ELECTRICAL COMMUNICATION BETWEEN DIFFERENT CELL TYPES IN THE COLONIC MUSCULATURE

ELECTRICAL COMMUNICATION BETWEEN DIFFERENT CELL TYPES IN THE COLONIC MUSCULATURE

by

Louis W. C. Liu, B. Eng.(McMaster University)

A Thesis

Submitted to the School of Graduate Studies

in Partial Fulfillment of the Requirements

for the Degree

M. Eng. in Engineering Physics

McMaster University

MASTER OF ENGINEERING (1991) McMASTER UNIVERSITY

(Engineering Physics) Hamilton, Ontario

TITLE: Electrical Communication Between Different Cells Types in the Colonic Musculature.

AUTHOR: Louis Wing Cheong Liu, B.Eng. (McMaster University)

SUPERVISOR: Dr. Jan D. Huizinga

NUMBER OF PAGES: xix, 165

Abstract

The major cell types in the canine colon musculature are interstitial cells of Cajal (ICC), circular muscle (CM) cells and longitudinal muscle (LM) cells. In isolated muscle strip studies, spontaneous membrane potential oscillations (slow waves) are generated in the submucosal border of the circular muscle where a gap junctionally well-coupled network of ICC and CM is found. CM devoid of LM and submucosal pacemaker region (CM preparations) are spontaneously quiescent. The research undertaken was to understand the mechanism of slow wave propagation into the circular muscle and to investigate the consequences to the electrical acitivity in CM after coupling with different electrical activities from different cells types.

Our results show that CM cells, although spontaneously quiescent because of high K^+ conductance, are excitable and can actively participate in slow wave generation. The electrical oscillations induced in the CM preparations could easily be potentiated by an L-type Ca^{2+} channel activator, Bay K 8644, and abolished by a L-type Ca^{2+} antagonist, D600, suggesting involvement of the conductance in the induced activity. The induced oscillations are similar to the SLAPs in the longitudinal muscle which shows that it is not necessary to have a specialized pacemaker cells for generating SLAPs. Using a cross sectioned preparation with all intact muscle layers, we also showed that the heterogeneity in the electrical activity of CM, such as: the resting membrane potential gradient, depolarization of plateau potential in the myenteric border and "apparent" decay in slow wave amplitude, is due to electrical interactions between different intrinsic activities from different cell types. Morphological evidence

was obtained for the possible communication pathways in the submucosal and the myenteric borders of the circular muscle. Different coupling mechanisms in different areas were hypothesized. In addition, the 3-dimensional aspects of the submucosal ICC network in the canine colon were clarified.

Acknowledgements

I would like to dedicate my deepest thanks to my supervisor, Dr. Jan D. Huizinga, for his unremitting guidance and encouragement during the last two years which made my Master's study a more enriching experience. Because of him, I learned how to think, speak, write, and survive as an engineer in the biological world.

I would also like to express my special thanks to all persons involved in the process of getting this dissertation in the final form, in particular Dr. Edwin E. Daniel for his constructive comments and recommendations, Dr. Irene Berezin for the preparation and photography of the electron micrographs concerning the structural communication study, and Dr. Lars Thuneberg for his inspiration related to the methylene blue study as well as the preparation of micrographs.

My special thanks are extended to Mrs. Laura Farraway for her technical assistance, friendship and, more importantly, spiritual support and comfort during hard times in the last two years.

Last but not the least, I would like to devote my sincere and heartfelt thanks to my family. To my mother, Mrs. Han-lan Chu Liu, for her continuous encouragement and support, financially and spiritually, in all these years while I was in Canada. Without her, my education would have not been successful. To my father, Mr. Yue-kwong Liu, who always believed that I could go far but who unfortunately did not live to see me begin my Master's career. I would like to dedicate this thesis to the memory of my father. To my sisters, Louisa, Julianna, Patricia and Vicky, for their support and taking care of mom so that I could leave home to pursue my career in

Canada. To my cousin, Anthony, for his companionship and support in the last two years. *I love you all.*

The financial support for this work came from the Medical Research Council of Canada, and scholarships from McMaster University.

Contents

1 Introduction **1**

1.1 Excitation-contraction-coupling 2

1.2 Morphology of the canine colon musculature 4

1.3 Literature review on colon physiology 6

1.3.1 Early history 6

1.3.2 Origin of slow waves 7

1.3.3 Ionic basis of slow waves 8

1.3.4 Slow wave propagation mechanism 9

1.3.5 Electrical heterogeneity within the circular muscle 10

1.3.6 Cellular organization in the pacemaker area 12

1.4 Choice of animal model 13

1.5 Objectives 13

2 Methodology **15**

2.1 Rationale of modus operandi 15

2.2 Tissue acquisition and preparations 17

2.2.1 FT preparation 17

2.2.2 ICC-CM preparation 19

2.2.3 CM preparation 20
2.3 Extracellular recording technique 20
2.4 Intracellular recording technique 22
2.4.1 Abe-Tomita bath 24

3 Excitability of Canine Colon Circular Muscle Disconnected from the Network of Interstitial Cells of Cajal 28

3.1 Abstract 28
3.2 Introduction 29
3.3 Method 31
3.3.1 Tissue preparations 31
3.3.2 Drugs and solutions 31
3.3.3 Result presentation and statistic analysis 32
3.4 Results 32
3.4.1 Spontaneous activities of ICC-CM preparations 32
3.4.2 Lack of spontaneous activity in CM preparations 33
3.4.3 Induced activities in CM preparations 34
3.5 Discussion 43
3.5.1 Circular muscle cells in canine colon can generate slow wave-like activity in the absence of the submucosal ICC network 43
3.5.2 Slow wave-like activity induced in spontaneously quiescent CM preparations lacks a D600-insensitive component 43
3.5.3 Role of K^+ conductance in depressing excitability of circular muscle 44

4 Properties of circular muscle of canine colon disconnected from pace-

maker cells **47**

4.1 Abstract 47

4.2 Introduction 49

4.3 Method 51

4.3.1 Tissue Preparation 51

4.3.2 Drugs and solutions 51

4.3.3 Result presentation and statistic analysis 52

4.4 Results 52

4.4.1 Comparison of activities in spontaneously quiescent CM preparations and ICC-CM preparations 52

4.4.2 Electrical oscillations induced by $BaCl_2$ 53

4.4.3 Excitability of spontaneously quiescent CM preparations . . . 58

4.4.4 Voltage sensitivity of the Ba^{2+} induced electrical oscillations . 59

4.4.5 Participation of L-type calcium channels in the generation of Ba^{2+} induced oscillations 63

4.4.6 Effects of forskolin on $BaCl_2$ induced electrical oscillations . . 68

4.5 Discussion 71

4.5.1 Role of membrane potential and K^+ conductance in generation of Ba^{2+} induced oscillations 71

4.5.2 Role of L-type calcium channels in generation of Ba^{2+} induced oscillations 73

4.5.3 Intrinsic differences in membrane properties of circular and longitudinal muscle cells 74

4.5.4 Role of circular muscle cells in the generation of electrical activity in the full thickness musculature 77

4.5.5 Is the metabolic clock present in the circular muscle cells of canine colon? 79

5 Electrophysiological and structural communication between circular and longitudinal muscle of the canine colon 81

5.1 Abstract 81

5.2 Introduction 83

5.3 Methods 85

5.3.1 Tissue Preparation 85

5.3.2 Intracellular recordings 86

5.3.3 Result presentation and statistical analysis 86

5.3.4 Tissue fixation and electron microscopic examination 90

5.4 Results 90

5.4.1 Resting membrane potential (RMP) gradient in the circular muscle 90

5.4.2 Plateau potential gradient in the circular muscle 96

5.4.3 Upstroke and plateau amplitudes 98

5.4.4 Frequency and duration of slow waves 100

5.4.5 Characteristics of spikes superimposed on slow wave plateaus . 101

5.4.6 Structural basis for electrical communication between longitudinal and circular muscle cells in the myenteric plexus 104

5.5 Discussion 109

5.5.1 Origin of membrane potential gradient 109

5.5.2 Structural basis for pulling of membrane potential 111

5.5.3 Active propagation of slow waves in circular muscle 114

5.5.4 Origin of the spikes in circular muscle 115

6 Selective accumulation of methylene blue by Interstitial Cells of Cajal in the canine colon with preservation of slow waves **117**

6.1 Abstract 117

6.2 Introduction 118

6.3 Method 120

6.3.1 Tissue preparation 120

6.3.2 Microelectrode recordings 120

6.3.3 Mechanical contraction measurements 121

6.3.4 Light and electron microscopy 121

6.3.5 Data Presentation and statistical analysis 124

6.4 Results 124

6.4.1 Selective accumulation of methylene blue by ICC 124

6.4.2 Effect of methylene blue on slow wave activity 128

6.4.3 Mechanical excitation by methylene blue 132

6.5 Discussion 134

6.5.1 Methylene blue is a specific probe for staining of canine colon submucosal ICC 134

6.5.2 The excitatory effects of methylene blue 135

6.5.3 The photosensitivity of methylene blue 136

7 Concluding remarks **138**

7.1 Physiological roles of ICC 138

7.1.1 As pacemaker cells 138

7.1.2 As an intercellular communication pathway 140

7.1.3 As a modulator of the frequency of bursts 142

7.1.4 As a metabolite supplier 142

7.2 Physiological roles of gap junctions 143
7.2.1 Metabolic coupling 143
7.2.2 Electrical coupling 144
7.2.3 Disadvantage of gap junction coupling 145
7.2.4 Gap junctions create a current sink in the canine colon pacemaker area 146

8 Extension of work **149**
8.1 Physiological aspects 149
8.1.1 Phase relationship between electrical oscillations 149
8.1.2 Selective action of methylene blue 150
8.2 Theoretical aspects 150
8.2.1 Oscillator modelling for slow wave origin 151
8.2.2 Propagation mechanism of slow waves 152
8.2.3 Chaos in proximal colon 153

Bibliography **154**

List of publications **165**

List of Figures

1.1 Schematic drawings of slow waves and corresponding phasic contractions illustrating the excitation-contraction-coupling 3

1.2 Schematic drawings of the cross section of canine colon musculature. . 5

2.1 The Full thickness preparation of Canine Colon. 18

2.2 ICC-CM preparation of canine colon. 19

2.3 Block diagram of the suction electrode set-up 21

2.4 Block diagram of the microelectrode set-up 23

2.5 Abe-Tomita bath 25

3.1 Effects of carbachol on ICC-CM and quiescent CM preparations (QCM) and their sensitivity to D600. 35

3.2 Effects of TEA on ICC-CM and quiescent CM preparations and their sensitivity to D600 36

3.3 Effects of $BaCl_2$ on ICC-CM and quiescent CM preparations and their sensitivity to D600 38

3.4 Slow wave frequency of the ICC-CM and frequency of electrical oscillations in CM preparations in different pharmacological conditions . . 39

3.5 Duration of slow waves in ICC-CM and oscillations in CM preparations under different pharmacological conditions 40
3.6 Normalized slow wave amplitude in the ICC-CM and oscillation amplitude in CM preparations under different pharmacological conditions 42

4.1 Input resistance of CM preparations in Krebs solution, 0.5 mM $BaCl_2$ and high extracellular K^+ concentration. 54
4.2 Different effects of depolarizing pulses on ICC-CM and quiescent CM preparations. 57
4.3 Voltage sensitivity of $BaCl_2$ induced oscillations in CM preparations and spontaneous slow waves in ICC-CM preparations. 60
4.4 High frequency oscillations induced by $BaCl_2$ and their sensitivity to elevation of extracellular K^+ concentration 62
4.5 Effect of L-type calcium channel blockade on $BaCl_2$ induced oscillations 64
4.6 Effects of Bay K 8644 on the Ba^{2+} induced oscillations 65
4.7 Appearance of bursting activity during hyperpolarization 66
4.8 Effects of Bay K 8644 on the spontaneous slow waves in ICC-CM preparations. 67
4.9 Effects of forskolin on $BaCl_2$ induced oscillations 69
4.10 Forskolin transforms regular activity induced in quiescent CM preparations by $BaCl_2$ into bursting activity. 70
4.11 Comparison of the electrical activity recorded at the same location of the circular muscle layer before and after removal of the submucosal ICC network with the spike like action potentials recorded in the longitudinal muscle. 75

5.1 Electrical oscillations in a FT preparation of canine colon 92
5.2 The average resting membrane potential and plateau potential of electrical oscillations recorded in the CM layer of the FT preparations. . 93
5.3 The average resting membrane potential and plateau potential at different locations of the circular muscle layer of the ICC-CM preparations. 94
5.4 Electrical oscillations in isolated muscle strips of canine colon. 95
5.5 A typical RMP and plateau potential gradient found in the submucosal surface of an ICC-CM preparation. 97
5.6 Maximum spike amplitude on the slow wave plateau phase of the circular muscle of the FT preparations. 102
5.7 Spikes in the canine colon circular muscle. 103
5.8 Low magnification micrographs of the narrow regions between the circular and longitudinal muscle. 105
5.9 Narrow regions between circular and longitudinal muscles at higher magnifications 107
5.10 High magnification micrographs of inner circular muscle. 112

6.1 Diagram to define the type of preparation used for methylene blue staining. 122
6.2 Light microscopical demonstration of methylene blue uptake in ICC of canine colonic submuscular plexus. 122
6.3 Montage of three light microscopical photographs of methylene blue stained ICC. 122
6.4 Low magnification myographs of the canine colonic musculature. . . . 125
6.5 Electron micrographs of canine colon incubated with methylene blue . 126
6.6 Effects of 50 μM methylene blue on the colonic slow wave activity . . 129

6.7 Effects of 50 μM methylene blue on colonic slow wave activity exhibiting intermittent prolonged slow waves. 130
6.8 Effects of 50 μM methylene blue on phasic contractions of ICC-CM and CM preparations. 133

7.1 Effects of hyperpolarization induced by extracellular electrodes in the FT preparations. 141

List of Tables

4.1 Effects of Bay K 8644 on ICC-CM preparations 52

4.2 Effects of $BaCl_2$ and $BaCl_2$ + Bay K 8644 on spontaneous quiescent CM preparations. 55

4.3 Effects of increasing extracellular K^+ on $BaCl_2$ induced oscillatory activity in CM preparations. 61

5.1 Summary of the exponential best fit parameters of the upstroke and plateau amplitudes in the FT and ICC-CM preparations. 99

5.2 Summary of the spike parameters in the FT preparation. 104

6.1 Pharmacological effects of 50 μM methylene blue on the slow wave parameters of canine colon. 128

6.2 Mechanical excitation of ICC-CM and CM strips by methylene blue and $BaCl_2$ 131

Nomenclature

AMP	Adenosine monophosphate
CM	Circular muscle
D600	Methoxyverapamil
EM	Electron microscopy
FT	Full thickness
ICC	Interstitial cells of Cajal
LM	Longitudinal muscle
MB	Methylene blue
MP	Membrane potential
P	Probability of happening of an event
PA	Plateau amplitude
PP	Plateau potential
$\mathbf{R_i}$	Input resistance
$\mathbf{R_j}$	Junctional resistance
$\mathbf{R_m}$	Membrane resistance
RMP	Resting membrane potential
SEM	Standard error of the mean
SLAP	Spike like action potential
TEA	Tetraethylammonium chloride
TTX	Tetrodotoxin

UA	Upstroke amplitude
cpm	Cycle(s) per minute
min	Minute(s)
n	Number of samples
$\mathbf{r^2}$	Pearson product moment correlation coefficient
$\mathbf{\bar{r}_{ab}}$	Ratio of input resistance in solution a to solution b
s	Second(s)
λ	Space constant

Chapter 1

Introduction

The major functions of the colon musculature are: (1) to provide mixing movements so as to optimally extract water and electrolytes from the fluid content received from the ileum; (2) to temporarily store colon contents before defecation; and (3) to contract in a coordinated fashion so as to move the contents towards the rectum and then provide, under voluntary control, defecation. The motility in the proximal colon is retarded and often antiperistaltic to provide enough time for reabsorption of water and electrolytes as well as for metabolization of the remaining carbohydrates by flora of bacteria to short chain fatty-acids which contribute to a nutritional value. During the temporary storage stage, reabsorption is continuous predominately in the middle colon. The motility is slow and segmental. In the final stage, co-ordinated phasic contractions are necessary for providing the peristaltic motion to move the faecal contents in the anal direction. Peristaltic movement relies on synchronized contractile activity in the muscle layers.

1.1 Excitation-contraction-coupling

The pattern of spread of contraction is highly correlated with the spread of electrical events in the colonic wall. The correlation between the phasic contractions and the electrical oscillations is governed by the mechanism of excitation-contraction-coupling [28, 33, 78] which, in simple terms, is the mechanism through which calcium enters the cell during the depolarizing phase of the electrical oscillation, whenever surpassing the threshold for opening calcium channels, causing the cell to contract by activating the intracellular contractile filaments. Hence, periodic calcium influxes caused by electrical oscillations with amplitudes that exceed the threshold for activating calcium channels can produce periodic phasic contractile activities. Out of the scope of this discussion, the force of contraction can also be enhanced by release of intracellular Ca^{2+} stores.

To produce a sustained and forceful contraction, it is more ideal to have a continuous supply of calcium for a long period of time. Consistently, in the canine colon, the electrical oscillations recorded in the circular muscle are of ≈5–8 s in duration and ≈6 cpm in frequency and consist of an upstroke phase and a plateau phase ([2, 5, 49], and see figures 4.3, 4.8, 5.1, 5.4). Because of the long period of depolarization during the plateau phase of electrical oscillations, the oscillations are also called slow-wave-type action potentials or *slow waves* in short. *In vitro* studies, phasic contractions can occur in the circular muscle strips without the appearance of spikes (compared to slow waves, spikes have a smaller duration—less than 2 s, and higher frequency—larger than 12 cpm) superimposed on the plateau phase, indicating that the plateau potential of slow waves has already surpassed the mechanical threshold of the muscle cells to initiate contraction [3]. Force of contractions can be further enhanced by induction of spikes superimposed on the plateau. Figure 1.1 schematically illustrates

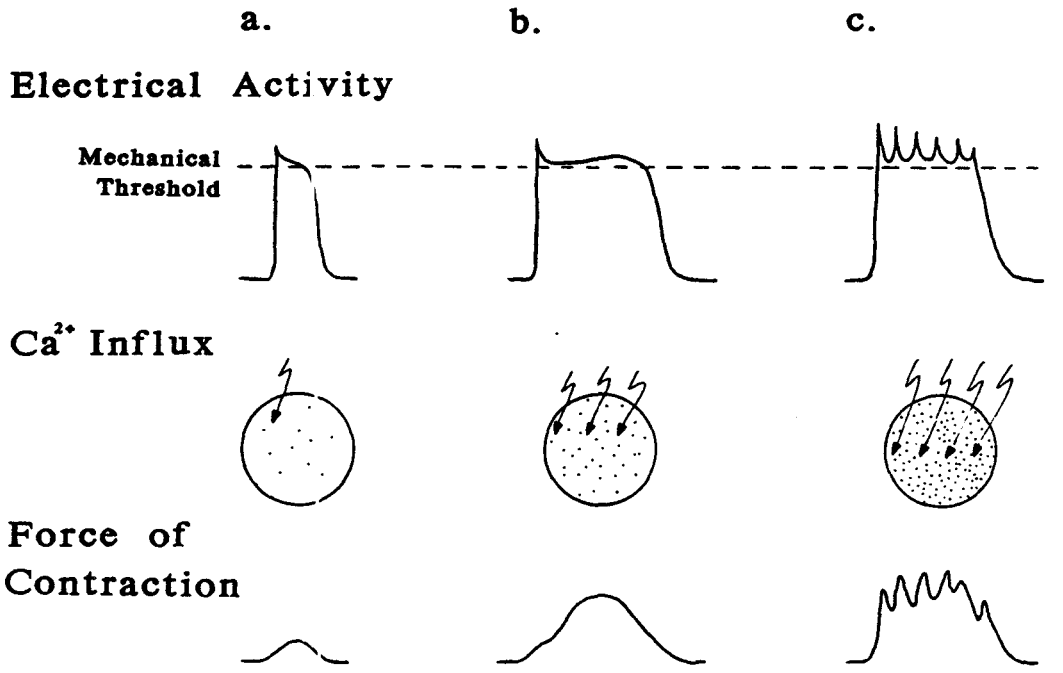

Figure 1.1: *Schematic drawings of slow waves and corresponding phasic contractions illustrating the mechanism of excitation-contraction-coupling*

Three different patterns of slow waves are shown in the first panel: (a) a regular duration slow wave; (b) a longer duration slow wave at a higher level of excitation than (a); and (c) a slow wave with spikes superimposed on the plateau at the highest level of excitation. The second panel represents corresponding calcium influxes. The third panel depicts the corresponding force development.

the correlation between force of contractions and different patterns of slow waves.

To understand the colonic motility, knowledge of where the electrical oscillations are originated (i.e. the location of the pacemaker), the mechanism of generation of the pacemaker potential, and mechanism of propagation of the pacemaker potential into the musculature is essential. Before describing the methodology employed and the research results, a brief description of the basic structure of the canine colon musculature and the existing literature in this area is presented to promote the appreciation of the present experimental findings.

1.2 Morphology of the canine colon musculature

Apart from nerve cells, blood vessels and mast cells, the major cell types in the canine colon musculature are interstitial cells of Cajal (ICC), circular muscle cells and longitudinal muscle cells (figure 1.2). As a global orientation, the long axis of circular muscle cells orient circumferentially around the colonic lumen; whereas, the long axis of longitudinal muscle cells run along the long axis (the axial direction) of the colon. Both the circular and longitudinal muscles are continuous (i.e no connective tissue septa are found) along the longitudinal axis of smooth muscle cells. Circular muscle is continuous in the circumferential direction but occurs in bundles separated periodically by connective tissue septa in the axial direction of colon (figures 6.1 and 6.5 of Chapter 6). The septal structure of the longitudinal muscle is less well-defined. The two muscle layers are separated by the myenteric plexus consisting of enteric neurons (axons and ganglions), blood vessels, ICC and connective tissue. ICC can also be found in the submuscular plexus (consists of the ICC network plus the immediately adjoining smooth muscle cells) located in the submucosal surface of the

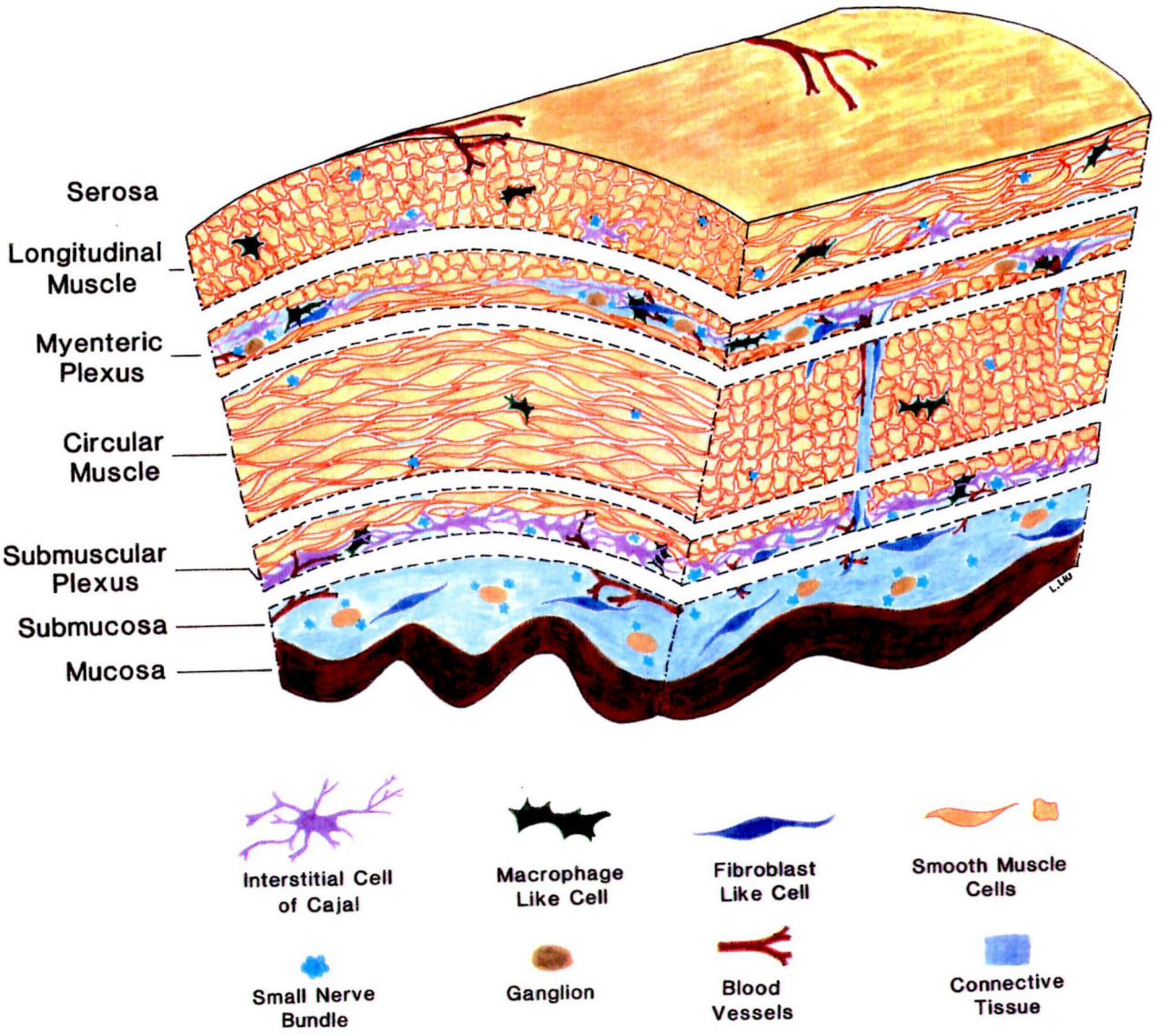

Figure 1.2: *Schematic drawing of the cross section of canine colon musculature.* The major structural divisions of canine colon are mucosa, submucosa, submuscular plexus, circular muscle, myenteric plexus (also called Auerbach's plexus), longitudinal muscle and serosa. The small space inserted between the major divisions indicates the line of dissection.

circular muscle layer. ICC in the submuscular plexus form a complete network with circular muscle cells by forming gap junctions between themselves and with smooth muscle cells ([14], also see Chapter 6). In areas where gap junctions are found, membranes of adjacent cells are in close apposition of a few nanometres; the gap between the membranes of adjacent cells are bridged by connexon proteins (channels) whose states of opening and closure can be regulated. Gap junctions are very rarely found elsewhere in the musculature. A description of the correlation between electrical oscillations and the gap junction distribution in the canine colonic musculature will be presented in Chapter 5.

1.3 Literature review on colon physiology

1.3.1 Early history

The 6 cycle per min (cpm) phasic contractions in the colon were first demonstrated in cats by Canon [18] using a radiography technique in 1902. A subsequent study performed in 1904 by Elliott and Barclay-Smith [37] confirmed Cannon's observations and found similar contraction patterns in other species such as dog, ferret, guinea pig, hedgehog, rabbit and rat. Consistent with these pioneer *in vivo* contraction studies, recent electrophysiological studies reported membrane potential oscillations, also called slow waves, of about 6 cpm. The latter studies proved a correlation between slow waves and phasic contractions. Reviews on the history of gut physiology were written by Christensen [21] and Szurszewski [78].

1.3.2 Origin of slow waves

In 1969, Christensen *et al.* [25] first demonstrated that slow electrical oscillations were generated in the isolated circular muscle layer but not in the isolated longitudinal muscle of cat colon. They concluded that slow waves were generated in the circular muscle. Almost fifteen years later, in 1983, Durdle *et al.* [33] proposed that not all the muscle cells in the dog colonic musculature could generate slow waves. At the submucosal surface, the slow wave amplitude is larger than at any other locations of the musculature. In addition, removal of the submucosal layer resulted in complete abolition of slow wave activity in both the isolated circular muscle and the intact muscle wall. Therefore, they suggested that "the appearance of slow waves in circular muscle ... was ... dependent on the integrity of the junction between the submucosa and the innermost circular layer" (p.381 of [33]). More recent studies by Barajas-López and Huizinga [2], Serio *et al.* [69] and Smith *et al.* [71] confirmed that the inner border of the canine colonic circular muscle is crucial for the generation of the spontaneous slow waves. Although the above mentioned studies show the area from where slow waves are generated, the type(s) of cells responsible for initiating these electrical oscillations are now under investigation.

Not more than a few years ago, it was generally accepted that there were no special pacemaker cells in the gut musculature but that every smooth muscle cell would act as pacemaker cell. In 1982, a paper written by Thuneberg [80] was instrumental in focusing research on the possibility that specialized cells might function as pacemaker cells and provided evidence that ICC might be the specialized cells. After this hypothesis, many research efforts have been devoted to looking for evidence that ICC are the gastrointestinal pacemaker cells. In the canine colon, apart from the electrophysiological evidence discussed above, there is a strong morphological basis

to support the theory that the submucosal ICC act as the colonic pacemaker cells since they not only form a highly gap junctionally coupled network at the submucosal surface with themselves and adjacent circular muscle cells but also house a lot of mitochondria [14] to provide sufficient energy for high energy consumption pacemaking processes since the slow wave generation mechanism has been shown to be metabolically dependent [56].

Slow waves recorded in the colon have long been thought to be *myogenic in nature* [35, 34, 37, 78]; that is, generation of slow waves is an intrinsic property of the muscle cells. It has been shown that slow waves are insensitive to TTX, which abolishes the propagation of nerve impulses along the axon by blocking the Na^+ channel, and atropine, which inhibits cholinergic impulse transmission at synapses. As the evidence that ICC are the gastrointestinal pacemaker cells is accumulating, the myogenic nature of the initiation mechanism of slow waves becomes *questionable* since ICC are not classified as smooth muscle cells.

1.3.3 Ionic basis of slow waves

The ionic basis of slow waves in canine colon has recently been characterized by Barajas-López and Huizinga [5]. The major portion of the slow wave is a consequence of voltage activation of L-type Ca^{2+} channels; the termination of the slow wave is, to a large extent, the consequence of activation of K^+ conductance. The ionic mechanism that initiates slow waves, related to the determination of the oscillating frequency, is insensitive to abolishment of Na^+ gradient, blockade of TTX sensitive Na^+ channels, replacement of 91% of extracellular Cl^- or blockade of L-type Ca^{2+} channel by D600. The upstroke component (initiation) of the slow wave is, however, abolished by either removal of extracellular Ca^{2+} or addition of Co^{2+} or Ni^{2+}. Hence, a Co^{2+}-sensitive

Ca^{2+} conductance is likely involved in the initiation of slow waves [57]. Two other studies performed by the same group suggests that the mechanism of slow waves generation is insensitive to K^+ conductance blockade [2, 3]. In addition, slow waves are sustained during hyperpolarization or depolarization of membrane potential [38, 56]. Therefore, slow waves are very unlikely to be initiated by sequential activation and inactivation of voltage dependent membrane conductances as observed in the cardiac pacemaker potentials. Consistently, in contrast to the slow depolarization preceding each cardiac pacemaker potential, the inter-slow-wave-interval is constant in canine colon. This led to the hypothesis that slow waves are initiated by activation of a membrane conductance caused by cyclic oscillation of intracellular metabolites [56].

A metabolic clock, that regulates the slow wave frequency, has recently been proposed by Huizinga *et al.* [56]. The period of the clock cycle is dramatically increased by increasing intracellular cyclic AMP. In the presence of 8-bromo-cyclic-AMP or forskolin, the slow wave frequency dramatically decreased without significant change in amplitude. Consistent with the idea of metabolic control of slow wave initiation, the slow wave frequency can also be reduced by decreasing temperature.

1.3.4 Slow wave propagation mechanism

After slow waves are initiated in the submucosal border of the circular muscle, they propagate to the neighbouring circular muscle cells in which contraction is generated. However, up to this point, whether slow waves propagate *actively* (that is, circular muscle cells possess regenerative mechanisms to restore the slow wave amplitude) or *passively* (slow waves generated by pacemaker cells decay exponentially according to the passive membrane parameters of circular muscle cells; in this case, the small volume of pacemaker cells in the submucosal border needs to drive the entire bulk of

circular muscle) from the submucosal to the myenteric border of the circular muscle is equivocal.

Using a cross-section preparation, slow waves have been suggested to be passively propagated through the circular muscle based on the observations that electrical activity could not be induced in the strips from which the pacemaker area had been removed and slow wave amplitude decayed exponentially from the submucosal to the myenteric border of the circular muscle [71]. This study also implied that circular muscle are passive and inexcitable cells. However, using a preparation with the longitudinal muscle removed, it was reported that the upstroke amplitude of slow waves in the myenteric border of circular muscle was 29.8 mV [2]. This amplitude is larger than what one predicts from the space constant (equal to 0.43 mm along the short axis of the circular muscle cells [51]) of this tissue. In other words, there seems to be a regenerative mechanism to restore a certain extent of the slow wave upstroke amplitude while slow waves are propagating across the circular muscle. That is, circular muscle may be composed of *active* cells. Noteworthy, active propagation of slow waves through circular muscle layer of feline colon has been observed [22, 23, 24]. Therefore, further experimentations are warrented to settle these paradoxical results.

1.3.5 Electrical heterogeneity within the circular muscle

Early electrophysiological studies performed by Christensen *et al.* [25] in 1969 using both surface glass pore electrodes and intracellular electrodes in cat colon revealed that slow waves were only dominant in the circular muscle; whereas, bursts of higher frequency oscillations (termed as spike-like-action-potentials, SLAPs) were recorded in the longitudinal muscle. In 1982, Durdle *et al.* confirmed their observations in canine colon. A subsequent, published almost at the same time, more sophisticated

and complete study carried out by El-Sharkawy [34] simultaneously recorded bursting activity from the longitudinal muscle and slow waves from the circular muscle. Although the patterns of oscillations were different, they were co-ordinated. The interaction mechanism of these two patterns of activities will be discussed in Chapter 5.

There are two divisions of thought about the origin of SLAPs. Because the SLAPs are so different from slow waves, one branch of idea is that a group of specialized cells located in the myenteric plexus is responsible for generating these SLAPs. This hypothesis is based on the observation that the amplitude of SLAPs decays exponentially in the circular muscle from the myenteric plexus either when all the muscle layers are intact or when the submucosal border is removed [71, 70]. Thus, the theory is that the canine colon musculature is embedded with two pacemaker regions: one located in the submucosal border generating slow waves; and the second one in the myenteric plexus area generating SLAPs [65]. Another branch of belief of the origin of SLAPs suggests that their appearance depends on the level of excitation of smooth muscle cells. Using circular muscle preparations with the longitudinal muscle and myenteric plexus area removed, SLAPs can be evoked in the circular muscle either by K^+ conductance blockade using TEA [2] or by cholinergic stimulation [3]. These observations suggested that it is not necessary to have specialize cells for generating SLAPs [50]; it could be considered as a property of smooth muscle cells. These controversial observations will be addressed from two different perspectives in Chapter 4 and Chapter 5.

When measuring across the transverse axis of the circular muscle, the two slow wave parameters that change the most are the plateau amplitude and resting membrane potential. The former has been discussed in the previous section; whereas, the

latter has been interpreted as a consequence of an heterogeneity in intrinsic membrane properties, namely the Na/K pump activity, of circular muscle cells across the layer [17]. It was observed that the resting membrane potential was equal to −80 mV and −43 mV in the submucosal and myenteric borders, respectively [70, 71]. If such a resting membrane potential gradient were to be due to the difference in intrinsic circular muscle membrane properties between the submucosal and myenteric borders, such gradient would have been preserved in the circular muscle layer isolated from longitudinal muscle; however, it was not observed. When the longitudinal muscle was removed, the resting membrane potential in the myenteric border equalled to −62 mV [2]. Therefore, the origin of resting membrane potential gradient across the transverse axis of the circular muscle remains to be resolved — one of the objective of this thesis.

1.3.6 Cellular organization in the pacemaker area

Although some physiological results of the canine colon as described above are disputable, the importance of the inner border of circular muscle is undeniable. Knowledge of the cellular organization in this region is limited but essential for identification of the cell(s) responsible for the generation of slow waves. Electron microscopic study has revealed the cellular structures of the ICC as well as the ultrastructure of gap junctions between cells in this area [14]. Unfortunately, the field of electron microscopy is limited to a tiny section of the entire tissue. It is necessary to obtain a method which allows one to visualize and characterize the entire 3-dimensional aspect of the submucosal ICC network.

Methylene blue, a vital stain, has been used for selective staining of the ICC network in the myenteric plexus of the small intestine of rabbit, guinea pig and

mouse (see review by Thuneberg [81]) which permits easy differentiation of ICC from the neighbouring smooth muscle cells under the light microscope. Methylene blue seemed to be a tool to be used to achieve the above stated objective. However, methylene blue has been shown to abolishe the canine colonic slow waves and stain the entire musculature pale blue [67] although these observations have been challenged by Thuneberg [82]. This thesis will present data on the use of methylene blue in the characterization of the colon ICC network.

1.4 Choice of animal model

The advantages of using the canine colon as our animal model for the study of cellular communication within one musculature are: (1) the circular and longitudinal muscle layer can be mechanically separated by dissection (whereas, for example, the muscle layers of human colon are interweave into each other at the interface [21, 58]; (2) the patterns of electrical oscillations are very distinct in the two muscle layers ([20, 29, 50, 78], see also Chapter 5) so that the investigation of electrical communication between muscle layers can be achieved by comparing the electrical events of the muscle layers in intact tissue and in isolated muscle strips; (3) preliminary data are available on the location of the pacemaker site [4, 70, 71, 78]; and (4) the submucosal ICC, candidates for the pacemaker cells, are organized in a distinct network that can be mechanically removed.

1.5 Objectives

As indicated by the title, the global objective of the research described in this thesis was to investigate the electrical inter-relationships between different cell types in the

canine colonic musculature. To approach this final goal, experiments were undertaken to: (i) provide further evidence for a role of ICC in colonic pacemaker activity; (ii) explore the intrinsic properties of circular muscle cells, and their roles in generation and propagation of action potentials so as to understand how circular muscle cells interact with ICC to generate the slow wave like action potentials; and (iii) investigate the mechanism of electrical communication between the circular and longitudinal muscles.

Chapter 2

Methodology

2.1 Rationale of modus operandi

The primary interest of this research is to investigate interactions between different cell types in the canine colon musculature. This demands knowledge of not only the characteristics of different intrinsic electrical oscillations in different cell types but also what the possible responses cells might be when they receive an input signal. Slow waves are generated in the submucosal surface of circular muscle. The mechanism through which slow waves propagate to the myenteric surface depends on the intrinsic properties of circular muscle cells. Since the excitability of circular muscle cells has been put in question, it was of our concern to investigate the excitability and intrinsic properties of circular muscle cells. Thus, the influences of electrical events from other sources in the musculature were needed to be eliminated which was accomplished by removing the longitudinal muscle and the submucosal pacemaker area; we called this the *circular muscle (CM) preparation.* Excitatory drugs were used for eliciting responses from the strips leading to a dramatic increase in the force of contraction

which created unstable impalements using intracellular recording techniques. Thus, extracellular suction electrodes were used in the determination of the possibility of inducing electrical oscillations in the quiescent CM preparations.

Owing to the inherent limitations of the suction electrode technique, the resting membrane potential, the absolute values of the amplitude, and rate of rise of oscillations could not be quantified. After knowing that electrical oscillations could be induced in the CM preparation, the intracellular recording technique was employed to characterize the parameters of the induced electrical oscillations. To compare the induced electrical oscillations with the spontaneous slow waves generated in tissue connected to pacemaker cells, similar pharmacological treatments were applied to strips with intact submucosal pacemaker area. This preparation consists of the submucosal ICC-network and the circular muscle layer and, therefore, referred to as the *ICC-CM preparation.*

With the knowledge that slow waves are recorded in ICC-CM preparations whereas SLAPs are observed in isolated longitudinal muscle (see figure 5.4 for diagramatic illustration of the difference in electrical activities displayed by the two muscle layers), the mechanism of electrical interaction between the two types of muscles at the interface was our next interest. For this purpose, a preparation with all intact muscle layers, including the submucosal pacemaker network, was required. Since this preparation was composed of the full thickness of the canine colon musculature, it was called the *FT preparation.*

2.2 Tissue acquisition and preparations

Dogs of either sex were killed by an overdose of pentobarbital sodium (100 mg/kg) given intravenously. Approximately 10 cm of proximal colon was taken starting from 5 cm distal to the ileocecal junction. The colon was opened flat. Colonic contents were carefully removed in a beaker containing oxygenated (95 % O_2 and 5 % CO_2) Krebs solution. The composition (in mM) of the Krebs solution was: NaCl—120.3; KCl—5.9; $CaCl_2$—2.5; $MgCl_2$—1.2; $NaHCO_3$—20.2; NaH_2PO_4—1.2 and glucose—11.5. The cleaned segment was then pinned flat to the Sylgard bottom of a dissecting dish which was filled with continuously oxygenated Krebs solution. The mucosa of the segment was carefully removed by sharp dissection.

2.2.1 FT preparation

A strip, approximately 1.5 mm thick and 10 mm long, cut along the long axis of the circular muscle was prepared. The width of this strip was similar to the thickness of circular and longitudinal muscle layers. Figure 2.1 shows a schematic drawing of the FT preparation. The strip was pinned (only 4 mm in the circular muscle long axis) on the Sylgard bottom of a transfer holder. The FT preparation was mounted by carefully putting insect pins along all four edges (serosal side of the longitudinal muscle, connective tissue at the submucosal surface circular muscle, two transverse edges determining the length of the strip) without damaging the muscle cells adjacent to the myenteric plexus and the submucosal ICC-circular muscle network.

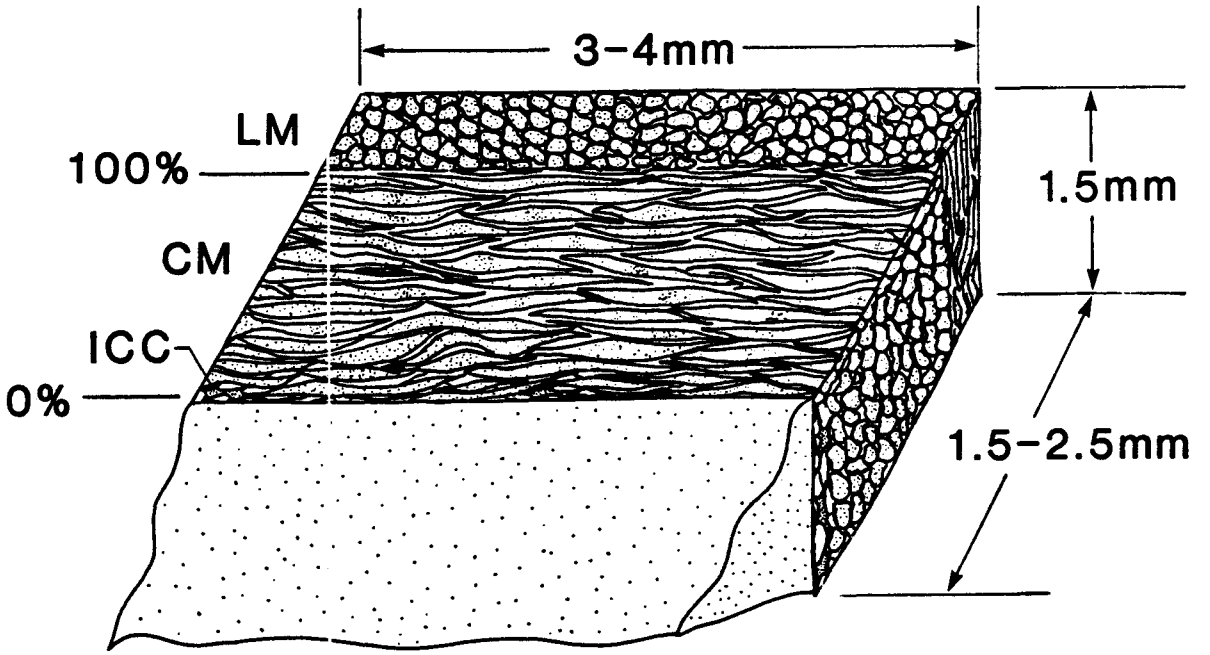

Figure 2.1: *The full thickness preparation of Canine Colon.*

The full thickness preparation consists of all the muscle layers of the colonic wall. Microelectrode recordings were made along the surface of the CM layer exposed by cutting along the longitudinal axis of the CM cells.

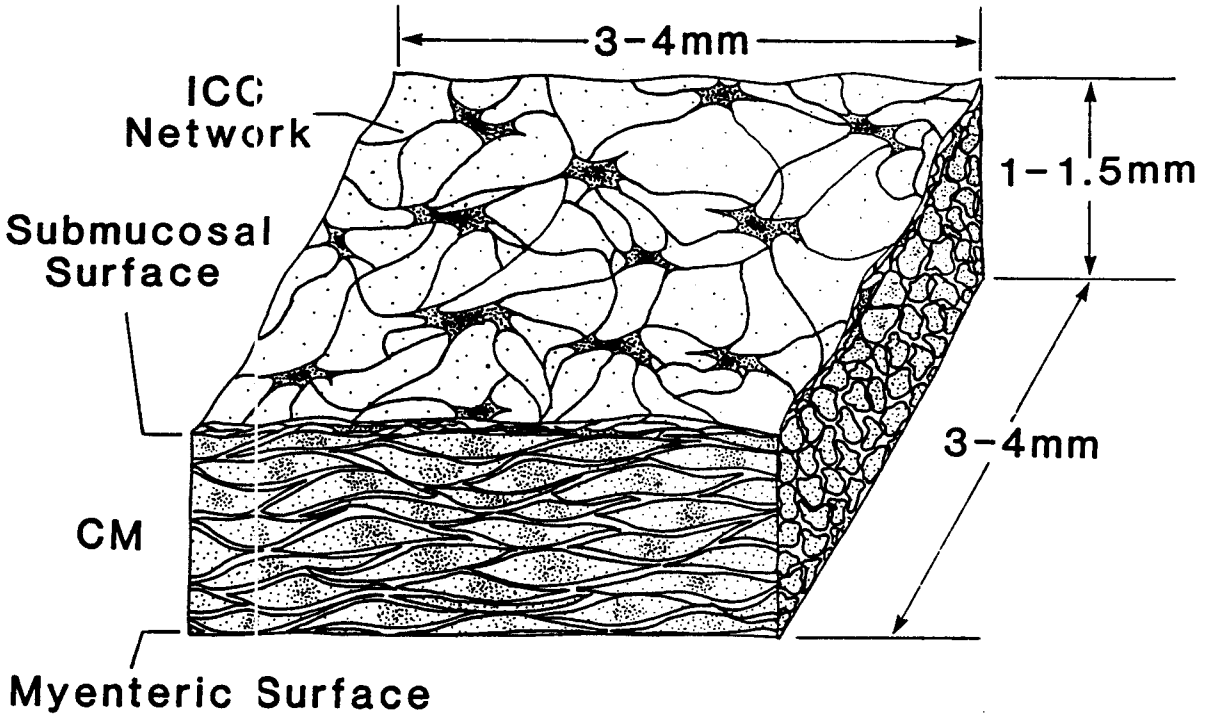

Figure 2.2: *ICC-CM preparation of canine colon.*
The ICC-CM preparation consists of only the circular muscle layer plus the submuscular plexus.

2.2.2 ICC-CM preparation

After removing the mucosa, the tissue was turned over; the longitudinal muscle and a few layers of circular muscle in the myenteric border were removed. A schematic drawing of the ICC-CM preparation is depicted in figure 2.2. The ICC-CM preparations were mounted differently according to the purposes of different studies and will be discussed accordingly.

2.2.3 CM preparation

After removing the longitudinal muscle layer and the myenteric plexus area, the tissue was then turned over again. The ICC-network (only the thin white layer with 2–5 layers of circular muscle attached) was carefully removed. This preparation was very similar to the ICC-CM preparation except that the ICC network at the submucosal surface shown in figure 2.2 was removed.

2.3 Extracellular recording technique

Figure 2.3 shows the block diagram of the suction electrode set-up. The tissue was cut into strips of 3 mm in width and 10 mm in length. The strips were then placed in an organ bath, filled with 500 ml of continuously oxygenated Krebs solution. The organ bath was surrounded by a warm water bath which kept the bathing solution at 37.0±0.5°C. One end of the strips was connected to a force transducer to record the mechanical contraction while the other end was tied to an adjustable hook to provide the optimal tension (≈ 100% of the original length of the strips) for pharmacological responses [54].

Monopolar suction electrodes, always attached to the submucosal side of the circular muscle, were used to measure the electrical activities of the ICC-CM and CM preparations. Both the recording and the ground electrodes were silver chloride-coated silver (Ag-AgCl) wires (0.015″ in diameter). The recording electrode was insulated by a plastic tubing with outer and inner diameters of 1.5 mm and 0.5 mm, respectively. Suction was provided by a mechanical pump. The electrical and mechanical activities were recorded on a Gould inkwriting recorder (2800S).

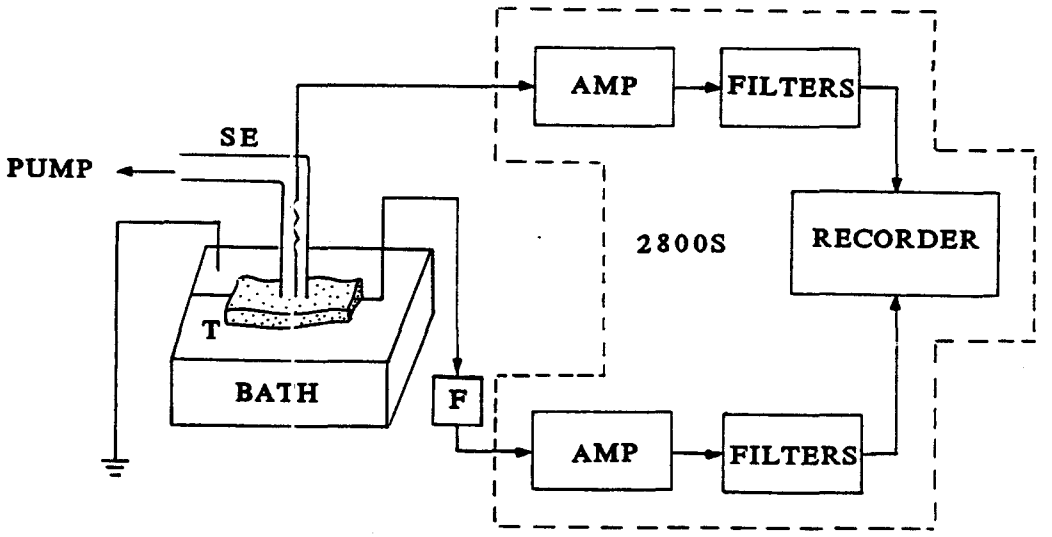

Figure 2.3: *Block diagram of the suction electrode set-up.*

Muscle strips (T) are hung in a muscle bath (BATH). Suction electrode (SE) is held on the surface of strip by suction created by a mechanical suction pump (PUMP). Electrode is connected to an amplifier (AMP) whose output is fed into a low-pass filter (cut-off at 30 Hz) and a notch (60 Hz) filter before recorded on an inkwriting recorder (RECORDER). F—force transducer.

2.4 Intracellular recording technique

The tissue was situated in an Abe-Tomita bath (see figure 2.5) consisting of a recording chamber and a stimulating chamber. The partitioned chamber was surrounded by a warm water bath which raised the perfusion solution temperature to 37.0±0.5°C before it reached the tissue. Before subjecting to experimentation, the tissue strips were allowed to equilibrate in the partitioned chamber for 2 hours so that it had recovered from temperature and stretch shocks due to the tissue preparation procedure. After the equilibration, synchronized electrical activity would always be observed.

Intracellular recordings were made by microelectrodes with 30–50 MΩ tip resistance because microelectrodes, having a tip resistance within this range, possess a tip diameter of approximately 150 nm which had been found to be appropriate for impaling cells in this tissue. Microelectrodes were filled with 3M KCl. A microelectrode was inserted into a microelectrode holder (WPI, MEH3SFW) which connected to an electrometer (WPI Duo773) which is a high impedance probe. The output of the electrometer was displayed on a Gould oscilloscope (1421) and recorded on a Gould inkwriting recorder (2400S).

Field stimulation was implemented by applying a stimulating pulse generated by a Grass stimulator (S88) to a pair of Ag-AgCl plates separated by 10 mm (see figure 2.5), through a Grass isolation unit (SIU5). The field strength was measured by a pair of Ag wire electrodes, 2 mm apart, locating in the middle of the stimulating chamber. The field strength (the voltage gradient recorded across the wire electrodes) was displayed on an oscilloscope and recorded on an inkwriting recorder.

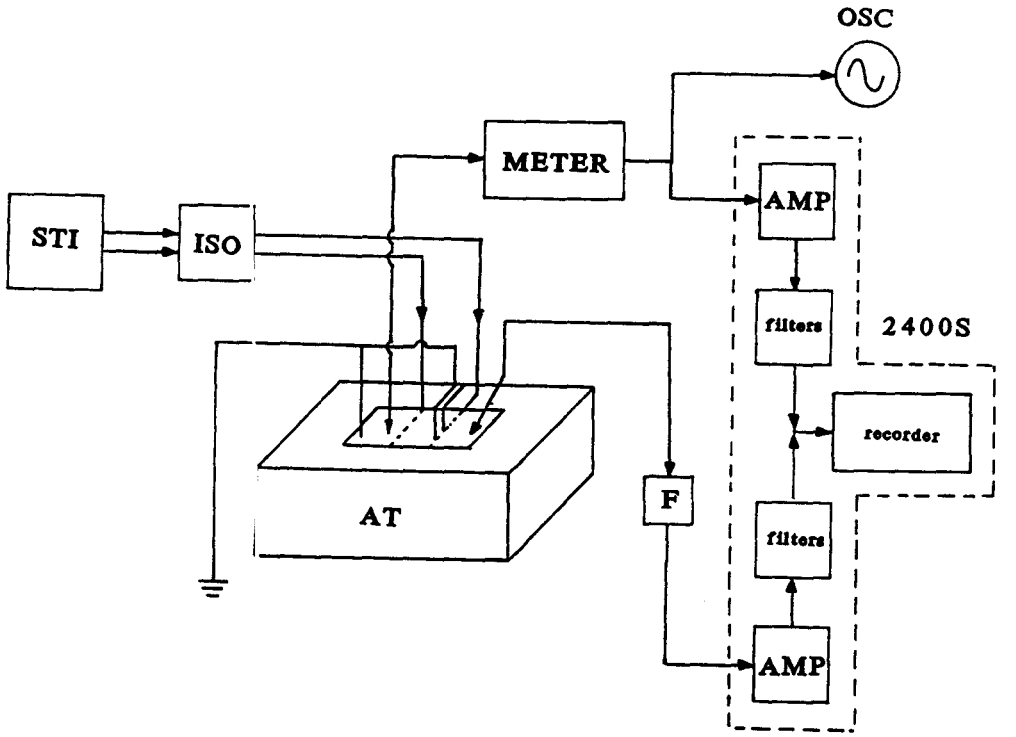

Figure 2.4: *Block diagram of the microelectrode set-up.*

The tissue is situated in a muscle bath (AT, see fig 2.5). Recording is made by a glass microelectrode connected to the probe of an electromemter (METER) whose output is displayed on an oscilloscope (OSC) and recorded on an inkwriting recorder (2400S) consisting of an amplifier (AMP), a low-pass filter (cut-off at 30 Hz), a notch filter at 60 Hz and a pen recorder (RECORDER). Stimulation pulses are sent to the muscle bath from a grass stimulator (STI) through an isolated unit (ISO). F—force transducer.

2.4.1 Abe-Tomita bath

The Abe-Tomita bath (figure 2.5) is divided into two partitioned chambers, namely a recording chamber and a stimulating chamber. The two chambers are separated by a Ag-AgCl plate coated with polyurethane coating on the side facing the recording chamber. A thin layer of dental wax is melted along the edge of the Ag-AgCl plate to ensure perfect insulation. Another Ag-AgCl plate (coated on the side away from the stimulating chamber) is situated at the other end of the stimulating chamber to allow application of a potential gradient across the stimulating chamber.

Perfusion solutions go into the Abe-Tomita bath through two separated tubings, which are coiled around a cylinder and bathed in water of 37.0±0.5 °C, at the inlet labelled as P_{in} in figure 2.5. The coiled tubing arrangement allows sufficient time for the ingoing perfusion solution to reach 37.0±0.5 °C before arriving at the partitioned chamber.

It is possible to induce an electrotonic pulse in the muscle strip by applying a potential gradient across the two Ag-AgCl plates located in the stimulating chamber. The electronic pulse then propagates passively to the site of the microelectrode recording and is seen as a membrane potential deflection. Thus, depending on the duration, intensity and polarity of field stimulation, different properties of the experimented tissue can be revealed.

Determination of excitability

The excitability of the tissue can easily be studied by brief depolarization field stimulating pulses of 0.1–0.3 s. The brief pulses replace the depolarization action of intrinsic pacemaking potentials. Therefore, membrane potential oscillations, following the frequency of the applied pulses are so called paced oscillations which, in gastrointestinal

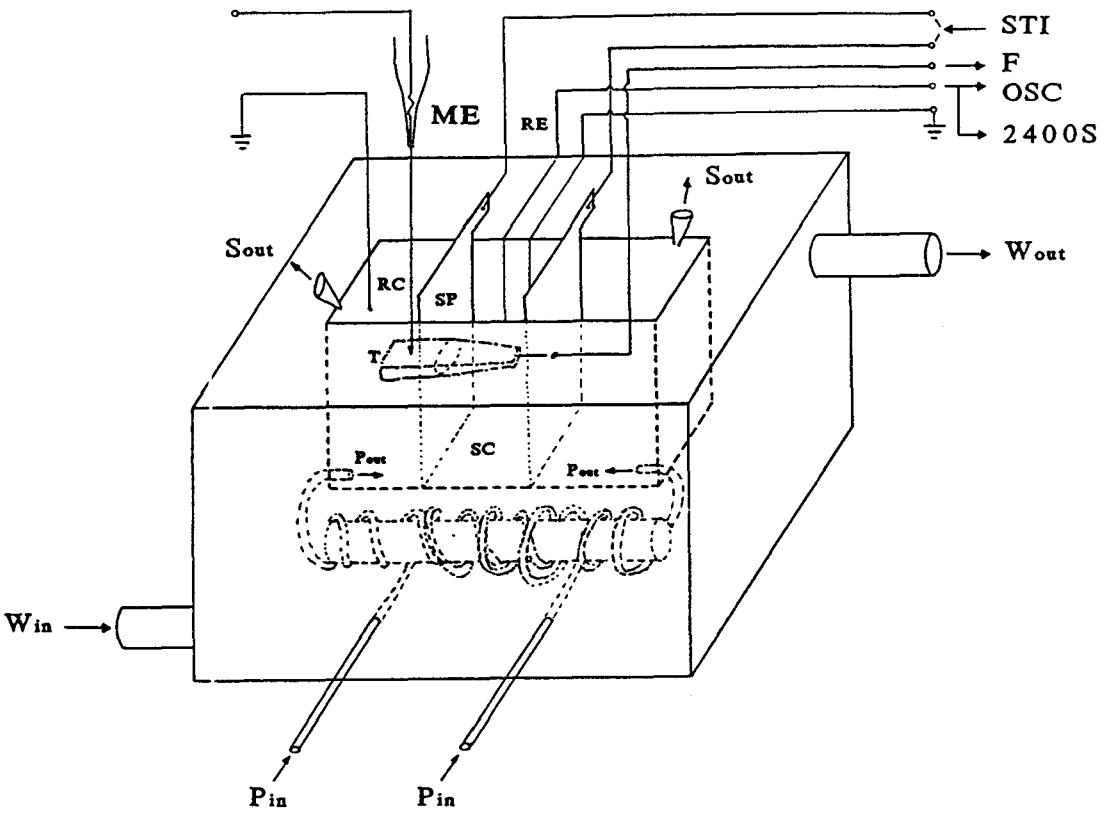

Figure 2.5: *Abe-Tomita bath*

The Abe-Tomita bath consists of a recording chamber (RC) and a stimulating chamber (SC). The SC is insulated from the RC by a Ag-AgCl stimulating plate (SP). The intensity of the field strength in the SC is recorded by a pair of Ag wire recording electrodes (RE). P_{in}—perfusion solution inlet; P_{out}—perfusion solution outlet; S_{out}—clearance outlet for perfusion solution from the bath; W_{in}—warm water inlet; W_{out}—warm water outlet; ME—microelectrode; F—force transducer; STI—stimulator; OSC—oscilloscope; 2400S—inkwriting recorder; T—tissue.

tissue with omnipresnt slow waves, are usually referred to as pre-mature slow waves since the paced frequency is usually higher than the intrinsic slow wave frequency. Figure 4.2 in Chapter 4 demonstrates the use of this concept to differentiate the intrinsic excitability of the ICC-CM and CM preparations.

Voltage dependence of activity

When long duration depolarizing or hyperpolarizing pulses (range from 20 s to 2 min) are applied across the two Ag-AgCl plates, the resting membrane potential of the tissue can be controlled for periods of maximally 2–3 minutes limited by the reduction rate of the Ag-AgCl plate. During either hyperpolarization or depolarization pulses, one of the two Ag-AgCl plates is continuously loosing Cl^- owing to the redox-reaction:

$$AgCl_{(s)} + e^- \rightleftharpoons Ag_{(s)} + Cl^-_{(aq)}$$

Therefore, the life-span of the stimulating plates can be extended by alternating application of depolarization and hyperpolarization pulses. Voltage sensitivity of electrical activities was studied using this approach in figure 4.3.

Measurement of input resistance

The input resistance of the tissue is reflected by the slope of the plot of the membrane potential deflections (mV) caused by pulses from the stimulating chamber versus different applied field strength (V/m) at the same location. This kind of plot is, very often, referred to as I/V curves. The duration of field stimulation is $\approx$3 s (to ensure steady amplitude of membrane deflection because the time constant of this tissue is $\approx$160 ms [51]) with varing amplitude. According to Ohm's Law, for the same

applied field strength (similar to the idea of current injection), the larger the input resistance, the larger the membrane potential deflection. Hence, an increase in slope after addition of a drug means an increase in input resistance (R_i) of the tissue. R_i is directly proportional to the membrane resistance, R_m, and junctional resistance, R_j. If the drug applied does not modify the R_j, an increase in R_i infers an increase in R_m. The average increase in R_i from different experiments was determined by

$$\bar{r}_{ab} = \frac{\sum_{t=1}^{n} \frac{m_{at}}{m_{bt}}}{n} \tag{2.1}$$

where $\bar{r}_{ab}$ is the average of the ratio of slope in solution a, m_a, to slope in solution b, m_b, in n trials. Since the amplitude of the membrane potential deflection decreases exponentially with distance away from the stimulating chamber, all the impalements were made very close to the pinned edge directly against the stimulating Ag-AgCl plate. In addition, the slopes before and after perfusion of a drug were compared only when recordings were obtained from the impalement of the same cell.

The resting membrane potential of the canine colon circular muscle has been shown to be insensitive to the abolishment of Na^+ gradient [5] or Cl^- gradient [5] indicating that the resting membrane potential is not determined by Na^+ or Cl^- conductances. The Ca^{2+} conductance is also very low at the resting potential. In addition, the resting membrane potential is very sensitive to change in extracellular K^+ and highly co-related to modification of the K^+ Nernst potential [3]. Hence, the membrane potential as well as the membrane resistance are dependent mostly on the K^+ conductance.

Chapter 3

Excitability of Canine Colon Circular Muscle Disconnected from the Network of Interstitial Cells of Cajal

3.1 Abstract

The 6 cpm omnipresent slow waves recorded in the circular muscle (CM) layer of canine colon are generated at the submucosal surface of the CM layer. After removal of the submucosal network of interstitial cells of Cajal, 66% of the CM preparations (25 out of 38) were quiescent in Krebs solution. In the presence of carbachol, 7 out of 9 of these spontaneously quiescent CM preparations demonstrated slow wave-like activity with mean frequency, duration and amplitude of 5.9±0.4 cpm, 2.8±0.5 s and 0.8±0.2 mV, respectively. Similar slow wave-like activities were induced by TEA

(7 out of 8 quiescent CM preparations) with frequency, duration and amplitude of 6.1±0.2 cpm, 2.7±0.5 s and 1.0±0.2 mV, respectively, and by $BaCl_2$ (8 out of 8 quiescent CM preparations) with frequency, duration and amplitude of 6.3±0.3 cpm, 1.8±0.2 s and 0.5±0.1 mV, respectively. All the induced activities were abolished in the presence of 1 μM D600. CM preparations with the submucosal ICC network intact (ICC-CM), showed slow wave activity in Krebs solution at a frequency of 6.2±0.2 cpm, a duration of 3.6±0.2 s, and an amplitude of 1.0±0.1 mV (n=22). When ICC-CM preparations were stimulated by carbachol, TEA or $BaCl_2$, the slow wave frequency did not change significantly, the duration increased as well as the amplitude. In the presence of D600, the slow wave upstroke and frequency were not affected in the ICC-CM preparations. The ability to generate slow wave-like activity after potassium conductance blockade in spontaneously quiescent CM disconnected from the ICC network suggested that circular muscle cells have ionic mechanisms for intrinsic oscillatory activity and are capable of actively participating in the conduction and generation of slow waves.

3.2 Introduction

Knowledge about the site of origin and propagation mechanisms of the slow wave type action potentials in gastrointestinal smooth muscle is crucial to our understanding of excitation-contraction-coupling mechanisms. Recent studies on canine colon have provided evidence that a network of Interstitial Cells of Cajal (ICC) and smooth muscle cells, located at the submucosal surface of the circular muscle layer, contains the cells from which slow waves are originated [4, 14, 71]. However, the role that colonic circular muscle cells play in the generation and conduction of slow waves is

unclear and controversial.

Circular muscle cells have been suggested to participate actively in the propagation of slow waves. In the cat colon, active propagation of slow waves from the submucosal side to the myenteric side of the circular muscle has been suggested [19, 22, 23, 24] based on the observation that the propagation velocity, 9.33±3.32 mm/s [19], is too slow for passive propagation. In the canine gastric antrum, slow waves observed in the circular muscle originate from multiple discrete foci located in the outer myenteric half of the circular muscle layer and have been shown to propagate regeneratively towards the submucosal border [10, 11, 12].

In the dog colon, data to determine whether the slow waves propagate passively or actively through the circular muscle layer is inadequate. Smith *et al.* [71] suggested that the circular muscle cells serve as a passive network allowing slow waves to propagate from the submucosal border to the myenteric border of the circular muscle layer: this conclusion was based on the observations that the slow wave amplitude *decays* exponentially as it propagates from the submucosal to the myenteric border, and that slow waves could not be induced in the circular muscle by acetylcholine after a thin strip of muscle along the submucosal border was removed. However, studying a circular muscle preparation without the attached longitudinal muscle, Barajas-López and Huizinga [2] reported that slow waves in the myenteric border of canine colon circular muscle layer had an average upstroke amplitude of 29.8 mV. With such a large slow wave upstroke amplitude present at the myenteric border (compared to 39.5 mV at the submucosal border), they concluded that such slow waves could not be transmitted passively through the circular muscle layer, whose thickness ranges from approximately 1 to 1.5 mm, as the space constant along the short axis of the circular muscle cells is only 0.43 mm [51]. In view of these contradictory conclusions,

further examination of the properties of circular muscle cells is warranted to clarify the possible roles that the circular muscle cells play in slow waves generation and conduction.

The objective of the present study was to investigate the excitability of the canine colonic circular muscle cells after disconnection from the ICC network.

3.3 Method

3.3.1 Tissue preparations

CM and ICC-CM preparations were studied using the suction electrode technique under different pharmacological conditions. Dimensions of strips of both preparations were cut at 3 mm in width and 10 mm in length. Sixty-six percent of the CM preparations were quiescent in Krebs solution and labelled as quiescent CM preparations in the text and abbreviated to QCM in figures. Approximately 34% of the CM preparations exhibited omnipresent slow wave like activity with similar frequency to that of the ICC- CM preparations in Krebs solution. These spontaneously active CM strips were discarded since they might suggest the presence of pacemaking activity. In each experiment, an ICC-CM strip was always present in the same bathing solution to provide the evidence that slow waves were present when ICC were in place and to serve as the control activity under different pharmacological situations.

3.3.2 Drugs and solutions

In carbachol experiments, an appropriate amount of 10 mM carbachol (Sigma Chemical Company, St. Louis, U.S.A.) stock solution was added directly to the organ bath containing Krebs solution. A similar procedure was performed for $BaCl_2$ experiments

using a 0.1 M $BaCl_2$ (Fisher Scientific Company, Fair Lawn, N.J., U.S.A.) stock solution. 30 mM TEA solution was made by replacing 30 mM of NaCl in the Krebs solution by an isomolar quantity of TEA-chloride (Kodak Co., Rochester, N.Y. U.S.A.). D600 experiments were prepared by adding the appropriate amount of 10 mM D600 stock solution to the premixed Krebs and drug solutions after induced activities in both ICC-CM and quiescent CM preparations remained steady for at least 3 min.

3.3.3 Result presentation and statistic analysis

All the data were expressed as MEAN±SEM. The analysis of the electrical activity consisted of the slow wave frequency, duration (measured at half maximum amplitude) and amplitude. To determine statistical significant differences of induced electrical activities in the ICC-CM and CM preparations under various pharmacological conditions, the total number of strips of either ICC-CM or CM preparations under different conditions was compared to the corresponding subset of the entire ICC-CM preparations in Krebs solution. Data on the induced electrical activities of ICC-CM and CM preparations were compared directly in different pharmacological bathing solutions. Either the t-test or the paired t-test, whichever appropriate, was performed to determine statistical significant differences of datum sets.

3.4 Results

3.4.1 Spontaneous activities of ICC-CM preparations

In the ICC-CM preparations, omnipresent slow wave activity was observed in all strips (n=22) with an average frequency, duration and plateau amplitude of 6.2±0.2 cpm, 3.6±0.2 s and 1.0±0.1 mV, respectively. Typical slow waves of ICC-CM preparations

are shown in figures 3.1a, 3.2a and 3.3a. Similar to the slow waves recorded by an intracellular recording technique, slow waves in the ICC-CM preparations possessed well-defined upstroke and plateau phases as reported previously [5, 49, 50]. Phasic contractions, at a frequency identical to the slow wave frequency, were observed spontaneously in all ICC-CM preparations.

3.4.2 Lack of spontaneous activity in CM preparations

66% of preparations (25 out of 38), from which the submucosal ICC network and directly associated circular muscle cells were removed (see method and Serio *et al.* [69]), were electrically quiescent. The lack of slow wave activity in CM preparations could be due to (a) the presence of high potassium (K^+) conductance: not only did we observe previously that slow wave activity disappears in the presence of the potassium channel activator, cromakalim [38], but also a relatively high K^+ conductance in circular muscle cells away from the pacemaker area has been reported to exist in the canine antrum [9]; (b) the absence of essential pacemaker cells. If the absence of slow waves is due to the absence of pacemaker cells, the question remains as to whether or not the circular muscle cells are intrinsically quiescent cells only capable of receiving information from pacemaker cells or inherently excitable requiring only an appropriate input or stimulus to initiate slow wave-like oscillations.

To test these hypotheses the effects of a cholinergic agonist (carbachol) and K^+ conductance blockers (TEA and $BaCl_2$) on the quiescent CM preparations were studied.

3.4.3 Induced activities in CM preparations

Effects of carbachol

In the ICC-CM preparations, 1 μM carbachol did not significantly change the slow wave frequency (from 6.2±0.5 cpm to 5.8±0.4 cpm; n=7) but induced a significant increase in the slow wave duration (from 3.4±0.3 s to 4.3±0.2 s) and plateau amplitude (from 1.1±0.2 mV to 1.8±0.3 mV). Figure 3.1b shows the carbachol induced activities in an ICC-CM preparation.

In quiescent CM preparations, slow wave-like activity as well as spiking activity with associated phasic contraction were induced by carbachol. Induced activity was observed in 7 out of 8 ($\approx$ 88%) preparations, 1 μM evoked slow wave-like activity in 5/7; 2/7 did not respond until 3 μM was used. Characteristics of the carbachol induced slow waves are graphically depicted in figures 3.4, 3.5 and 3.6. The shape of the electrical oscillations induced in quiescent CM preparation is shown in figure 3.1e. The carbachol induced oscillations in quiescent CM preparations had a similar frequency (5.9±0.4 cpm, n=7) to those in the ICC-CM preparations (5.8±0.4 cpm) in the presence of carbachol. The duration and amplitude of the induced oscillations in quiescent CM preparations were 2.8±0.5 s (n=7) and 0.8±0.2 mV (n=7), respectively, and were significantly smaller than those in the ICC-CM preparations. The carbachol-induced electrical activities were associated with the generation of phasic contractions occurring at the oscillations frequency.

Effects of TEA

The effects of 30 mM TEA on ICC-CM preparations are characterized graphically in figures 3.4, 3.5 and 3.6 and are qualitatively similar to the effects previously observed

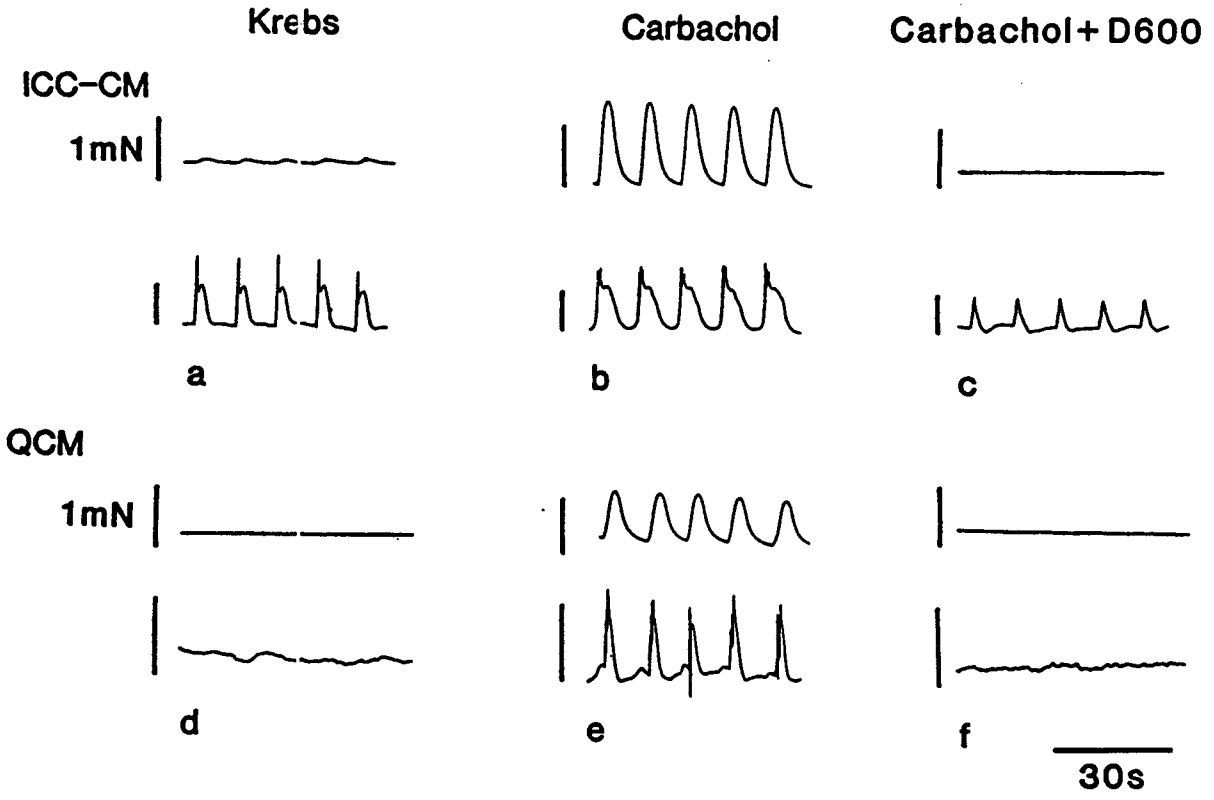

Figure 3.1: *Effect of carbachol on ICC-CM and quiescent CM preparations (QCM) and their sensitivity to D600.*

The top trace of each panel shows the mechanical activity; the bottom trace shows the electrical activity recorded by surface electrodes (the same holds for figures 3.2 and 3.3). Carbachol (1 μM) increased the slow wave duration and amplitude leading to increase in the force of phasic contraction of the ICC-CM preparations. 1 μM carbachol induced slow wave-like activity in the QCM strips with a similar frequency but smaller in duration and amplitude. The carbachol induced activities were abolished by 1 μM D600. All calibration bars next to the electrical recordings represent 1 mV. Force of mechanical contraction is measured in the unit of mN.

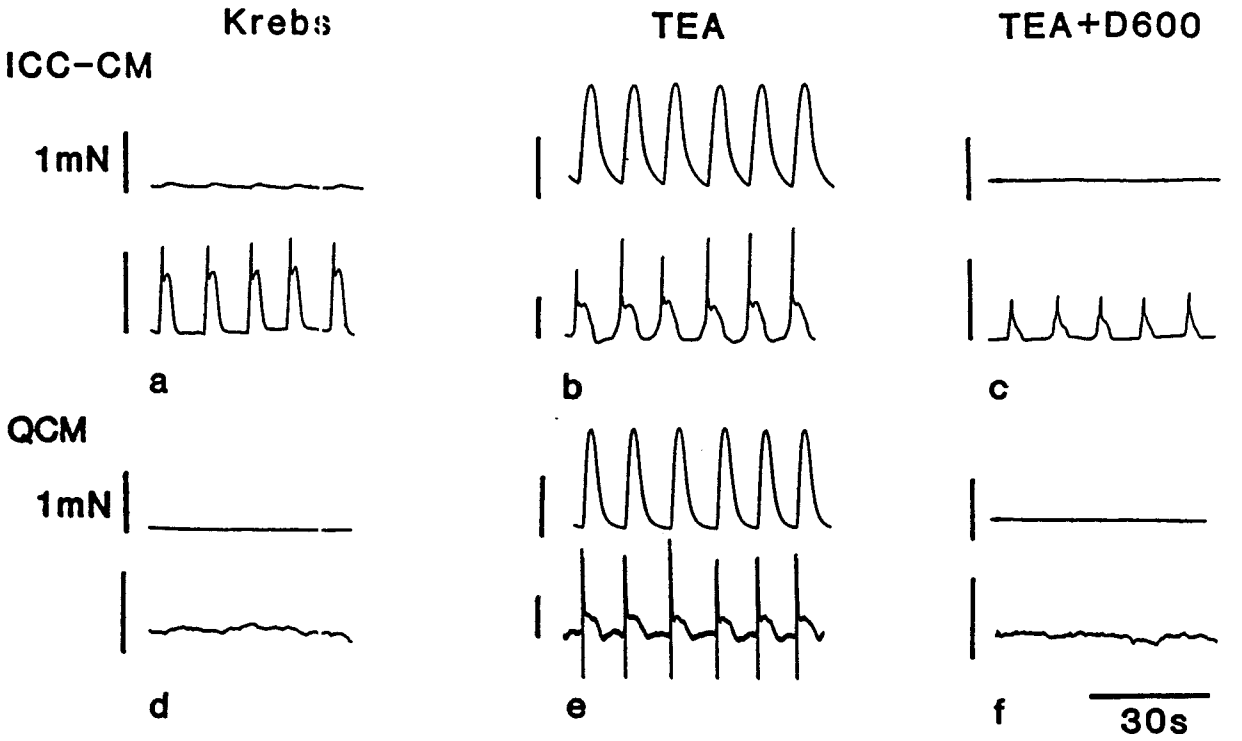

Figure 3.2: *Effects of TEA on ICC-CM and quiescent CM preparations and their sensitivity to D600.*

TEA (30 mM) significantly increased the slow wave duration and amplitude of the ICC-CM preparations (b) and the force and duration of the corresponding phasic contractions. 30 mM TEA induced slow wave-like activity in QCM. Note the similarity of the shape between the induced slow waves in the ICC-CM and QCM preparations. The TEA induced activities were abolished by 1μM D600. All calibration bars next to the electrical recordings represent 1 mV. Force of mechanical contraction is measured in the unit of mN.

with intracellular recording techniques [2]. The slow wave duration increased from 3.6±0.2 s to 5.5±0.6 s (n=7) and the amplitude from 1.1±0.3 mV to 1.6±0.3 mV (n=7), with no significant change in frequency. The force of contraction was drastically enhanced compared to that in Krebs solution. Figure 3.2b demonstrates the TEA induced electrical and mechanical activities in the ICC-CM preparations.

In the presence of 30 mM TEA, electrical activity was evoked in 78% (7/9) of spontaneously quiescent CM preparations (figures 3.2e, 3.4, 3.5 and 3.6). The induced oscillation frequency of CM preparations in the presence of TEA was not significantly different from that of the ICC-CM preparations. The duration and amplitude of the induced oscillations in the CM preparations were significantly smaller than those in the ICC-CM preparations and equal to 2.7±0.5 s and 1.1±0.1 mV (n=7), respectively. The mechanical activity in the presence of 30 mM TEA in the CM preparations changed from no recordable mechanical contraction to amplitudes similar to that recorded in the ICC-CM preparations.

Effects of barium chloride

0.5 mM $BaCl_2$ slightly increased the slow wave frequency (from 5.9±0.3 cpm to 6.6±0.3 cpm, n=8, $P < 0.05$) in the ICC-CM preparations, but decreased the slow wave duration (from 3.7±0.3 s to 2.8±0.1 s) and amplitude (from 0.8±0.2 mV to 0.6±0.1 mV, n=8). The decrease in slow wave amplitude might be due to the depolarization induced by $BaCl_2$ as a result of K^+ conductance blockade [57]. Figure 3.3b illustrates the $BaCl_2$ induced electrical and mechanical activities in the ICC-CM preparations.

$BaCl_2$ evoked activities in all spontaneously quiescent CM preparations (n=8) tested (with 0.5 mM in 6 out of 8 strips and 1 mM in the rest). The induced slow

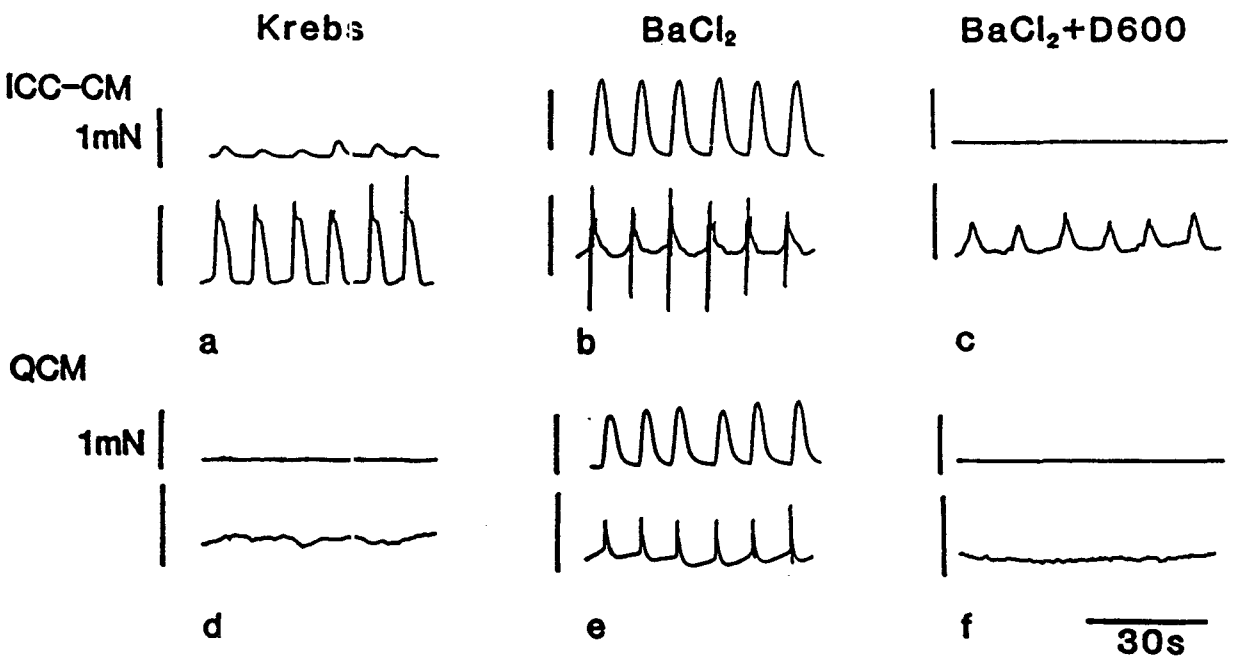

Figure 3.3: *Effects of $BaCl_2$ on ICC-CM and quiescent CM preparations and their sensitivity to D600.*

$BaCl_2$ (0.5 mM) induced electrical activity is dominated by spikes superimposed on the plateau phase of the slow waves in both ICC-CM preparations (b) and QCM preparations (e). The $BaCl_2$ induced activities were abolished by 1 μM D600. All calibration bars next to the electrical recordings represent 1 mV. Force of mechanical contraction is measured in the unit of mN.

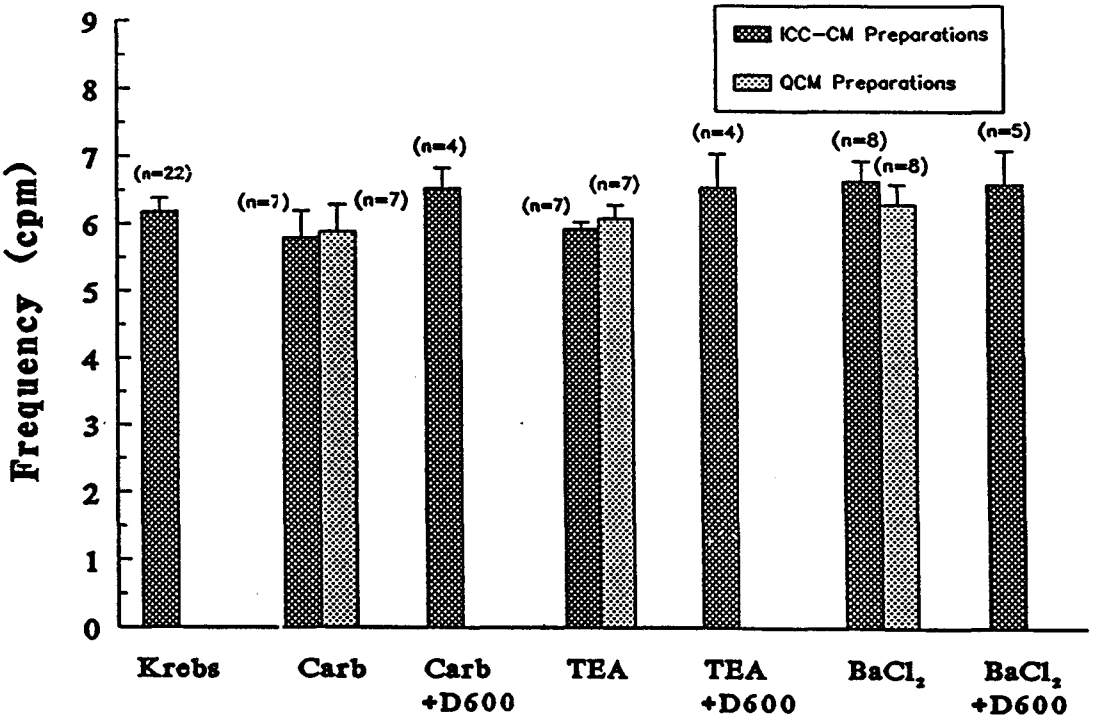

Figure 3.4: *Slow wave frequency of the ICC-CM and frequency of electrical oscillations in CM preparations in different pharmacological conditions.*

Frequency of slow waves in ICC-CM preparations under different pharmacological conditions was not different from that in Krebs solutions, except in the presence of $BaCl_2$ under which the slow wave frequency was slightly increased ($P < 0.05$). The oscillation frequencies of the ICC-CM preparations and the CM preparations were not statistically different under identical pharmacological condition.

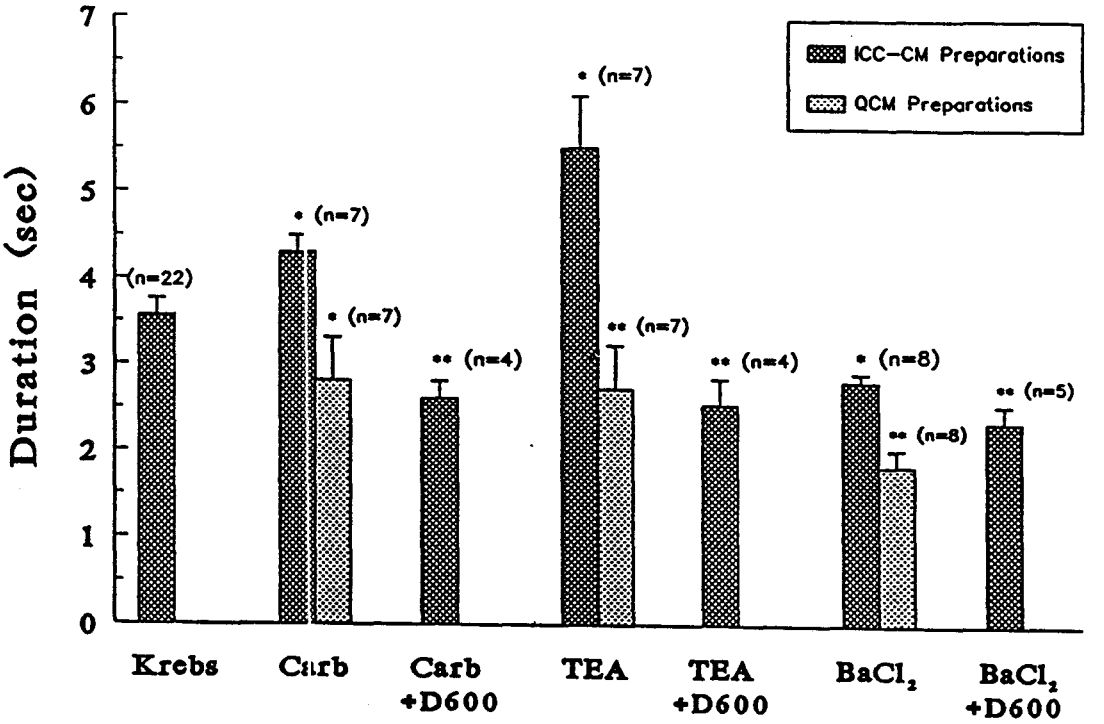

Figure 3.5: *Duration of slow waves in ICC-CM and oscillations in CM preparations under different pharmacological conditions.*

1 μM Carbachol and 30 mM TEA significantly increased but 0.5 mM $BaCl_2$ significantly decreased the slow wave duration in ICC-CM preparations. The duration of the induced oscillations in the spontaneously quiescent circular muscle (QCM) preparations was significantly smaller than that in the ICC-CM preparations under the same pharmacological condition. 1 μM D600 reduced the slow wave duration in ICC-CM preparations and abolished induced activity in CM preparations. The slow wave duration in ICC-CM preparations in the presence of D600 was significantly smaller than that in the Krebs solution.

* represents ($P < 0.05$); ** represents ($P < 0.01$)

wave-like activity is shown in figure 3.3e. Similar to actions of TEA and carbachol, the $BaCl_2$ induced electrical oscillations were similar in frequency (6.3±0.3 cpm; figure 3.4) but smaller in duration (1.8±0.2 s; figure 3.5) compared to those induced in the ICC-CM preparations. Although the average value of the induced oscillation amplitude of the CM preparations (0.5±0.1 mV; figure 3.6) was not statistically different from that of the ICC-CM preparations, the induced slow wave amplitude in the quiescent CM preparations was always smaller than that in the ICC-CM preparations in the same experiment. CM preparations recovered fully from the action of carbachol, TEA and $BaCl_2$ upon washout.

Effects of D600 on induced electrical activities

1 μM D600 abolished all electrical activity induced by carbachol (n=4), TEA (n=4), and $BaCl_2$ (n=5) in spontaneously quiescent CM preparations (see figure 3.1f, 3.2f and 3.3f, respectively) although electrical oscillations, less than 0.1 mV in amplitude, oscillating at irregular frequency still remained in two out of four strips in the presence of carbachol. The effects of 1 μM D600 on the induced electrical activities of the ICC-CM preparations are graphically demonstrated in figures 3.4, 3.5 and 3.6. Compared to the spontaneous slow waves of ICC-CM preparations in Krebs solution, the presence of 1 μM D600 did not significantly modify the frequency (from 6.3±0.2 cpm to 6.7±0.2 cpm, n=13) but significantly reduced the slow wave duration (from 3.5±0.2 s to 2.5±0.1 s, n=13) and amplitude (from 0.8±0.1 mV to 0.6±0.1 mV, n=13). D600 abolished phasic contractions in both the ICC-CM and CM preparations.

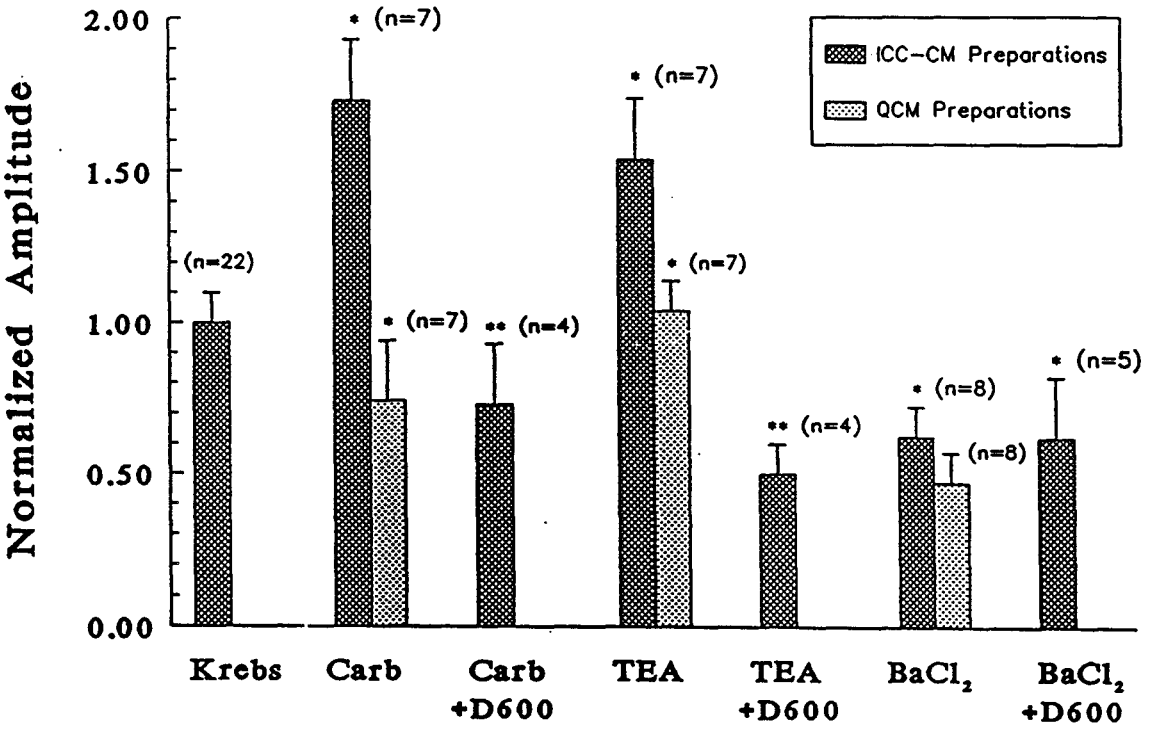

Figure 3.6: *Normalized slow wave amplitude in the ICC-CM and oscillation amplitude in CM preparations under different pharmacological conditions.*

The amplitude of the induced oscillations was normalized to the slow wave amplitude of the entire population of ICC-CM preparations in Krebs solution (n=22) so that the relative size of the oscillation amplitudes of various preparations under different pharmacological conditions could be compared directly. Both carbachol and TEA significantly increased but $BaCl_2$ significantly decreased the slow wave amplitude in ICC-CM preparations. Under the same pharmacological condition, the induced oscillation amplitude in CM preparations was significantly smaller (except for the case of $BaCl_2$ where no statistical significant difference was observed) than that in the ICC-CM preparations.

* represents ($P < 0.05$); ** represents ($P < 0.01$)

3.5 Discussion

3.5.1 Circular muscle cells in canine colon can generate slow wave-like activity in the absence of the submucosal ICC network

Preparations without the ICC network and without spontaneous electrical activities do, after inhibition of K^+ conductance by $BaCl_2$, TEA and cholinergic agonist (carbachol), generate oscillatory activity with characteristics similar to that of the slow waves generated in ICC-CM preparations. In particular, the oscillation frequency observed using different stimulating agents is not different from the slow waves frequency. In addition, the contractile activity generated is similar in CM and ICC-CM preparations. The presence studies indicate that the circular muscle cells are excitable and capable of actively participating in the generation of slow waves. The synchronization between the phasic contractions and the electrical activities indicate that the excitation-contraction-coupling in the circular muscle is not affected by the removal of the ICC network.

3.5.2 Slow wave-like activity induced in spontaneously quiescent CM preparations lacks a D600-insensitive component

The induced activity in CM preparations was completely abolished by blocking voltage dependent calcium channels. Consistently, in cat jejunum, Dahms *et al.* [27] showed that either 1 μM D600 or Krebs solution lacking calcium abolished the acetylcholine induced activity in quiescent preparations. In contrast, slow waves generated

at the submucosal surface of the ICC-CM preparations maintained a major portion of the upstroke potential in the presence of D600, as previously described [2, 5, 57]. The D600 insensitive component of the slow wave was recently characterized by Huizinga *et al.* [57]. This initial part of the upstroke potential is generated at least, in part, by a non-L-type calcium conductance, is insensitive to the organic calcium channel blockers, D600 and nitrendipine, but is sensitive to Ni^{2+} or Cd^{2+} or to reduction in extracellular calcium [56]. The data from the present study suggest that conductances, generating the D600 insensitive upstroke which are present in the ICC-CM preparations, are not present in the CM preparations. They may therefore be exclusive to the interstitial cells of Cajal.

3.5.3 Role of K^+ conductance in depressing excitability of circular muscle

Removal of the submucosal ICC network, caused 66% of the CM preparations to become electrically quiescent. Our data are consistent with the idea that both removal of the pacemaker area and the presence of high K^+ conductance in circular muscle contribute to the low level of excitation. Blockade of K^+ conductance by TEA and $BaCl_2$ induced oscillatory activity involving activity of L-type calcium channels in spontaneously quiescent CM preparations. Inhibition of slow wave activity by high K^+ conductance was recently demonstrated by Farraway and Huizinga [38]. The potassium channel activator, cromakalim, first abolished the plateau phase of the slow waves, then reduced the slow wave amplitude and eventually abolished the activity. A relatively high K^+ conductance of circular muscle cells away from the pacemaker sites has also been observed in the canine antrum by Bauer and Sanders [9]. The absence of spontaneous excitation occurs despite the fact that the CM cells under

discussion are at a more depolarized resting membrane potential than the ICC-CM preparation [69]; hence, the K^+ conductance involved in depression of the excitability is not the one responsible for governing the resting membrane potential; it is likely the voltage activated outward rectifier which, in intact tissue, is activated upon depolarization and an important determinant of the slow wave plateau amplitude. This is consistent with the observation in the canine antrum where the conductance of the outward rectifier (K^+ conductance) is higher in the submucosal circular muscle where a more depolarized resting membrane potential is found [10, 12, 9]. This high K^+ conductance is, in part, responsible for the smaller slow wave amplitude recorded in the submucosal border of the antral circular muscle [11] and myenteric border of the canine colon circular muscle [72, 2, 35] observed in ICC-CM preparations. In cardiac tissue, differences in electrical activity between sinus node cells and atrial cells has been proven to be due, in part, to differences in the composition of plasma membrane K^+ channels [41].

It is of particular interest that the induced oscillatory activity in the spontaneously quiescent CM preparations oscillates at a frequency very similar to that of the slow waves in the ICC-CM preparations. One can hypothesize two mechanisms of generation of the oscillations in circular muscle: (1) depolarization, resulting from decrease in K^+ conductance, brings circular muscle cells above the threshold for activation of voltage activated calcium channels. This brings in motion sequential activation of voltage activated channels leading to induction of regular slow wave-like activity. The oscillation frequency will be regulated by the kinetics of the membrane conductances. Consistent with this hypothesis is the fact that different pharmacological agents induce slow wave-like activity at similar frequency; or (2) the mechanism that gives the network of submucosal ICC and smooth muscle cells its auto-rhythmicity

(the intracellular metabolic clock, see Huizinga *et al.* [56]) may also operate in circular muscle cells. The validation of either hypothesis need further investigation.

Chapter 4

Properties of circular muscle of canine colon disconnected from pacemaker cells

4.1 Abstract

1. The electrical activity in canine colonic circular muscle is dominated by slow wave activity originating from a network of interstitial cells of Cajal (the pacemaker cells). In order to understand the contribution circular muscle cells make to the slow waves and to understand regulatory mechanisms intrinsic to circular muscle, preparations were developed where circular muscle cells were disconnected from the submucosal ICC network. These "CM preparations" were spontaneously quiescent with a resting membrane potential of -62.9 ± 0.6 mV.

2. CM preparations were found to have the capacity for generation of membrane potential oscillations. $BaCl_2$ (0.5 mM) depolarized the cells to $-51.\pm0.6$ mV

and induced electrical oscillations with frequency, duration, amplitude and rate of rise equal to 6.6±0.4 cpm, 2.2±0.2 s, 19.4±0.9 mV and 21.±1.7 mV/s, respectively.

3. Ba^{2+} induced oscillations were preceded by pre-potentials of 4.4±0.3 mV with a rate of rise equal to 1.1±0.1 mV/s (in contrast to slow waves which have a constant inter-slow-wave resting potential).

4. Ba^{2+} markedly decreased K^+ conductance which was responsible for oscillation generation and not depolarization per se since depolarization up to or above that induced by Ba^{2+} caused by either application of extracellular electric field or elevation of extracellular K^+ did not evoke electrical oscillations.

5. Ba^{2+} induced electrical activity was abolished by 1 μM D600 without change in resting membrane potential as well as by repolarizing the membrane potential by 6–12 mV, indicating the participation of voltage sensitive L-type Ca^{2+} channels in the generation of the oscillations (in contrast to slow waves that are not abolished by these procedures).

6. 0.1 μM Bay K 8644 further depolarized the Ba^{2+} excited circular muscle cells to −42.4±0.8 mV and greatly increased the oscillation frequency to 16.8±1.8 cpm.

7. 1 μM forskolin, previously shown to dramatically decrease the slow wave frequency without change in amplitude, did the opposite to the Ba^{2+} induced oscillations, suggesting that the metabolic clock, regulating the slow wave frequency, is not present in CM preparations.

8. The results provide strong evidence for an exclusive role for the network of interstitial cells of Cajal in colonic pacemaker activity. Circular muscle cells are

shown to be excitable and capable of generating oscillatory activity. Activity generation is dominated by L-type calcium channel activity which is regulated by K^+ conductance and is dependent on the membrane potential.

4.2 Introduction

The peristaltic movement of contents down the gastrointestinal tract depends on the phasic contractions of its muscle wall which in turn rely on electrical oscillations, in particular the slow wave type action potentials [27, 49]. Circular muscle and interstitial cells of Cajal play a role in the generation of this activity. Elucidation of the physiology of gastrointestinal motility requires understanding of excitation-contraction-coupling mechanisms in the different cell types; hence, understanding of the location of pacemaker sites and the ionic basis of the electrical oscillations generated in the pacemaker sites as well as in circular muscle cells, which are indeed responsible for producing the force of phasic contractions is essential.

Recent studies have revealed the pacemaker site in various segments of the gastrointestinal tract of different mammals. Slow waves are generated at the myenteric border of the circular muscle layer of the stomach of dog [11], and the small intestine of mouse [80], dog [47], cat [47, 77] and rabbit [47]. Whereas, slow waves are generated at the submucosal surface of the circular muscle layer of colon of pig [55], cat [19, 25], and dog [4, 71].

In canine colon, the ionic basis of the slow waves generated in the submucosal surface has recently been characterized [5, 49]. In addition, a recent study provided evidence that the frequency of slow waves in canine colon is governed by a metabolic clock possibly dependent on oscillations in intracellular cyclic AMP [56].

Canine colonic circular muscle disconnected from the pacemaker cells is most often electrically quiescent ([62, 71, 70], see also Chapter 3). Whether the circular muscle cells have the capacity to generate electrical activity is controversial. This tissue was reported to be insensitive to stimulation [71] whereas a recent study employing extracellular electrodes revealed the generation of oscillatory activity in the presence of TEA, $BaCl_2$ or carbachol at similar frequency to the slow wave activity observed in circular muscle preparations connected to pacemaker cells ([62] and Chapter 3). The fact that the induced activity was of similar frequency as the original slow wave activity raised the question whether or not the circular muscle could generate slow waves through a mechanism similar to that in pacemaker cells.

The electrical activity in canine colonic circular muscle is dominated by slow wave activity originating from a network of interstitial cells of cajal (the pacemaker cells). In order to understand the contribution circular muscle cells make to the slow waves and to understand regulatory mechanisms intrinsic to circular muscle, preparations were developed where circular muscle cells were disconnected from the submucosal ICC network. The objective of the present study was to fully characterize the electrical activities that can be generated by circular smooth muscle disconnected from pacemaker cells. Since such preparations are spontaneously quiescent, activity was induced by $BaCl_2$. Particular attention was given to the ionic basis of induced activity. Since slow wave type action potentials in intact tissue are governed by a metabolic clock in the submucosal ICC network, a central question was whether the oscillatory activity in smooth muscle cells disconnected from pacemaker cells is governed by a similar metabolic clock.

4.3 Method

4.3.1 Tissue Preparation

CM and ICC-CM preparations were examined using microelectrode technique in this study. Approximately 3x3 mm of the tissue, with the submucosal surface facing up, was pinned on the Sylgard bottom of a transfer holder. The tissue was then cut along the pinned edges, except one edge from which a strip of 10 mm long (3 mm wide at the pinned edge and gradually reduced to 1 mm at the free end) was cut along the longitudinal axis of the circular muscle. The end of the strip was tied to a thread (0.5 mm in diameter). The holder was transferred to a Abe-Tomita partitioned chamber [1] with the pinned section in the recording chamber and the free strip in the stimulating chamber. The free end of the strip was tied to a force transducer.

4.3.2 Drugs and solutions

All the solutions perfused into the partitioned chamber were prewarmed to 37±0.5 °C and oxygenated with 95% O_2 and 5% CO_2. The extracellular potassium concentration was increased from 6 mM to 10 and to 15 mM by adding KCl directly into the Krebs solution. $BaCl_2$ experiments were implemented by perfusing Krebs solution premixed with an appropriate amount of 0.1 M $BaCl_2$ (Fisher Scientific Company, Fair Lawn, N.J., U.S.A.) stock solution. Bay K 8644 and forskolin were dissolved in dimethyl sulfoxide (DMSO). DMSO in the concentrations applied did not have any effect.

Table 4.1: *Effects of Bay K 8644 on ICC-CM preparations*

	Krebs	Bay K 8644
Resting Membrane Potential (mV)	-71.1 ± 2.1	-73.5 ± 1.9
Frequency (cpm)	6.1±0.7	5.3±0.5
Duration (s)	2.6±0.2	4.2±0.4*
Upstroke Amplitude (mV)	44.5±4.0	45.3±3.8
Plateau Ampliude (mV)	37.8±3.7	38.0±3.6
Rate of Rise (mV/s)	304.1±59.2	371.5±64.3*

n = 21

* significantly different from that in Krebs solution ($P < 0.05$)

4.3.3 Result presentation and statistic analysis

All the data were expressed as MEAN ± SEM. Statistical significance between datum set were compared by paired t-test.

4.4 Results

4.4.1 Comparison of activities in spontaneously quiescent CM preparations and ICC-CM preparations

Spontaneous activity in ICC-CM preparations (circular muscle plus network of ICC) was identical to that described previously (table 4.1) [2, 3, 5]. Removal of the network of interstitial cells of Cajal and adjoining smooth muscle cells resulted in quiescent CM preparations, with resting membrane potentials ranging from −56 mV

to −66 mV.

4.4.2 Electrical oscillations induced by $BaCl_2$

$BaCl_2$ (0.5 mM) depolarized quiescent circular muscle cells by approximately 11 mV to −52 mV (range from −45 mV to −56 mV; n=18; table 4.2). This depolarization was accompanied by a 2.4 fold increase in input resistance (figure 4.1a). After a stable depolarization level was obtained, the membrane potential oscillated at an average frequency of 6.6±0.4 cpm (range 4.8–11.6 cpm). The amplitude, duration, and rate of rise of the oscillations are shown in table 4.2. Three different patterns of membrane potential oscillations were identified.

Oscillations with pre-potentials

The most dominant activity observed, in 13 out of 18 experiments, was the occurrence of regular membrane potential oscillations preceded by pre-potentials. This pattern of induced electrical oscillations is illustrated in figures 4.3b, 4.5, 4.6 and 4.9. Figures 4.3b, 4.5 and 4.6 show continuous recordings depicting the transition from the quiescent state to the excited state of three CM preparations. During the gradual depolarization phase, a few small amplitude oscillations were always observed preceding the appearance of regular oscillatory activity. When the resting membrane potential became steady (−52.3±0.6 mV), the membrane potential oscillated at a frequency, ranging from 4.8 cpm to 8.3 cpm, with an average of 6.0±0.2 cpm. The amplitude, duration and rate of rise of the induced oscillations were 20.5±1.0 mV, 2.4±0.3 s and 22.1±2.1 mV/s, respectively.

In contrast to the constant resting membrane potential observed in the inter-slow-wave-interval in ICC-CM preparations (see figures 4.2a, 4.3b and 4.8) the fast

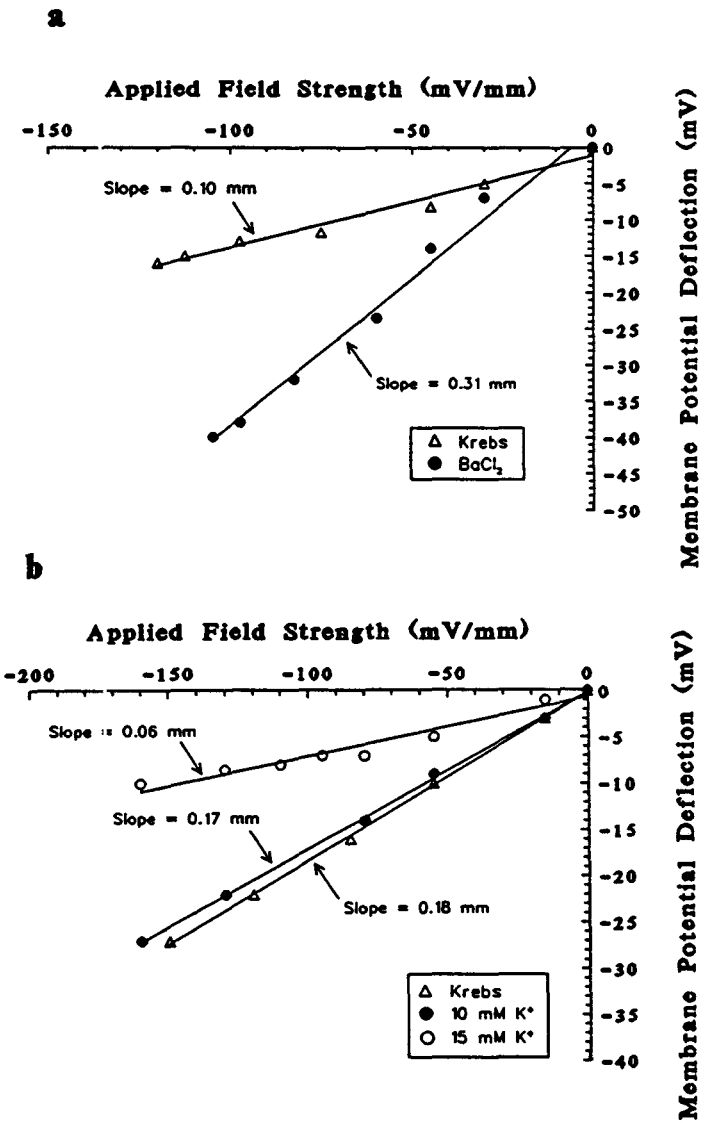

Figure 4.1: *Input resistance of CM preparations in Krebs solution, 0.5 mM $BaCl_2$ and high extracellular K^+ concentration.*

Both (a) and (b) are plots of the membrane potential deflection (mV) in response to a hyperpolarizing pulse versus the applied field strength (in mV/mm). (a) shows that the slope increases from 0.10 mm to 0.31 mm in response to 0.5 mM $BaCl_2$. (b) illustrates the effects of elevation of $[K^+]_o$ concentration. The slope slightly decreases from 0.1 mm to 0.17 mm in 10 mM K^+ indicating that the input resistance only changes slightly despite membrane depolarization. The slope (0.06 mm) is dramatically decreased by 15 mM $[K^+]_o$.

Table 4.2: *Effects of $BaCl_2$ and $BaCl_2$+ Bay K 8644 on spontaneous quiescent CM preparations.*

	n	Krebs	$BaCl_2$ (0.5 mM)	$BaCl_2$ + Bay K8644[1]
Resting Membrane Potential (mV)	18	-62.9 ± 0.6	-51.8 ± 0.6*	-42.4 ± 0.8**
Frequency (cpm)	18	—	6.6±0.4	16.8±1.8***
Duration (s)	18	—	2.2±0.2	1.0±0.1**
Upstroke Amplitude (mV)	18	—	19.4±0.9	17.4±1.7
Rate of Rise (mV/s)	18	—	21.8±1.7	50.5±8.3**
Slope (mm)	6	0.18±0.04	0.35±0.04**	—
r	6	0.96±0.16	0.98±0.01	—

Slope = change of membrane potential deflection with respect to applied field (representing the input resistance)

Significant differences are indicated by * = $P < 0.001$, ** = $P < 0.01$, *** = $P < 0.05$; $BaCl_2$ data are compared with data in Krebs solution; $BaCl_2$+ Bay K 8644 data (1: n = 7) are compared with $BaCl_2$ data.

upstroke phase of the $BaCl_2$ induced oscillations was preceded by a slow depolarization, termed pre-potential. The amplitude and rate of rise of the pre-potentials were 4.4±0.3 mV and 1.1±0.1 mV/s, respectively.

Oscillations preceded by bursting activities

In 3 out of the 18 preparations, 0.5 mM $BaCl_2$ induced transient bursting activity with variable duration before regular oscillations were achieved (figure 4.10). The oscillations were not different from that described in the previous section in terms of frequency, duration, amplitude and rate of rise. The time required to induce

oscillations in these strips was much longer than that in the strips described in the last section and the activity occurred at a more depolarized level (−50.3±0.3 mV, n=3). At this membrane potential the occurrence of pre-potentials was less obvious.

High frequency oscillations

In the remaining two preparations, 0.5 mM $BaCl_2$ induced oscillations at a faster frequency (10.3±1.4 cpm), occurring at a more depolarized resting membrane potential (−48.0±2.0 mV) (figure 4.4), compared to the preparations described in the last two sections. Associated with a higher frequency, a smaller duration (1.1±0.2 s) was observed. The amplitude and rate of rise of the induced oscillations were 17.5±1.5 mV and 27.0±5.0 mV/s, respectively.

High frequency oscillations were also observed when higher concentrations of $BaCl_2$ were necessary for evoking activity. This was observed in 5 preparations, different from the 18 described above, in which activity could not be induced by 0.5 mM $BaCl_2$. When the $BaCl_2$ concentration was increased to 1 mM, 4 of the 5 preparations established steady oscillations whereas steady oscillations were not achieved in the remaining one until 2.5 mM $BaCl_2$ was used. No positive correlation was found between the Ba^{2+} concentration and induced electrical oscillation parameters. The resting membrane potential, frequency, duration, amplitude and rate of rise of the electrical oscillations were −47.0±1.1 mV, 11.9±0.7 cpm, 1.2±0.2 s, 17.6±3.5 mV and 25.6±6.3 mV/s, respectively. Also in these preparations, the pre-potential was less obvious when high frequency oscillations occurred at more depolarized membrane potentials.

When studying the Ba^{2+} induced activity, it was observed that (a) the resting membrane potential depolarized before electrical oscillations were evoked; (b) the

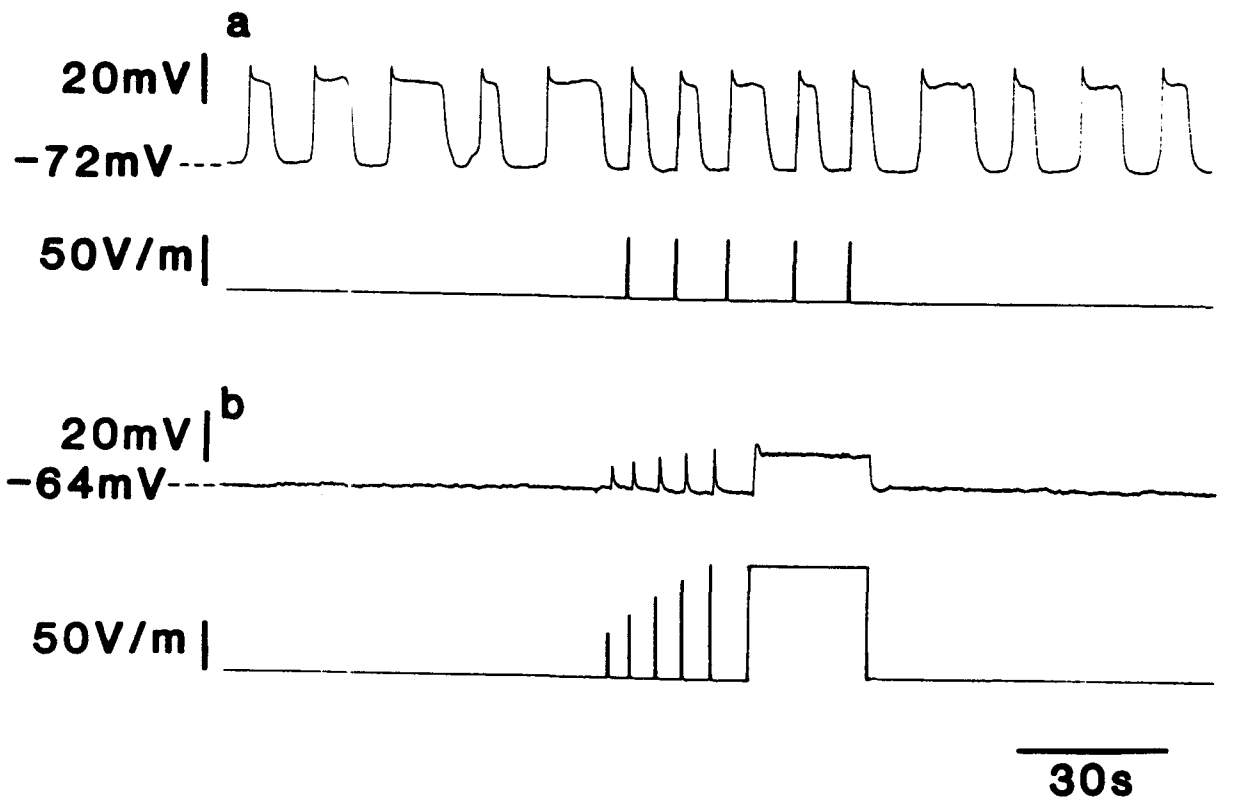

Figure 4.2: *Different effects of depolarizing pulses on ICC-CM and quiescent CM preparations.*

(a) Premature slow waves were evoked in ICC-CM preparations by brief depolarization pulses. (b) In contrast, depolarization pulses, double the intensity of those applied to the ICC-CM preparations, could not induced oscillations in quiescent CM preparations. A long lasting pulse (25 s), reaching −48 mV did also not evoke oscillations.

frequency of the Ba^{2+} induced electrical oscillations was related to the resting membrane potential (compare 6.6±0.4 cpm and −51.±0.6 mV in 0.5 mM Ba^{2+} (n=18) to 11.9±0.7 cpm and −47.0±1.1 mV in higher Ba^{2+} concentrations (1 mM and 2.5 mM, n=5)). Therefore, it was important to examine the effects of changes in membrane potential on the spontaneously quiescent CM preparations.

4.4.3 Excitability of spontaneously quiescent CM preparations

Field depolarization

An electric field was applied to the muscle through Ag-AgCl plates in the stimulating chamber. Voltage pulses of 0.5 s in duration and of varying amplitude (50 V/m to 150 V/m) were applied. Electrical oscillations were not induced in any of the preparations (n=18) although the resting membrane potential reached as low as −48 mV (see figure 4.2b). Pulses of 0.5 s in duration and of 50–70 V/m in amplitude always induced premature slow waves in the ICC-CM preparations (n=4). Figure 4.2 compares the different effects of field induced depolarization in the ICC-CM and CM preparations.

Elevation of the extracellular potassium concentration, $[K^+]_o$

The resting membrane potential of the CM preparations (n=4) decreased from −63.8±0.3 mV to −58.8±1.0 mV ($P < 0.05$) in 10 mM $[K^+]_o$ and to −47.8±1.4 mV ($P < 0.01$) in 15 mM $[K^+]_o$ without inducing any membrane potential oscillation. The depolarization by 10 mM $[K^+]_o$ was not associated with a change in input resistance. Slope of I/V curve was 0.20±0.05 mm ($r = 0.99 \pm 0.01$) in Krebs solution and

0.19±0.06 mm (r = 0.98±0.01) in 10 mM $[K^+]_o$. The input resistance in 15 mM $[K^+]_o$ (0.11±0.04 mm, r = 0.96±0.02, $P < 0.01$) was only 48% of that in Krebs solution (figure 4.1).

4.4.4 Voltage sensitivity of the Ba^{2+} induced electrical oscillations

The upstroke potential of the slow waves in ICC-CM preparations was found to be insensitive to changes in membrane potential (figure 4.3b and [56]), insensitive to L-type calcium channel blockers but sensitive to Ni^{2+} and Co^{2+} [57]. This led to the conclusion that the initiating conductance of the slow waves is a non-L-type calcium conductance. To investigate if $BaCl_2$ would activate a similar conductance to evoke the oscillations, the sensitivity of the $BaCl_2$ induced oscillations to voltage changes and L-type calcium channel blockers was investigated.

Field induced voltage changes

The electrical oscillations induced by Ba^{2+} in the CM preparations were extremely sensitive to hyperpolarization. Figure 4.3 compares the sensitivity of slow waves in ICC-CM to that of the oscillations in CM preparations to hyperpolarization. In the ICC-CM preparations (figure 4.3a), slow waves still remained when the resting membrane potential was hyperpolarized to about −90 mV. Consistent with previous reports [57, 38], during hyperpolarization the slow wave duration decreased but the amplitude increased, and the frequency remained unchanged. In contrast, the electrical oscillations induced in the CM preparations were abolished by as little as 6–12 mV (n=18) repolarization of the resting membrane potential.

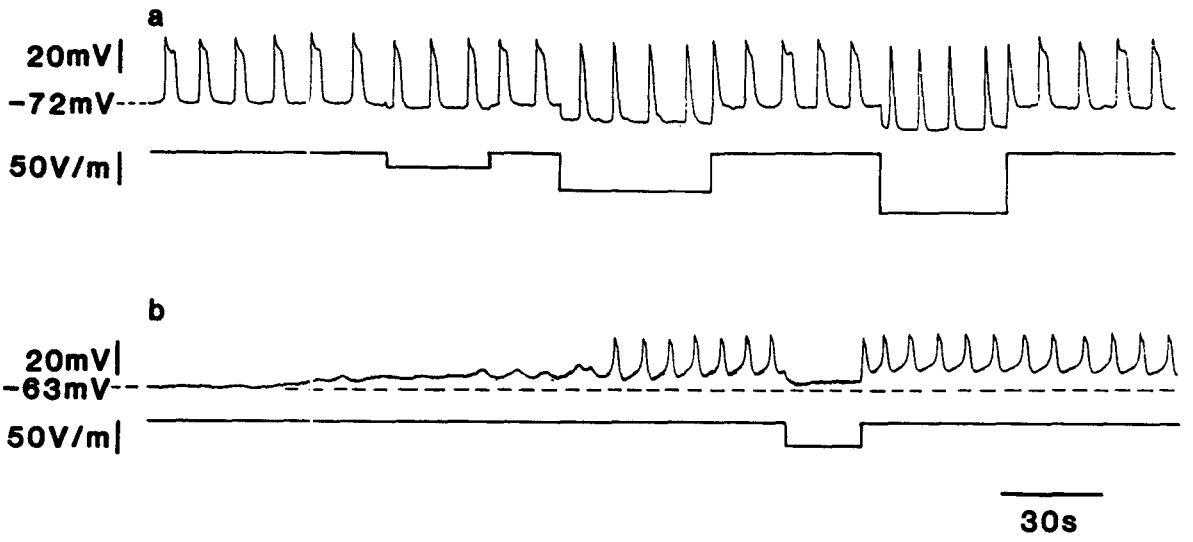

Figure 4.3: *Voltage sensitivity of $BaCl_2$ induced oscillations in CM preparations and spontaneous slow waves in ICC-CM preparations.*

(a) The frequency of the slow waves in the ICC-CM preparations was not sensitive to hyperpolarization. Hyperpolarization decreased the slow waves duration but increased the slow wave amplitude and left the frequency unchanged.

(b) 0.5 mM $BaCl_2$ induced oscillations were abolished by field induced hyperpolarization of 6 mV.

Table 4.3: *Effects of increasing extracellular K^+ on $BaCl_2$ induced oscillatory activity in CM preparations.*

	Krebs	$BaCl_2$	$BaCl_2$ + 10 mM $[K^+]_o$	$BaCl_2$ + 15 mM $[K^+]_o$
Resting Membrane Potential (mV)	−62.3 ± 2.1	−49.0 ± 1.1	−49.0 ± 1.1	−49.3 ± 1.1
Frequency (cpm)	—	7.4±1.4	6.6±1.0	5.3±1.4[a]
Duration (s)	—	2.6±0.7	2.4±0.8	2.2±0.7
Upstroke Amplitude (mV)	—	14.8±2.9	13.3±2.8**	6.3±2.6*
Rate of Rise (mV/s)	—	16.6±2.9	13.4±1.7	7.7±2.7**
Slope (mm)	0.16±0.05	0.28±0.05	0.25±0.05**	0.21±0.04**
r	0.97±0.01	0.98±0.01	0.96±0.01	0.98±0.01

n=4; [a] within bursts

Slope = change of membrane potential deflection with respect to applied field (representing the input resistance)

Significant differences are indicated by * = $P < 0.01$, ** = $P < 0.05$; data in elevated $[K^+]_o$ are compared with $BaCl_2$ data.

Effects of elevation of $[K^+]_o$

The pattern of the Ba^{2+} induced oscillations was sensitive to the elevation of $[K^+]_o$ (figure 4.4). The experimented group (n=4) covered almost the entire frequency spectrum of the Ba^{2+} induced oscillations (ranging from 5.6 cpm to 11.6 cpm with an average frequency of 7.4±1.4 cpm, table 4.3). After increasing the $[K^+]_o$ to 10 mM, the oscillation frequency reduced from 7.4 cpm to 6.6 cpm, while the amplitude also decreased slightly but significantly (table 4.3). These changes occurred without a change in resting membrane potential, but were accompanied by a reduction in input resistance (table 4.3). In 15 mM $[K^+]_o$, the Ba^{2+} induced oscillations were abolished in one of the strips. The rest of the four strips exhibited bursting activity having

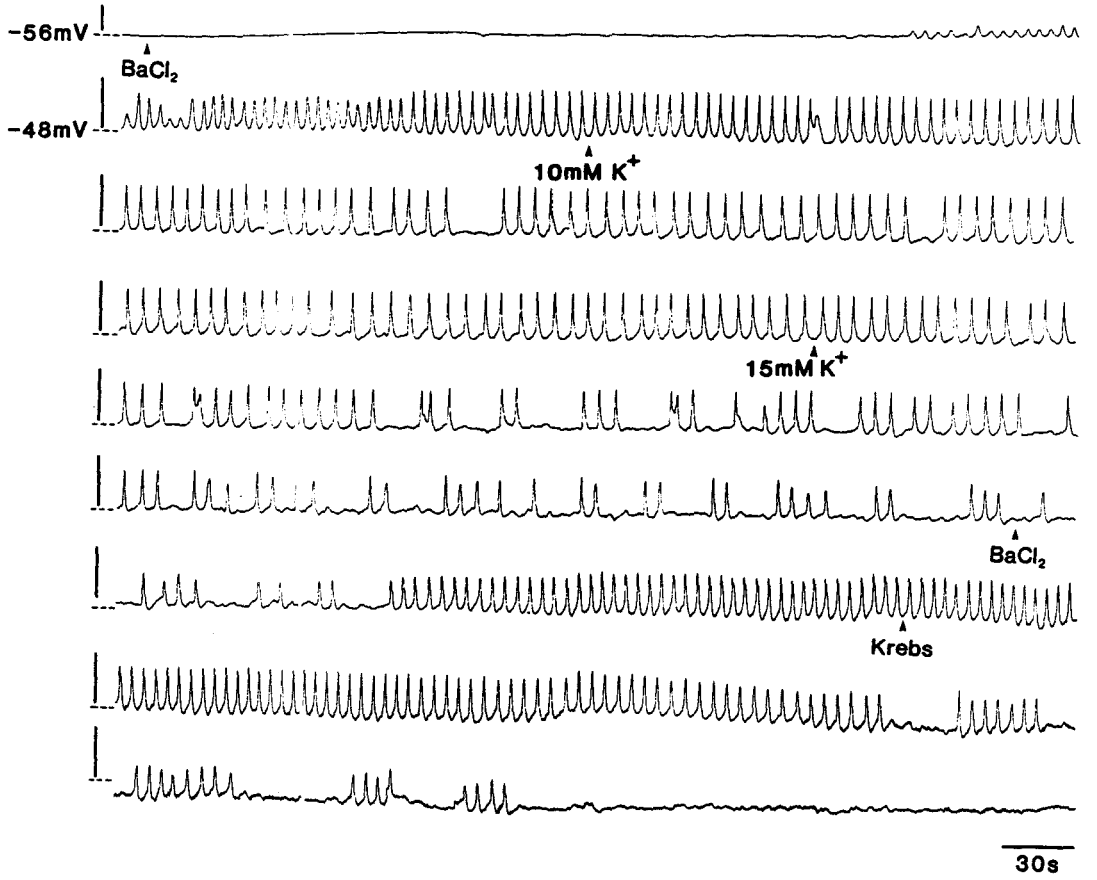

Figure 4.4: *High frequency oscillations induced by $BaCl_2$ and their sensitivity to elevation of extracellular K^+ concentration*

High frequency oscillations (11.6 cpm) were induced by 0.5 mM $BaCl_2$ (added at the arrow in the first panel) in a CM preparation whose resting membrane potential was the most depolarized among all the preparations (n=18) examined. 10 mM $[K^+]_o$ (arrow in the second panel) decreased the slow wave frequency and introduced short quiescent periods in between. 15 mM $[K^+]_o$ (arrow in the fourth panel) further reduced the level of excitation leading to bursting activity of variable duration. Reperfusion of 0.5 mM $BaCl_2$ (arrow in the sixth panel) caused recommencing of the high frequency oscillations. Washing the preparation by Krebs (arrow in the seventh panel) produced bursting activity and eventually abolished all the membrane potential oscillations. The above traces display a continuous recording from a single cell throughout the entire experiment. Dotted lines indicate the membrane potential of −48 mV in all panels except in the first panel (−56 mV).

durations ranging from 5–30 s with bursting frequency between 0.5–2.0 bursts/min. The frequency, amplitude and rate of rise of oscillations within the burst were decreased (table 4.3). The resting membrane potential remained unchanged; but, the input resistance was decreased to 77% of that in 0.5 mM $BaCl_2$. In addition, bursting activity was also observed prior to complete abolishment of induced activity when the strip was washed by Krebs. Therefore, the appearance of bursting activity with decreasing oscillation frequency within the burst indicated a lower level of excitation compared to that during continuous high frequency oscillations.

4.4.5 Participation of L-type calcium channels in the generation of Ba^{2+} induced oscillations

The $BaCl_2$ induced electrical oscillations were abolished by 1 μM D600 without causing a change in the resting membrane potential (n=5; figure 4.5).

0.1 μM Bay K 8644 produced no effect on the membrane potential of the quiescent CM preparations (n=3) but dramatically modified the Ba^{2+} induced oscillations (n=4; figure 4.6). Moreover, 0.1 μM Bay K 8644 evoked membrane potential oscillations in three CM preparations in which 0.5 mM $BaCl_2$ only induced irregular small amplitude oscillations of less than 4 mV.

Bay K 8644, in the presence of $BaCl_2$ first decreased the resting membrane potential accompanied by an increase in frequency and decrease in amplitude and duration of Ba^{2+} induced oscillations (see figure 4.6a). A similar depolarization was observed in the three preparations in which only irregular small amplitude electrical oscillations were observed. When the resting membrane potential reached -42.4 ± 0.8 mV, the frequency of the electrical oscillations became 16.8 ± 1.8 cpm, ranging from 12 cpm to 24 cpm (n=7). The rate of rise increased significantly (table 4.2). In

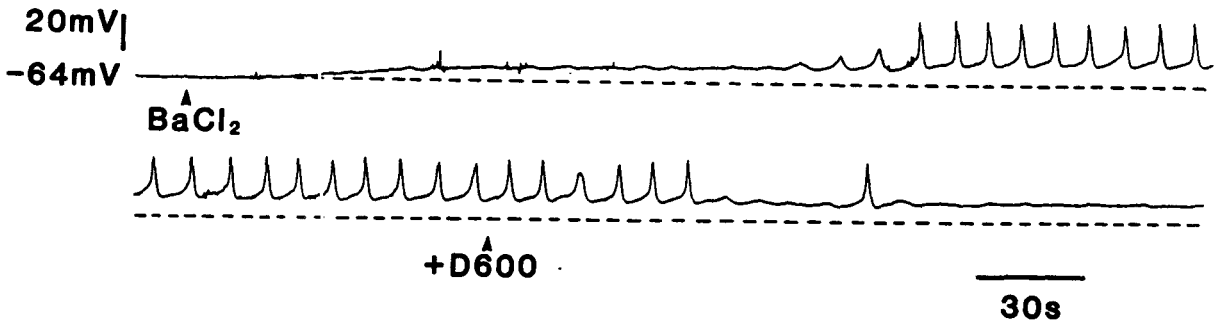

Figure 4.5: *Effect of L-type calcium channel blockade on $BaCl_2$ induced oscillations* $BaCl_2$ (0.5 mM) induced oscillations were abolished by 1 μM D600. D600 did not change the resting membrane potential. The top and the bottom traces are part of a continuous recording from a single cell.

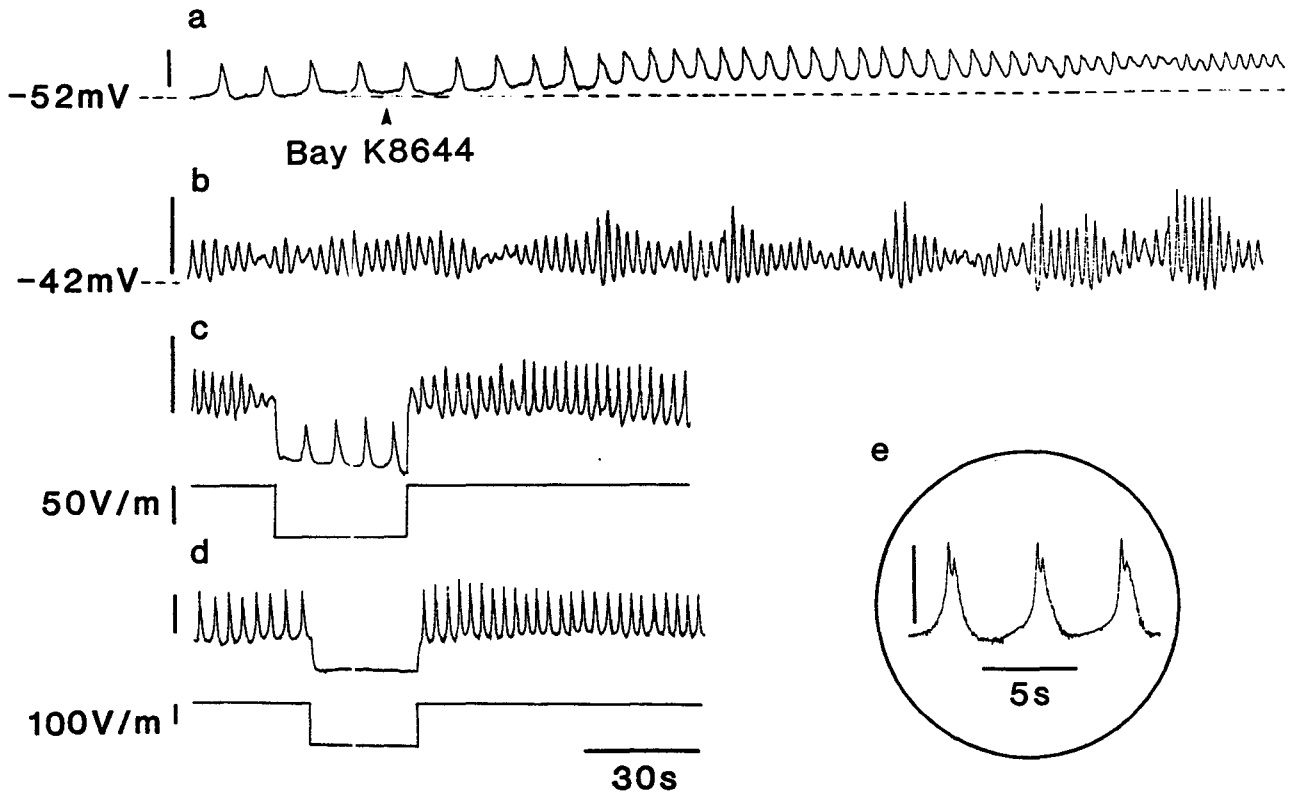

Figure 4.6: *Effects of Bay K 8644 on the Ba^{2+} induced oscillations*

(a) 0.1 μM Bay K 8644 (added at arrow) dramatically increased the frequency of the Ba^{2+} induced activity which was accompanied by depolarization and a decrease in oscillation duration. (b) Periodical changes in oscillation amplitude were observed prior to the occurrence of steady amplitude oscillations. (c) When the membrane was hyperpolarized to a value approximately the same as that in $BaCl_2$, oscillations with similar frequency to that in $BaCl_2$ were observed. (d) An additional 8 mV hyperpolarization completely abolished the oscillations. A second spike could be distinguished after the upstroke phase (e). All calibration bars for electrical oscillations represent 20 mV.

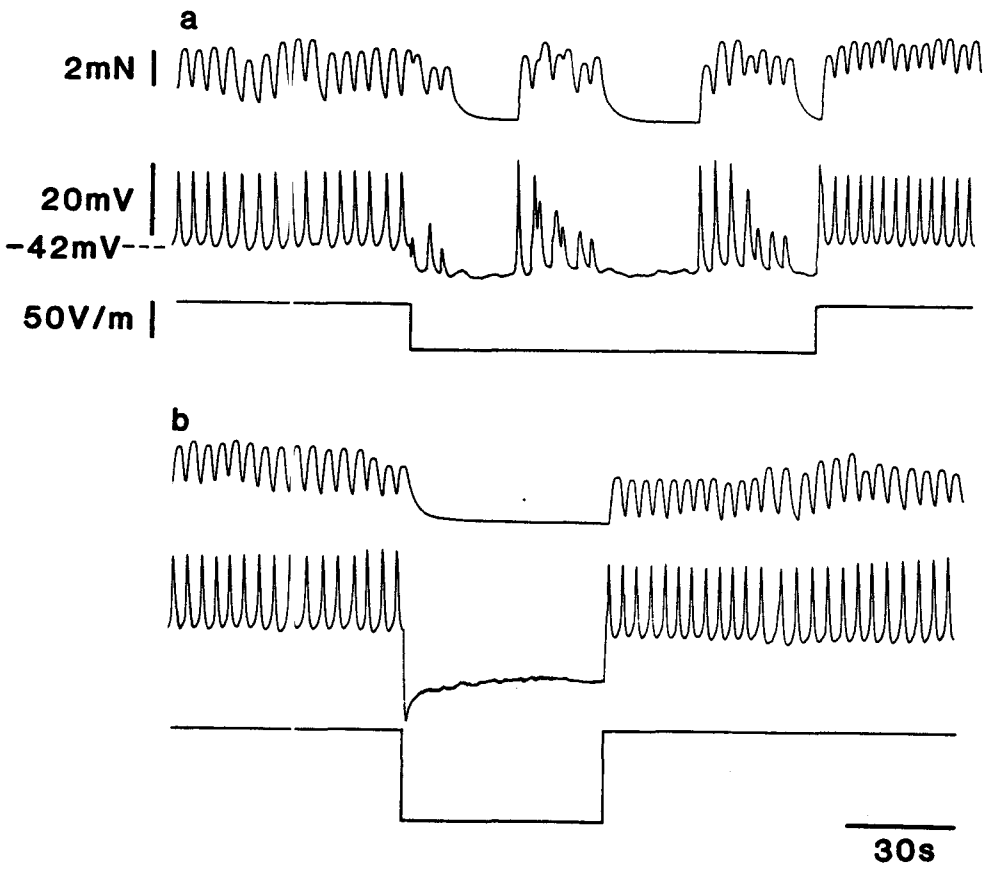

Figure 4.7: *Appearance of bursting activity during hyperpolarization*

Regular high frequency oscillations induced in Ba^{2+} and Bay K 8644 changed to a burst type pattern oscillation during hyperpolarization (trace a). The oscillations were completely abolished when an additional 12 mV hyperpolarization was induced (b). Mechanical (top panel) and electrical (middle panel) activities, as well as the field strength (bottom panel) in the stimulating chamber, are shown. Calibration bars in (a) are also applicable to (b).

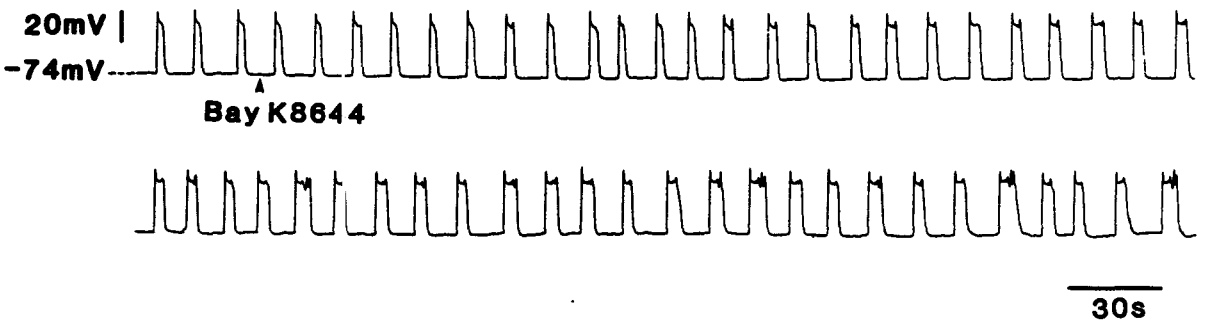

Figure 4.8: *Effects of Bay K 8644 on the spontaneous slow waves in ICC-CM preparations.*

Bay K 8644 (0.1 μM) increased the duration and induced spikes on the plateau phase of slow waves recorded at the submucosal surface of ICC-CM preparations.

4 preparations, when cells were hyperpolarized to a level similar to that in 0.5 mM $BaCl_2$, the oscillation frequency decreased and the pattern of the electrical oscillations resumed to that similar in 0.5 mM $BaCl_2$ (figure 4.6c). All electrical oscillations were inhibited by 12–16 mV hyperpolarization (see figure 4.6d). In 2 preparations, bursting activity with durations ranging from 20 s to 40 s were observed during 6–8 mV hyperpolarization. Figure 4.7 illustrates the appearance of bursting activity in the presence of 0.1 μM Bay K 8644 in Ba^{2+} induced activity during hyperpolarization.

For comparative purposes, the effects of Bay K 8644 on ICC-CM preparations were studied. In contrast to the dramatic modification of the Ba^{2+} induced oscillations by Bay K 8644, 0.1 μM Bay K 8644 only increased the duration (from 2.6±0.2 s to 4.2±0.4 s, n=4) and rate of rise (from 304.1±59.2 mV/s to 371.5±64.3 mV/s) of the ICC-CM slow waves (table 4.1). In addition, spikes were observed superimposed on the plateau phase of slow waves in the presence of Bay K 8644. Figure 4.8 shows a continuous recording from a single cell of an ICC-CM preparation illustrating the effects of 0.1 μM Bay K 8644 on the slow wave activity.

4.4.6 Effects of forskolin on $BaCl_2$ induced electrical oscillations

Since forskolin had a dramatic effect on the frequency of the slow wave type action potential in ICC-CM preparations revealing characteristics of a metabolic clock [56], it was of interest to study its effects on the induced activity in CM preparations. The effects of 1 μM forskolin on the Ba^{2+} induced activity could be separated into two categories: (1) complete abolishment of Ba^{2+} induced activity after a gradual decrease in amplitude without an effect on the frequency (4 out of 6); and (2) appearance of bursting activity (2 out of 6). In either situation, cells slightly repolarized to

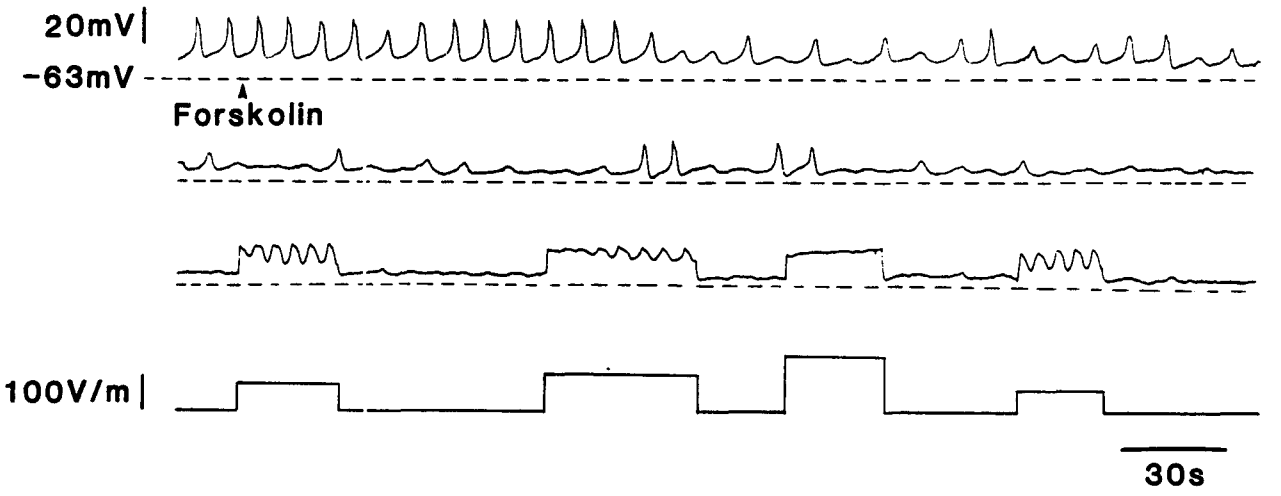

Figure 4.9: *Effects of forskolin on $BaCl_2$ induced oscillations*

1 μM forskolin slightly repolarized the cells, decreased the oscillation amplitude without significant change of the frequency. The beginning of recording shows $BaCl_2$ induced activity in quiescent CM preparations. When the oscillations were abolished (observed in 4 of the 6 tested preparations), oscillations could be re-evoked again by long lasting depolarization pulses unless the peak potential of the induced oscillations was surpassed. The above experiment shows a continuous recording from the same cell. The fourth pulse showed that the inability of producing membrane potential oscillations during the third pulse was not due to extensive damage to the tissue by intensive electrical stimulations.

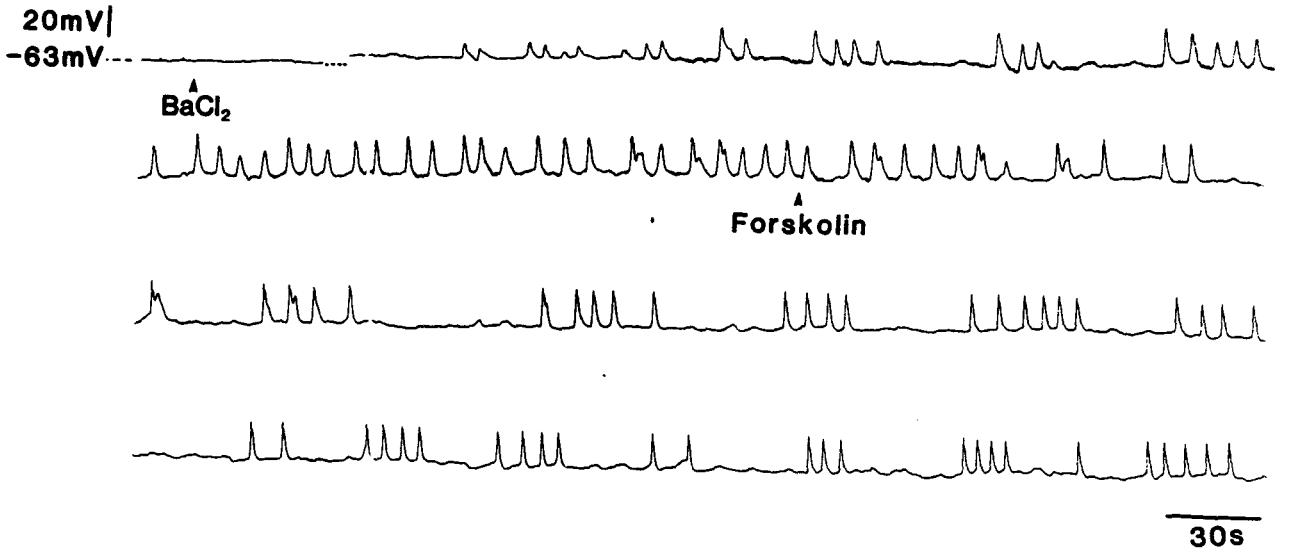

Figure 4.10: *Forskolin transforms regular activity induced in quiescent CM preparations by $BaCl_2$ into bursting activity.*

1 μM forskolin transformed regular oscillatory activity induced by 0.5 mM $BaCl_2$ into bursting activity of variable burst duration but regular oscillation frequency within the burst. 8 min of recording is omitted between the first and the second part in the first panel. There is a gap of 5 min between the end of the third panel and the beginning of the fourth panel.

-56.7 ± 1.1 mV (n=6, $P < 0.01$) as compared to that in the 0.5 mM $BaCl_2$ solution. Figure 4.9 shows the first situation and illustrated that oscillations can be re-evoked during long lasting depolarization pulses. In the latter case, bursting activity was irregular with durations of burst ranging from 10–30s. Figure 4.10 illustrates the conversion of regular Ba^{2+} induced activity into bursting activity in the presence 1 μM forskolin.

4.5 Discussion

The present study shows that the circular muscle of canine colon, which becomes electrically quiescent after removal of the submucosal network of interstitial cells of Cajal and the adjoining smooth muscle cells, responded to $BaCl_2$ by generating oscillatory activity accompanied by contractile activity. This proves that the circular muscle cells are excitable, unlike otherwise proposed [65, 70, 71]), and have intrinsic mechanisms to produce oscillatory activity.

4.5.1 Role of membrane potential and K^+ conductance in generation of Ba^{2+} induced oscillations

The electrical activity generated by $BaCl_2$ in the smooth muscle cells is evoked as a consequence of inhibition of K^+ conductance. $BaCl_2$ inhibits K^+ conductance [13, 74, 76] reflected in this study by a decrease in input resistance. Although the $BaCl_2$ induced activity is accompanied by depolarization, it is not the depolarization per se that induces activity since depolarization alone, by field depolarization via extracellular electrodes or by elevation of $[K^+]_o$, did not evoke oscillatory activity. Consistent with the hypothesis that decrease in K^+ conductance is responsible for

the appearance of oscillatory activity is the fact that oscillations can also be evoked by TEA ([62], and Chapter 3). The situation may be similar to that observed in chick heart cells where decrease in K^+ conductance can turn a quiescent non-pacemaker cell into a cell which generates electrical activity very similar to that in the spontaneous active pacemaker cells by a mechanism independent of depolarization [74].

The $BaCl_2$ induced oscillations were preceded by a slow depolarization amounting to approximately 4.5 mV, except when the tissue was depolarized above −50 mV. The appearance of pre-potentials was also observed with acetylcholine induced oscillations in the cat small intestine after spontaneous slow waves were abolished by ouabain [27]. Interestingly, in CM preparations, electric field induced depolarization pulses of the same or higher magnitude than the depolarization caused by $BaCl_2$, did not evoke oscillations. Similar depolarization pulses applied approximately four seconds after the repolarization phase of slow waves in ICC-CM preparations always evoked premature slow waves. The inability of current induced depolarization to induce slow waves does not necessarily indicate a voltage insensitivity of the conductances involved in the generation of the oscillations: it may indicate the presence of a high potassium conductance. Hara *et al.* [46] reported that depolarization caused by increasing $[K^+]_o$ in the quiescent isolated outer circular muscle of dog jejunum to the same membrane potential as caused by acetylcholine could not induce slow waves; but acetylcholine did. Thus, consistent with other studies, a high potassium conductance may be responsible for the low level of excitability in CM preparations [38]. Consistent with this hypothesis is our observation that Bay K 8644 did not evoke any activity in CM preparation except during K^+ conductance blockade by Ba^{2+}.

Our results indicate that K^+ conductance of the CM preparations is increased by elevation of $[K^+]_o$ since the input resistance decreases markedly. The frequency of

Ba^{2+} induced oscillations was reduced in 10 mM $[K^+]_o$ and transformed into bursting activity (or even abolished) in 15 mM $[K^+]_o$. It suggests that the level of excitation in CM preparations was decreased probably due to an increase in K^+ conductance. Sperelakis and Lehmkuhl [74] reported a decrease in membrane resistance of cultured chick heart cells and hyperpolarization instead of depolarization when $[K^+]_o$ was increased from 2.7 mM to 10 mM. Consistently, elevation of $[K^+]_o$ has been shown to increase the permeability of K^+ channels and shift positively their voltage-dependence [44, 48].

The oscillations evoked by the presence of $BaCl_2$ have, strikingly, a frequency similar to that of the slow wave type action potentials generated by the ICC-CM preparations. To investigate the similarities and/or differences between their mechanisms of generation, the role of L-type calcium channels and the voltage sensitivity was investigated.

4.5.2 Role of L-type calcium channels in generation of Ba^{2+} induced oscillations

$BaCl_2$ induced activity in CM preparations was abolished by L-type calcium channel blockers and also by hyperpolarization. This suggests that the $BaCl_2$ induced activity is generated through voltage activation of L-type calcium channels. The upstroke phase of the slow waves in the ICC-CM preparations has a component insensitive to L-type calcium channel blockers and hyperpolarization [2, 3, 5, 57]. From the present study, there is no evidence that the CM preparations can generate this component. The present study therefore suggests that the mechanism of generation of the slow waves and the $BaCl_2$ induced oscillations are different. It also suggests that the D600 insensitive component present in the ICC-CM preparations may originate exclusively

from the ICC network that is absent in the CM preparations.

The actions of Bay K 8644 (a L-type Ca^{2+} channel agonist [31]) substantiated the differences between the mechanism of generation of slow waves and $BaCl_2$ induced oscillations and confirmed the involvement of L-type calcium channels in the generation of the $BaCl_2$ induced activity. Bay K 8644 increased the duration of the slow wave plateau and induced spiking activity; both are known to be generated by L-type Ca^{2+} channels. Bay K 8644 did not affect the slow wave frequency known to be regulated by a non-L-type calcium conductance [57]. In contrast, Bay K 8644 markedly increased the frequency and decreased the duration of the $BaCl_2$ induced oscillations. These effects are compatible with a patch study in which Bay K 8644 was shown not only to enhance the magnitude of Ca^{2+} inward current but also to increase the rate of inactivation of the current in canine colon myocytes [61].

4.5.3 Intrinsic differences in membrane properties of circular and longitudinal muscle cells

In the presence of Bay K 8644 and after K^+ conductance blockade, the CM preparations generate high frequency oscillations with characteristics very similar to that in the spontaneous electrical oscillations generated by colonic longitudinal muscle [20]. Figure 4.11 compares electrical oscillations recorded in the circular muscle (adjacent to the submucosal surface) in the presence and absence of the submucosal ICC network to the spike like action potentials recorded in the longitudinal muscle. The high frequency oscillations in the circular muscle (a) are sensitive to L-type calcium channels blockers, (b) are voltage sensitive, (c) are variable in frequency, and (d) can be induced to go into a burst type activity. Since this is the exact description of longitudinal muscle activity, the $BaCl_2$ induced activity can therefore be classified as

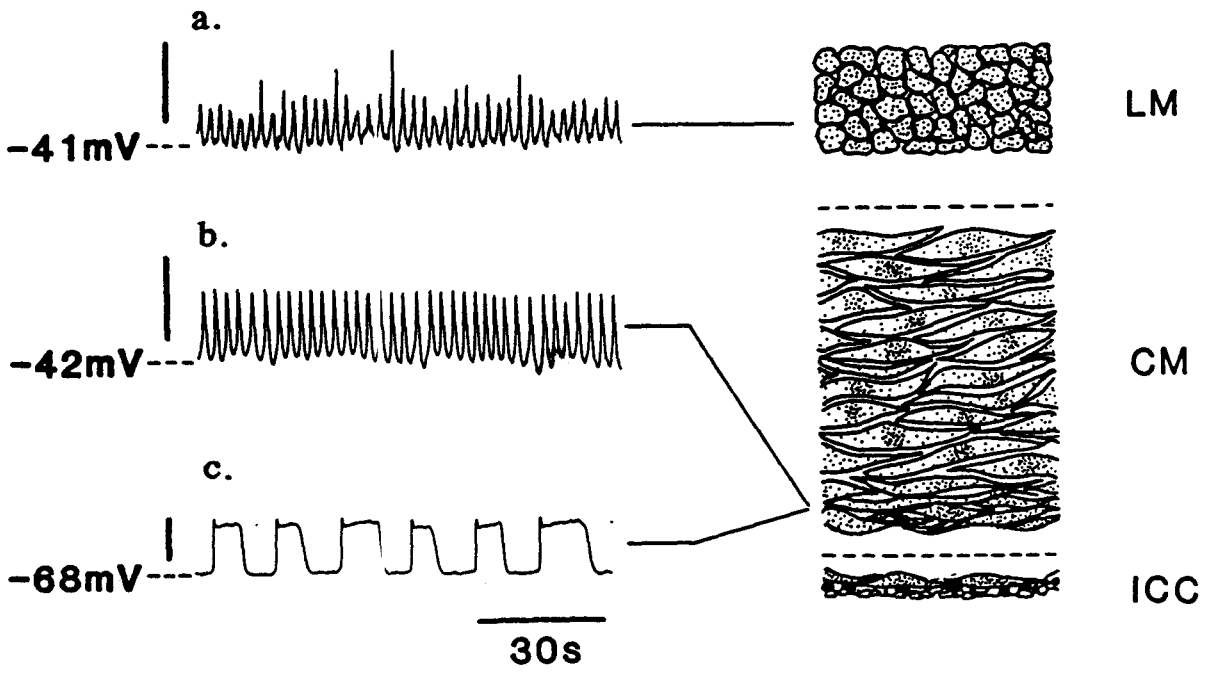

Figure 4.11: *Comparison of the electrical activity recorded at the same location of the circular muscle layer before and after removal of the submucosal ICC network with the spike like action potentials recorded in the longitudinal muscle.*

(a) Intracellular recording from the isolated longitudinal muscle layer which exhibited high frequency spike like action potentials spontaneously in Krebs solution. Calibration bar represents 20 mV (the same in (b) and (c)).

(b) Intracellular recording from a CM preparation in the presence of 0.5 mM $BaCl_2$ and 0.1 μM Bay K 8644.

(c) Intracellular recording at the same location of the circular muscle layer as that recorded in (b), except that the submucosal ICC network was intact. The preparation was pinned flat with the cut-edge of the circular muscle layer faced up so that impalement could be made at different locations of the circular muscle layer. The recording was made at about 15% (0% being the submucosal surface and 100% being the myenteric surface) away from the submucosal surface.

spike like action potentials [49, 50].

Normally, the electrical activity of the circular muscle is dominated by the slow wave type action potentials generated by the ICC network. However, spikes can appear superimposed on the slow waves, again, usually after K^+ conductance blockade. These spikes have the same ionic basis and voltage sensitivity as the spike like action potentials in longitudinal muscle. CM preparations used in the present study do not contain the myenteric plexus area; hence, this study indicates that special pacemaker cells in the myenteric plexus region are not essential for the generation of spike like action potentials as suggested previously [65, 70, 71]. Consistently, spikes superimposed on the plateau phase of slow waves have been reported in the circular muscle with the longitudinal muscle layer removed [2, 3, 54].

It is intriguing that circular muscle can behave very much like longitudinal muscle after removal of the pacemaker cells. The question becomes if circular muscle cells intrinsically are identical to longitudinal muscle cells. From this study it seems possible, if not likely, that they have the same ion channel composition. However, based on the characteristics of our dissected preparations, circular muscle cells seem to be more hyperpolarized and seem to have a lower excitability than longitudinal muscle cells. Based on the hypothesis that a high K^+ conductance suppresses excitability of circular muscle cells, one can suggest that circular muscle cells have a higher probability of opening and/or a higher density of K^+ channels, possibly the outwardly rectifying K^+ channel. Also, the probability of opening and/or density of L-type Ca^{2+} channels may be different in circular muscle versus longitudinal muscle. These differences can be caused by differences in membrane properties or by trophic factors.

Another fascinating similarity between the excited circular muscle cells and longitudinal muscle cells is the ability to generate bursting activity without underly-

ing slow oscillating potentials, i.e. bursts of spike like action potentials with a burst frequency of 0.5 to 2.0 bursts/min and an action potential frequency within a burst ranging from 8 cpm to 22 cpm. An intriguing question is what the mechanism that regulates the frequency and duration of the bursting activity is. In the longitudinal muscle of the human colon, continuous spike like action potentials can be transformed into bursting pattern in the presence of carbachol [59] or by increasing the stretch [58]. Similar observations have been made in the longitudinal muscle of canine colon (Huizinga and Chow, unpublished results). In the excited CM preparations, bursting activity can be observed when repolarizing the resting membrane potential by approximately 6 mV, elevating $[K^+]_o$, washing the Ba^{2+} excited strips by Krebs solution, or in the presence of forskolin which slightly repolarizes the cell membrane. In all these situations, the bursting activity is observed when the level of excitation is decreased. The conditions for the appearance of burst type activity do not seem to be identical for the circular and longitudinal muscle cells; an explanation will need further experimentation.

4.5.4 Role of circular muscle cells in the generation of electrical activity in the full thickness musculature

Results of the present study indicate that the circular muscle cells possess ionic conductances to generate spike like action potentials and resemble colonic longitudinal muscle cells. In ICC-CM preparations the electrical activity in circular muscle is distinctly different from that of longitudinal muscle cells because of the dominating influence of the activity from the pacemaker cells in the submucosal ICC network. From other studies it is known that in ICC-CM preparations, circular muscle cells actively contribute to the generation of the upstroke potential: Barajas-López *et al.*

[2] recorded full amplitude upstroke potentials from the myenteric plexus surface of the circular muscle layer. Evidence has been presented in an abstract that circular muscle cells also actively contribute to the generation of the plateau potential ([62], and Chapter 3). If circular muscle cells were to only passively transmit slow wave activity, as has been suggested [70, 71], intrinsic calcium channels would never be activated and contraction would never occur. We know this ought not to be the case.

The present study indicates that the circular muscle cells do not exhibit the D600 insensitive component of the slow wave type action potentials observed in the ICC-CM preparations. It is therefore conceivable that the conductance responsible for the generation of the D600 insensitive component (the initial part of the upstroke potential) is only found in the cells located in the network of ICC and smooth muscle cells at the submucosal border. This is then passively propagated to the circular muscle cells which respond by voltage activation of Ca^{2+} and K^+ channels generating a full slow wave type action potential. The present study provides evidence to indicate that the extent of contribution of circular muscle cells depends on the activity of the K^+ conductance. That is why it is probably important that excitatory substances like carbachol inhibit K^+ conductance [3], allowing the circular muscle cells to fully participate in generation of slow waves and hence generate contractile activity. Consistently, a recent patch study showed that an inward current was activated at around -60 mV in isolated circular muscle cells of canine colon [61].

Circular muscle cells contribute also directly to the generation of the slow wave type action potentials recorded from the submucosal ICC network region. If one records from an ICC-rich preparation consisting of the submucosal ICC network and a few layers of adjacent smooth muscle cells, one observes that the slow waves are oscillating from a membrane potential of -83 mV with the frequency, duration

and upstroke amplitude equal to 3.7 cpm, 6.8 s, 46.3 mV, respectively [69]. Slow waves observed from exactly the same area when the whole muscle layer is intact are of faster frequency (about 6 cpm), smaller amplitude and duration, and oscillate at about −70 mV. The ICC network is coupled to adjacent smooth muscle cells by gap junctions. It is conceivable that when the submucosal ICC and circular muscle cells are intact, circular muscle cells (at least those in the submucosal border) generate slow wave-like oscillations with faster frequency, smaller duration and amplitude at more depolarized resting membrane potential than the slow waves in the ICC-rich preparations. As a consequence of the high density of gap junctions in the submucosal border, these two kinds of electrical oscillations interact and produce the resultant 6 cpm slow waves which is normally recorded in the intact ICC-CM preparations.

The present study indicates that the excitability of the circular muscle is dramatically decreased once the submucosal ICC network is removed. This reduction in excitability could be a direct effect of removal of certain trophic factors which are normally supplied by the metabolically active ICC-network. This is consistent with the morphological observation that ICC possess numerous mitochondria and form a complete network with circular muscle connected through abundant large gap junctions which permit metabolic coupling.

4.5.5 Is the metabolic clock present in the circular muscle cells of canine colon?

Data from the present study indicate that the mechanism underlying Ba^{2+} induced oscillations in CM preparations is different from the mechanism that gives ICC-CM preparations its auto-rhythmicity. The frequency of Ba^{2+} induced oscillations can easily be modified by changes in K^+ conductance or changes in activity of calcium

channels (present study); in contrast, it is insensitive to changes in intracellular cyclic AMP. Ba^{2+} induced oscillations seem to be initiated and regulated directly by voltage activated Ca^{2+} and K^+ conductances.

Forskolin decreased the amplitude of the Ba^{2+} induced oscillations. Forskolin also abolishes the plateau phase of the ICC-CM slow waves [56]. It is therefore likely that intracellular cyclic AMP modifies L-type calcium channels either directly or through induction of (de-)phosphorylation of the channel.

The slow wave frequency in ICC-CM preparations is rather insensitive to changes in Ca^{2+} or K^+ conductance. In contrast the slow wave frequency is dramatically altered by changes in intracellular cyclic AMP. The insensitivity of the slow waves to voltage and their sensitivity to changes in intracellular metabolites suggested that the slow wave frequency was regulated by an intracellular metabolic clock [56]. Since the present study provides no evidence that such a clock is operating in circular muscle preparations from which the ICC cells are removed, the hypothesis is warranted that the regulatory mechanism of the slow wave frequency, the metabolic clock, is exclusive to the submucosal ICC network. Hence the present study strengthens the hypothesis that ICC are the pacemaker cells of the gut [4, 14, 80, 83].

Chapter 5

Electrophysiological and structural communication between circular and longitudinal muscle of the canine colon

5.1 Abstract

1. Electrical and structural interactions between the circular and longitudinal muscle and interstitial cells of Cajal were investigated and the hypothesis was tested that longitudinal muscle pulls circular muscle to create a circular muscle membrane potential gradient.

2. Using cross-sectioned full thickness (FT) preparations, cut along the long axis of the circular muscle cells, a resting membrane potential gradient of about

23 mV was revealed (−71 mV at the submucosal and −48 mV at the myenteric surface).

3. In preparations with the longitudinal muscle removed (ICC-CM preparations), the resting membrane potential (RMP) gradient was only 10 mV. The RMP remained constant in the submucosal border up to −76 μm. In this area, the ICC network is present and contains dense gap junctions. From 76 μm, the cell depolarizes abruptly up to about 18% from the submucosal border, after which the resting membrane potential was constant at −62 mV.

4. The differences in RMP gradient in the FT and ICC-CM preparations indicate that the RMP gradient is not caused by a gradient in intrinsic circular muscle properties (otherwise, it would have persisted in the preparation with longitudinal muscle removed), but are caused by the *pulling* forces from the more hyperpolarized submucosal ICC network and the more depolarized longitudinal muscle.

5. The upstroke and plateau amplitudes in the FT preparations decayed apparently and exponentially across the circular muscle with space constants equalled to 0.59 mm and 0.51 mm, respectively. The upstroke and plateau amplitudes were measured to be 4.8 mV and 2.4 mV in the myenteric border (100%).

6. The upstroke and plateau amplitudes in the ICC-CM preparations decayed exponentially only in the submucosal border but remained very similar in the rest of the circular muscle reaching 13.3 mV and 10.1 mV at the myenteric surface.

7. Comparison of the upstroke and plateau amplitudes at the myenteric surface of the FT and ICC surfaces indicates that the decrease in upstroke and plateau amplitude is caused by the decrease in RMP in the myenteric border of FT preparations; hence, exponential decay of upstroke and plateau amplitudes in the circular muscle of FT preparations cannot provide evidence for passive propagation when the resting membrane potential also changes in the same direction.

8. In the FT preparations, the amplitude of spikes superimposed on plateau potentials of the circular muscle did not decay exponentially as measured from the myenteric interface. The amplitude reached a maximum in between 70–75% of circular muscle away from submucosal surface. Spikes were born from intrinsic properties of circular muscle and not created by specialized pacemaker cells in the myenteric plexus.

9. Longitudinal and circular muscles were not always separated by a wide myenteric plexus. At many points, the two types of muscle cells were directly apposing to each other with small gaps of 50–100 nm. In these narrow areas, ICC frequently coupled with circular and longitudinal muscle cells with close apposition contacts and hence might provide a pathway for electrical coupling.

5.2 Introduction

One of the intriguing questions in the physiology of colonic motility is the communication and subsequent coordination of the circular and longitudinal muscle layers. This question is of particular interest in the colon because the two muscle layers display markedly different patterns of electrical and mechanical activities, yet they can be seen to contract synchronously.

In intact tissue, performing simultaneous recordings using extracellular electrodes on both muscle layers of the canine colon, El-Sharkawy [35] showed that although there is no significant electrotonic spread of activity between the two muscle layers, the motor and electrical activities can be seen to be co-ordinated, particularly during the period when spiking activity occurs in the longitudinal muscle. It was suggested that the co-ordination of the two muscle layers might be commanded by a common input from periodically active, cholinergic intramural neurones. Sabourin *et al.* [64] also recorded simultaneously from both muscle layers using an L-shaped preparation with a dual sucrose gap technique and found that the activities of the two muscle layers were most often uncoordinated but became synchronized after cholinergic stimulation. In addition, TTX did not abolish, even enhanced some aspects of the interaction between the muscle layers indicating that neural conduction does not form an essential part of the interaction pathway. Therefore, it is essential to seek for another communication pathway for the two muscle layers.

The structural pathway for electrical communication between the two orthogonally orientated muscle layers of the canine colon is not known. Unlike in the small intestine where gap junctions and other specialized membrane structures have been identified between the muscle layers [40, 79], in the colon a wide area of the myenteric plexus separating the two muscle layers has been documented [15]. One of the objectives of the present study was to find the structural basis for cellular communication between the two muscle layers.

Recent electrophysiological studies provided challenging questions about the electrical communication between the two muscle layers in canine colon. Using a cross-sectioned preparation with both the muscle layers intact, the resting membrane potential of smooth muscle cells in the longitudinal and circular muscle adjacent to

either side of the myenteric plexus was found to be around −40 mV [71, 70, 72]. These studies indicate a resting membrane potential gradient of more than 35 mV in the circular muscle layer from the submucosal to the myenteric surface. Such a gradient could be entirely due to gradients in intrinsic properties of circular muscle cells. A current hypothesis is that muscle cells have a gradient in sodium pump activity [17]. An alternative hypothesis is that the coupling of the relatively more depolarized longitudinal muscle to the circular muscle cells induces the membrane potential gradient. The importance of this hypothesis lies in the fact that if proven to be correct it may mean that there is no heterogeneity in electrical properties of circular muscle cells. Interestingly, if one separates the longitudinal muscle from the circular muscle, the resting membrane potential gradient is reduced to approximately 10 mV providing some support for the latter hypothesis.

The present study was undertaken (a) to investigate the hypothesis that because of coupling to longitudinal muscle cells, the resting membrane potential of circular muscle cells in the myenteric border is *pulled* from −62 mV to −48 mV, (b) to find structural evidence for electrical communication between the longitudinal and circular muscle layers, and (c) to explore consequences of coupling of circular muscle cells to both the network of submucosal interstitial cells of Cajal and the longitudinal muscle layer.

5.3 Methods

5.3.1 Tissue Preparation

To study whether the presence of longitudinal muscle is responsible for the *pulling* up of the RMP in the myenteric border of the circular muscle, comparative studies

were performed on the FT and the ICC-CM preparations. The FT preparations were mounted as described in Chapter 2. The ICC-CM preparation (3 × 3 mm) was mounted flat onto the Sylgard bottom of a transfer holder with either the submucosal or the myenteric surface faced up.

5.3.2 Intracellular recordings

For the FT preparations, impalements were made at the surface cells along the transverse axis of the circular muscle cells with 0% referred to the submucosal surface and 100% referred to the myenteric surface. The resolution in identifying the location of impalement across the circular muscle layer in the FT preparations is better than ±50 μm. For the ICC-CM preparations, impalements were made at successive cells by penetrating deeper into the transverse axis of the circular muscle layer. The accuracy in determining the depth of penetration is better than ±2.5 μm. The percentage of penetration away from the submucosal surface could be calculated from the thickness of the circular muscle.

5.3.3 Result presentation and statistical analysis

Numeric results were presented as MEAN±SEM. Graphical presentations showed the mean with the upper and lower limits obtained by adding and subtracting SEM from the mean value, respectively. Owing to the variation of circular muscle thickness and the quantal displacement of the micromanipulator, the locations of impalement, in terms of the percentage from submucosal surface, varied from one experiment to another. Therefore, averages of slow wave parameters at various locations within the circular muscle could not be obtained by simply determining the mean of discrete measurements at different locations from different experiments. As a result, different

curve fitting techniques for estimating the spacial variation of different slow wave parameters were performed on each individual experiment. The precision in data fitting was indicated by r value which represents the square root of coefficient of determination (an r value of 1.0 is a "prefect" fit). The average slow wave parameters at different locations of the circular muscle layer could then be determined from the estimated curves at an arbitrary interval of percent in the circular muscle.

Nomenclature and abbreviations

Experiments are performed on two types of preparations — FT = full thickness (longitudinal muscle + circular muscle + ICC, see above), and ICC-CM (circular + submucosal ICC, see above). The electrical activity of the circular muscle is described as: RMP = resting membrane potential; slow wave starts with the upstroke potential, then follows by a partial repolarization; and, the plateau potential (PP) which maintains during the plateau phase. The plateau amplitude is the difference between the RMP and the plateau potential.

Resting membrane potential (RMP) and plateau potential (PP)

In the FT preparations, the RMP and PP recorded at different locations of the circular muscle (percentage from submucosal surface) in each experiments were fitted by fifth order polynomial using the least square method.

$$MP = A_0 + A_1 x + A_2 x^2 + A_3 x^3 + A_4 x^4 + A_5 x^5 \tag{5.1}$$

where MP is either the RMP or PP of slow waves at $x\%$, and

A_i ($i = 0$ to 5) are the coefficient of x of order i.

The RMP and PP at different locations (0%, 2%, 4%, ..., 100%) of each experiment were obtained from the best fitted equations. The RMP and PP at the same percentage from different experiments could then be obtained; thus, the average of RMP and PP at various locations could be determined.

In the ICC-CM preparations, the RMP and PP in the submucosal border had similar patterns as those in the FT preparations. They were fitted by fifth order polynomial. However, the RMP and PP in the myenteric border were fairy steady and estimated by linear regression.

$$MP = m \cdot x + c \tag{5.2}$$

where MP is either the RMP or PP of slow wave at x%,

m is the slope, and

c is the y-intercept.

To estimate how far away from the submucosa the RMP remained constant (see result section), the tangent at the point of inflection of the fifth order best fit curve closest to the submucosal surface and the linear regression of RMP from the first 4 to 5 successive impalements (less than 50 μm measured from submucosal surface) were determined (see figure 5.5). The intercept of these two lines gives the estimated location up to which the RMP remained constant.

Upstroke and plateau amplitudes

In the FT preparations, the gradient of the upstroke and plateau amplitude of the circular muscle layer in each experiment was estimated by exponential fit; In the ICC-CM preparations, only the submucosal recordings could be fitted by exponential functions.

$$V(x) = V_0 \cdot e^{-\frac{x}{\lambda}} \tag{5.3}$$

where $V(x)$ is the amplitude at x mm away from submucosa,

V_0 is the amplitude at 0 mm, and

λ is the space constant.

Frequency and duration

Both frequency and duration of slow waves in the circular muscle layer of canine colon remained quite constant throughout the entire thickness of FT and ICC-CM preparations. Thus, the frequency and duration of slow waves at various locations were estimated by linear regression.

Amplitude of the spikes superimposed on the slow wave plateau in the myenteric border of circular muscle

The amplitude of spikes was obtained by measuring the absolute magnitude of the biggest spike on the plateau phase of slow waves. The spike amplitude gradient was determined using third order polynomial fit. That is,

$$MP = A_0 + A_1 x + A_2 x^2 + A_3 x^3 \tag{5.4}$$

where AMP_{spike} is the maximum amplitude of spikes at x%, and

A_i (i = 0 to 3) are the coefficient of x of order i.

5.3.4 Tissue fixation and electron microscopic examination

Four dogs were anaesthetized with sodium pentobarbital (30 mg/kg i.v.) and segments of proximal colon were fixed by local perfusion with 2% glutaraldehyde in 0.075 M cacodylate buffer (pH 7.4) containing 4.5% sucrose and 1 mM CaCl2, as previously described [14, 15]. Following fixation, circular and longitudinal strips of muscularis externa were cut, washed overnight in 0.1 M cacodylate buffer, containing 6% sucrose and 1.24 mM $CaCl_2$ (pH 7.4) at 4 °C, postfixed with 2% OsO_4 in 0.05 M cacodylate buffer (pH 7.4) at room temperature for 90 min, stained with saturated uranyl acetate, and embedded in Epon 812. Tissues were oriented in moulds to cut the circular muscle layer in either a cross or longitudinal direction. To locate narrow regions of the myenteric plexus, 0.5 μm thick serial and semi-serial sections were cut and stained with 2% toluidine blue. Both the longitudinal and circular strips of colonic muscularis externa were used for this study. After suitable areas were found on the toluidine blue stained sections, ultrathin sections were cut, mounted on either 200 mesh grids or 400 mesh ultra light transmission grids, and double stained with uranyl acetate and lead citrate. The grids were examined in a JEOL-1200 EX Biosystem electron microscope at 80 kv.

5.4 Results

5.4.1 Resting membrane potential (RMP) gradient in the circular muscle

FT preparations

In the FT preparations, the RMP gradient in the circular muscle layer was found to be triphasic. Figure 5.1 shows slow waves recorded in the circular muscle layer of the FT preparations. Figure 5.2 shows the average RMP and plateau potential at various locations of 9 FT preparations. The average thickness of the circular muscle layer was 1.3±0.2 mm. The RMP at the submucosal surface (0%) and myenteric surface (100%) was 70.5±0.4 mV and 47.8±0.7 mV, respectively. In phase I of the RMP gradient, the RMP remained fairy constant for the first 5 % away from the submucosa and rose slowly for the following 10%, after which the RMP depolarized abruptly to approximately −64 mV at about 30%. A point of inflection was always found in phase I. Phase II of the RMP gradient extended approximately from 30% to 60%. In this phase, the RMP depolarized gradually with a slope very similar to that of the initial portion (between 5% to 15%) of phase I. Phase III of the RMP gradient increased abruptly when compared to phase II; the RMP depolarized from −58 mV to −48 mV (from 60% to 100%). A point of inflection could also be found in this phase. The RMP of the longitudinal muscle was −47.4±0.9 mV (n=9) at the myenteric plexus surface and −43.6±0.5 mV (n=5, $P < 0.05$) in the middle of the longitudinal muscle layer, approximately 150 μm away from the myenteric plexus.

ICC-CM preparations

In contrast to the triphasic RMP gradient found in the FT preparations, the RMP gradient in the ICC-CM preparations was biphasic (figure 5.3). Typical slow waves recorded at the submucosal and the myenteric surfaces of a ICC-CM preparation are illustrated in figure 5.4. The RMP of the circular muscle layer at the submucosal surface was −7..7±0.8 mV, very similar to that in the FT preparations. The

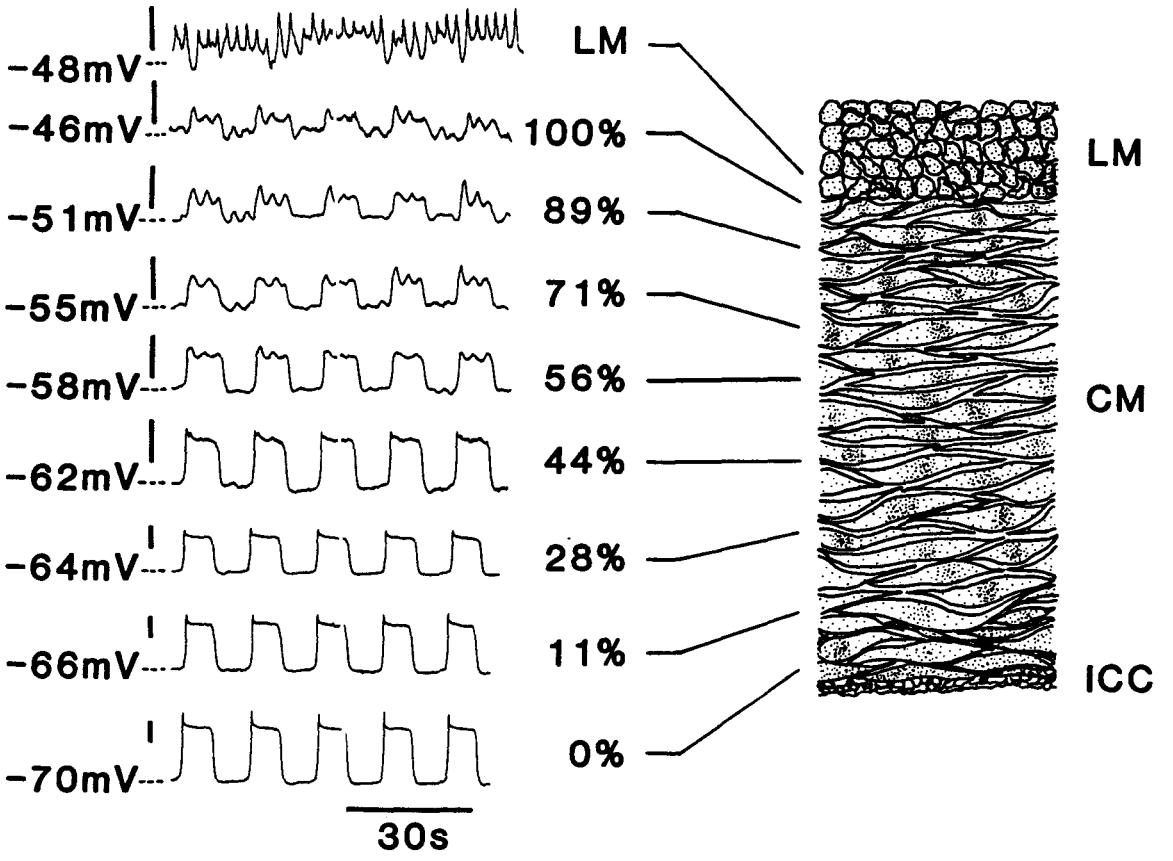

Figure 5.1: *Electrical oscillations in a FT preparation of canine colon*

Microelectrode recordings were made at different locations of the CM layer as well as the myenteric border of the longitudinal muscle. The 0% location is the submucosal surface and 100% is the myenteric border of the CM layer. The slow wave pattern remains distinguishable throughout the entire thickness of CM layer despite the change in RMP. Note the similarity in frequency and duration of slow waves throughout the whole thickness of the CM layer although recordings were not made simultaneously. The spikes start to appear at about 56% in this particular preparation. Also note that the RMP in the myenteric border of the longitudinal muscle fluctuated as compared to the steady RMP in the isolated LM strips (see figure 5.4). Calibration bars are 20 mV.

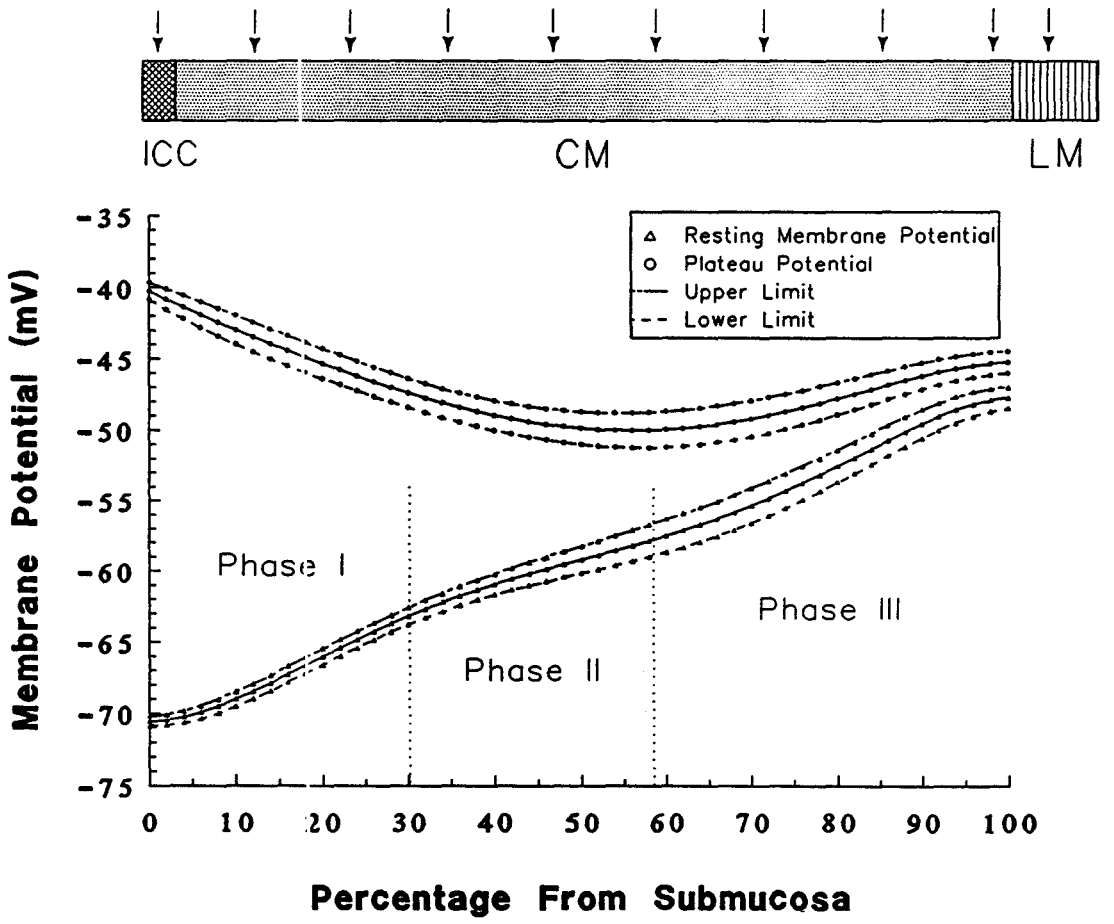

Figure 5.2: *The average resting membrane potential and plateau potential of electrical oscillations recorded in the CM layer of the FT preparations.*

The upper and lower limits represent the deviation from the mean by SEM. The RMP in the CM layer of the FT preparations can be described by three phases. Beginning of phase I is influenced strongly by the pacemaking region in the submucosal surface. The intrinsic properties of the CM cells start to take over as moving away from the submucosal surface. Phase II reflects the intrinsic properties of CM cells the most and sees the pulling forces from either sides (see results). The RMP rises sharply as approaching the myenteric plexus where the more depolarized LM is adjacent to it. The plateau potential can be divided into two phases: a decreasing phase and a delayed increasing phase as getting close to myenteric border.

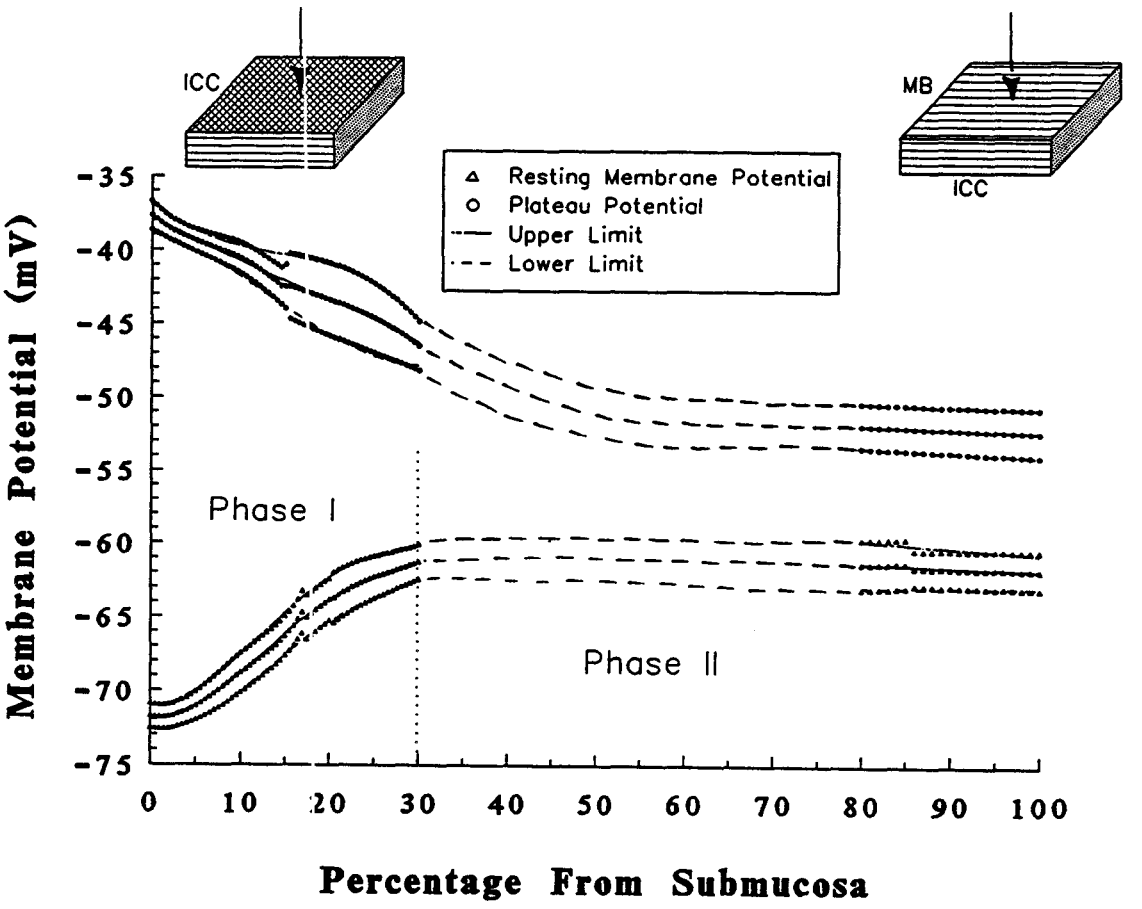

Figure 5.3: *The average resting membrane potential and plateau potential at different locations of the circular muscle layer of the ICC-CM preparations.*

Averages of 7 experiments in the submucosal border and 4 in the myenteric border are plotted. The upper and lower limits represent the deviation from the mean by SEM. Note the ***biphasic*** RMP gradient. After an abrupt increase in RMP in the submucosal border, the RMP remained very similar in the rest of the CM layer. The data recorded in the submucosal and the myenteric border were arbitrarily joined by dashed lines.

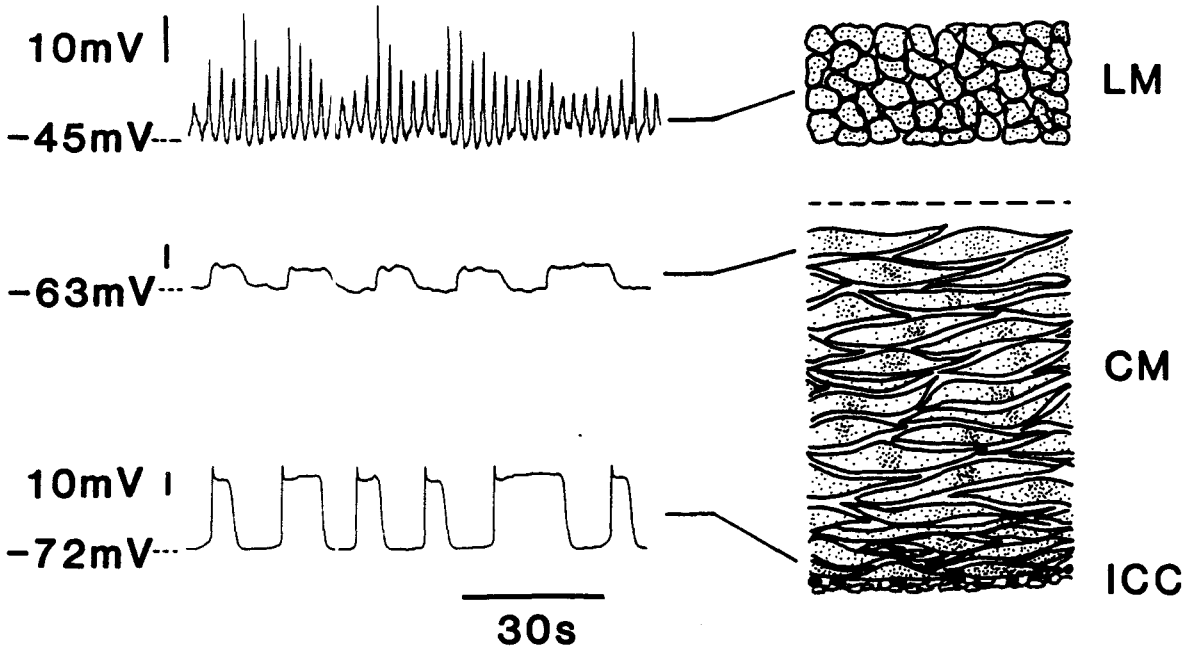

Figure 5.4: *Electrical oscillations in isolated muscle strips of canine colon.*
Microelectrode recordings were made on the myenteric surface of isolated LM, myenteric surface of an ICC-CM preparation, and the submucosal surface of an ICC-CM preparation. The patterns of electrical oscillations were very different in the LM and CM layers. Note that the difference of RMP between the two surfaces of the circular muscle is only 9 mV in the experiment shown above, compared to 24 mV in FT preparations shown in figure 5.2).

RMP at the myenteric surface of the circular muscle was -61.7 ± 1.3 mV compared to -47.8 ± 0.7 mV in FT preparations measured at the same location, a difference of approximately 14 mV ($P < 0.001$).

The behaviour of the RMP in the submucosal border is quantified by determining the intercept point as described in the method section. Figure 5.5 shows a typical distribution of RMP in the submucosal surface. The RMP remained constant for the first 76.3 ± 6.1 μm (corresponding to approximately 6.5% of the circular muscle away from the submucosal surface since the average thickness of the circular muscle was 1.1 ± 0.2 mm, n=7). Thereafter, it depolarized abruptly within the next 123.4 ± 10.3 μm (11.3%) with a slope of 55.2 ± 4.1 mV/mm reaching -64.7 ± 0.8 mV at about 18% away from the submucosal surface. The RMP rose less steep again for the remaining part of phase I reaching -62 mV at the end of phase I at 30%. The RMP remained constant in phase II.

5.4.2 Plateau potential gradient in the circular muscle

FT preparations

The plateau potential in the FT preparations could be divided into two phases and were fitted by fifth order polynomial (figure 5.2). The plateau potential at the submucosal surface was -40.2 ± 0.6 mV (n=9) and became more negative going into the muscle layer reaching a minimum at approximately 60% (50.0 ± 1.3 mV, n=9), corresponding to the beginning of phase III of the RMP gradient. Thereafter, the plateau potential started to rise approaching the myenteric surface and eventually reached -45.3 ± 0.8 mV (n=9).

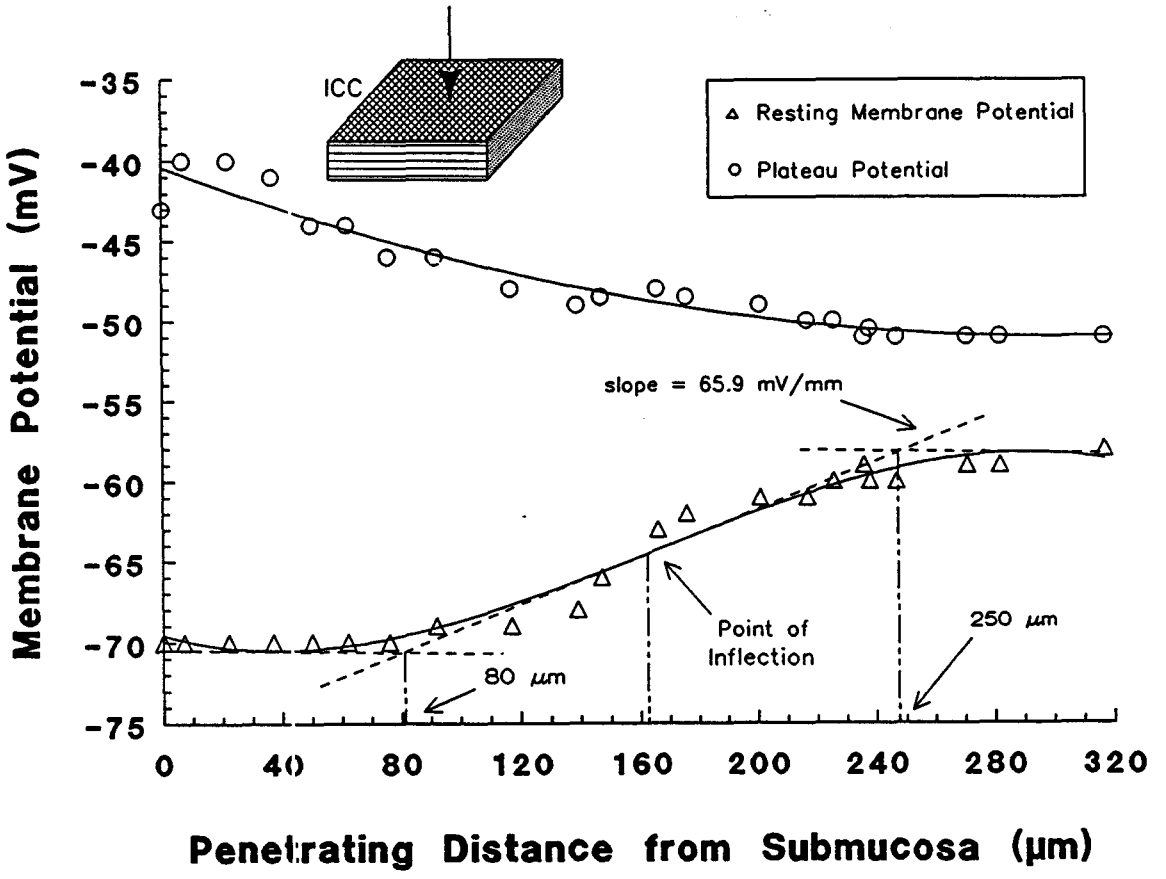

Figure 5.5: *A typical RMP and plateau potential gradient found in the submucosal surface of an ICC-CM preparation.*

The RMP gradient was fitted by third order polynomial (to simplify the calculation of determining the point of inflection) using the least square method. The RMP remained fairy constant in the submucosal border of the CM layer. The distance for which the RMP remained constant was estimated by determining intercept of the tangent at the point of inflection and the linear square fit of the first 5 points in the submucosal border.

ICC-CM preparations

The plateau potential at different locations within the circular muscle layer were depicted in figure 5.3. The plateau potential at the submucosal surface of the ICC-CM preparations was -37.7 ± 1.0 mV (n=7) which was not significantly different from that in the FT preparations. The plateau potential decreased abruptly in the submucosal half of the circular muscle layer and remained basically unchanged in the myenteric half (at least from 80% to 100%) of the circular muscle layer. The plateau potential at the myenteric surface was -52.1 ± 1.6 mV (n=4) which was very similar to the minimum plateau potential in the FT preparation at approximately 60% but significantly different from that at the myenteric border (100%) of the FT preparations ($P < 0.05$). The gradual depolarization of the plateau potential in phase III of the FT preparations was not seen in ICC-CM preparations.

Cross sectioned preparations similarly cut as the FT preparations but without the longitudinal muscle were difficult to prepare because strips could only be mounted by pins along three edges (since no pin could be put in the myenteric border of circular muscle) causing unstable impalements. Two successful preparations confirmed the constant RMP (≈ -60 mV) and plateau potential (≈ -50 mV) throughout the circular muscle from approximately 40% to 70%.

5.4.3 Upstroke and plateau amplitudes

FT preparations

The upstroke and plateau amplitudes of slow waves in the FT preparations decreased exponentially throughout the circular muscle layer. However, this should not immediately be considered as an indication of passive decay of slow waves since

Table 5.1: *Summary of the exponential best fit parameters of the upstroke and plateau amplitudes in the FT and ICC-CM preparations.*

	Upstroke Amplitude		Plateau Amplitude	
	FT	*ICC-CM*	*FT*	*ICC-CM*
V_o (mV)	35.3±1.9	43.5±1.9	32.8±1.8	37.2±1.6
λ (mm)	0.59±0.05	0.28±0.04	0.51±0.04	0.32±0.05
r	0.982±0.004	0.952±0.012	0.985±0.03	0.949±0.012
x-range (mm)	0–1.3	0–0.25	0–1.3	0–0.25

x-range = the range that λ is applicable as measured in mm from the submucosal surface.

the resting membrane potential was decreasing (depolarizing) in the same direction. Conclusion should only be drawn after comparison with data from ICC-CM preparations (see below). Table 5.1 summarizes the best fit curve parameters, such as the amplitude at 0% (V_o), space constant (λ) and r values. The average r values of the best exponential fits equalled to 0.982±0.004 and 0.985±0.003 for the upstroke and plateau amplitudes, respectively. The r values were larger than 0.96 in all of the best fit curves. The average thickness of the CM layer was 1.3±0.1 mm (n=9). The space constants of the upstroke and plateau amplitudes were 0.59±0.05 mm and 0.51±0.04 mm, respectively. Using these estimated exponential decay parameters, the upstroke and plateau amplitudes of slow waves at the myenteric plexus of the circular muscle were calculated to be 3.9±0.7 mV and 2.6±0.5 mV, respectively. Consistently, the plateau amplitude obtained from the best fit curves of the RMP gradient and plateau potential gradient was 2.5±0.7 mV (see figure 5.2) which indicated the consistency in the best fit equations. The upstroke and plateau amplitudes recorded were 4.8±0.8 mV and 2.4±0.2 mV (n=9), respectively. These results demonstrated

the precision of the estimated best fit curve parameters in representing the physiological data. The upstroke amplitude of spike like action potentials (SLAPs) in the longitudinal muscle adjacent to the myenteric plexus was 7.4±0.8 mV (n=9).

ICC-CM preparations

In the ICC-CM preparations, the upstroke and plateau amplitudes did not decay according to a simple exponential function throughout the entire circular muscle. Both the upstroke and plateau amplitudes decayed exponentially only for the first 30% from the submucosal border. The upstroke and plateau amplitudes remained very similar from 80% to 100% in the myenteric border of the circular muscle. Table 1 summarizes the exponential best fit curve parameters of the upstroke and plateau amplitude in the submucosal border of the ICC-CM preparations. The upstroke and plateau amplitudes recorded physiologically in the myenteric border of the circular muscle were 13.3±3.1 mV and 10.1±2.0 mV, respectively; whereas the plateau potential was found to be equal to 9.5±1.1 mV in the best fit curves of RMP gradient and plateau potential gradient (figure 5.3). Both the upstroke and plateau amplitudes were much larger than the values predicted from the space constants obtained from the exponential fit of these parameters in the submucosal side, indicating that the upstroke and plateau amplitudes did not decay exponentially throughout the circular muscle layer.

5.4.4 Frequency and duration of slow waves

The frequency and duration of slow waves in the circular muscle layer did not exhibit spatial variation and were similar in both FT (see figure 5.1) and ICC-CM (see figure 5.4) preparations. The absolute value of the slopes ontained from the plots

of the slow wave frequency versus various locations varied from 0.0001 cpm/percent to 0.0063 cpm/percent in FT preparations (n=9) and from 0.0025 cpm/percent to 0.0087 cpm/percent in ICC-CM preparations (n=4) with averages in both cases very close to zero. Similarly, the average of the slopes of curves plotting the slow wave duration versus different locations in the circular muscle layer of either preparations were also very close to zero. These results indicate that both the duration and frequency of slow waves were not affected by removal of longitudinal muscle and very similar in any location of the circular muscle measured during different time domains.

5.4.5 Characteristics of spikes superimposed on slow wave plateaus

Spikes were observed in the myenteric half of the circular muscle layer of the FT preparations. The spike amplitude gradient was estimated by third order polynomial fit (figure 5.6) with an r value of 0.96±0.05 (n=5) indicating that the estimation of the spike amplitude gradient by each fitting was very reliable. In one preparation, the spike was observed as close to the submucosal surface as 35% (figure 5.7). The maximum spike amplitude was found between 70% and 75%. It indicates that the spikes were not passively propagated from the myenteric plexus (as previously suggested [65, 71]) since the spike amplitude gradient does not follow an exponential decay function. Unlike the amplitude, the frequency and duration of the spikes in any location of the myenteric half of the circular muscle were very similar, and also similar to the spike like action potentials in the longitudinal muscle (table 5.2).

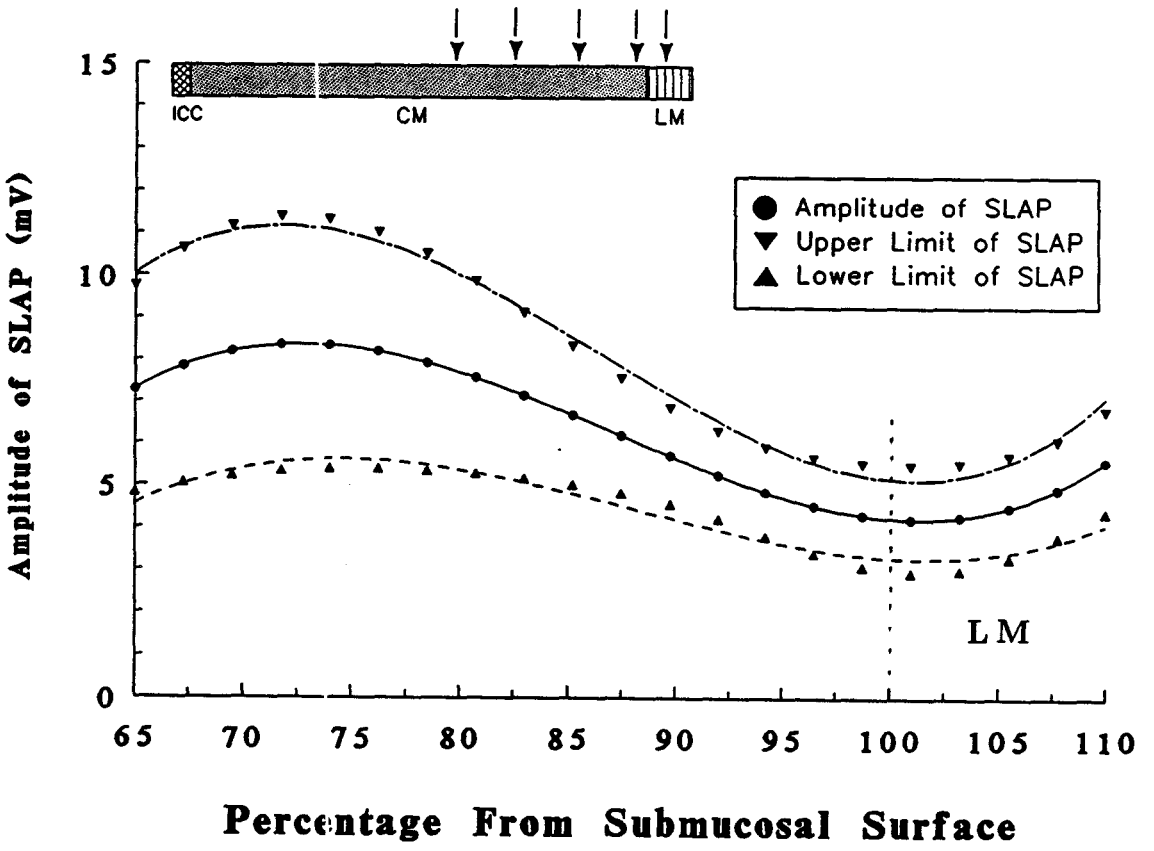

Figure 5.6: *Maximum spike amplitude on the slow wave plateau phase of the circular muscle of the FT preparations.*

The upper and lower limits represents the deviation from the mean by SEM (n=5). Spikes reache the maximum amplitude in between 70–75% as measured away from the submucosal surface of circular muscle.

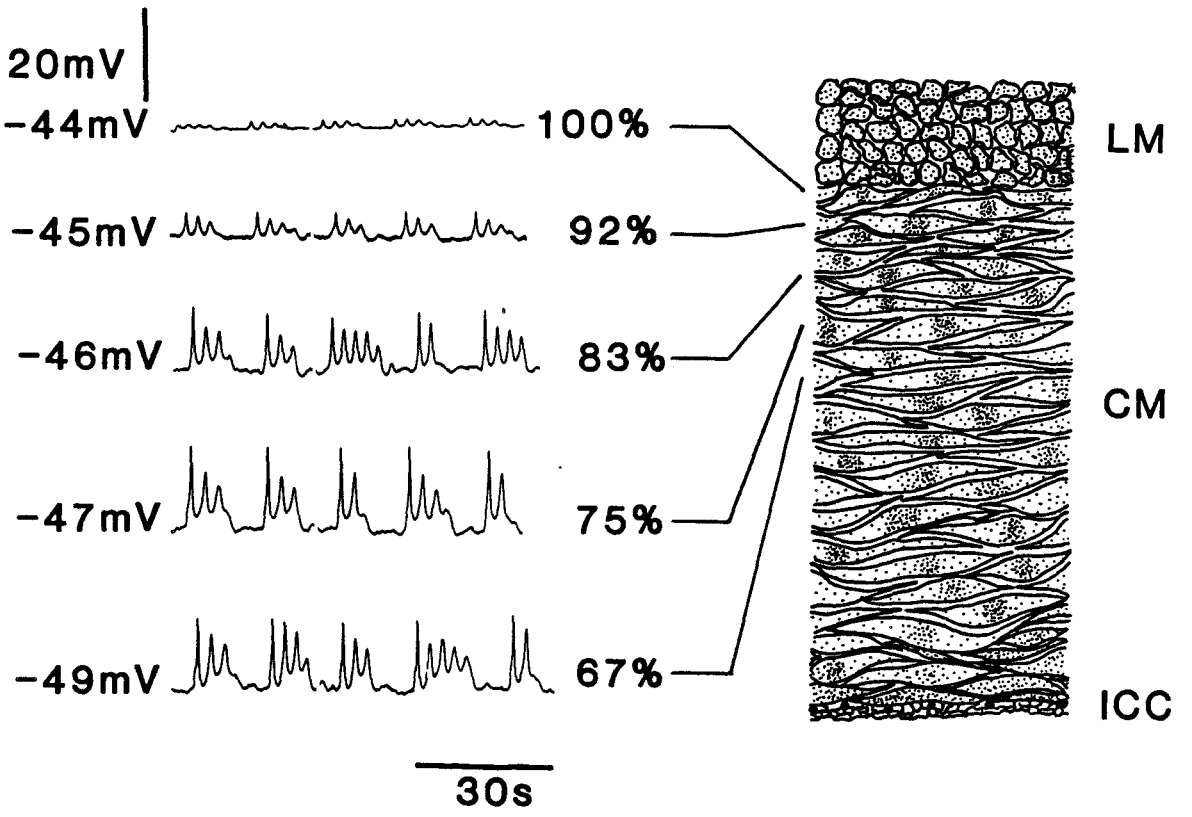

Figure 5.7: *Spikes in the canine colon circular muscle.*

Intracellular recordings in the myenteric half of the circular muscle in a FT preparation. This experiment shows the most obvious spike amplitude gradient from all 5 experiments. The maximum spike amplitude was found at 75% of the circular muscle.

Table 5.2: *Summary of the spike parameters in the FT preparation.*

Location (%)	Frequency (cpm)	Duration (s)	Amplitude (mV)
65	20.7±0.4	1.3±0.1	6.2±2.6
72	21.2±0.5	1.1±0.1	8.3±3.1
85	21.3±0.9	1.0±0.1	6.8±1.7
92	21.3±1.3	1.0±0.2	5.1±1.1
100	23.7±0.8	1.0±0.1	4.0±0.8
LM	22.7±0.9	1.2±0.2	5.3±1.5

5.4.6 Structural basis for electrical communication between longitudinal and circular muscle cells in the myenteric plexus

A recent study has revealed the structural characteristics of different cell types in the myenteric plexus of the canine colon [15]. The present examination of the whole myenteric plexus area indicates that longitudinal and circular muscle layers of the canine colon are not always separated by a wide myenteric plexus. Figure 5.8 shows a low magnification micrograph of a cross section illustrating the narrow regions of the myenteric plexus (arrows). In the narrow regions (see figure 5.9), the membranes of longitudinal and circular muscle cells were found to be separated by a small gap of as small as 50 nm or directly apposing each other for a long distance by approximately 100 nm. The intercellular gaps between longitudinal or circular muscle cells within their own layers were similar to that between a longitudinal and a circular muscle cell in these narrow areas (see figure 5.9c). In the areas where the two muscle types were

Figure 5.8: *Low magnification micrographs of the narrow regions between the circular and longitudinal muscle.*

a. A low magnification micrograph of a longitudinal section through a narrow region of myenteric plexus (arrows). The width of the gap between the longitudinal (LM) and circular (CM) muscle layers varies between 0.1 μm and 4 μm within the same section, but can widen up to 7 μm, if a small blood vessel (bv) occurs between two muscle layers. No crossover of muscle cells was seen between muscle layers in the narrowed region. Bar, 25 μm.

b. A low magnification micrograph of the longitudinal section through the narrowed interval between the longitudinal (LM) and circular (CM) muscle layers (small arrows). In the narrowed region of the myenteric plexus the majority of the nerves of the tertiary plexus and associated with them interstitial cells (arrowheads) frequently enter the longitudinal muscle layer (large arrow) in the same direction as the blood vessels (bv). Only a few nerves and interstitial cells can be seen between the longitudinal and circular muscular layers (small arrows). The two branches of the tertiary plexus join each other again in the widened part of the myenteric plexus. There are no structural differences between the inner longitudinal muscle cells (iLM) interposed between the narrowed myenteric plexus and blood vessel region, and cells of the main longitudinal muscle layer (oLM). Although, in thin serial sections, as one approaches a widening in the myenteric plexus, the cells of inner longitudinal muscle layer often appear to be oblique to cells of the main longitudinal muscle layer. Bar, 25 μm.

directly apposing each other, distinguishable cell-to-cell membrane specialization was not observed.

Very frequently, ICC were found to be present in the narrow gaps between the longitudinal and circular muscles (see figure 5.9. Close apposition contacts and tiny gap junctions were occasionally found between the longitudinal muscle cells and ICC, and between the circular muscle cells and ICC (see figure 5.9b, and figures 9 & 11 of [15]) but not between longitudinal and circular muscle cells. These findings urge us to consider that ICC may play a role in electrical communication between both muscle layers.

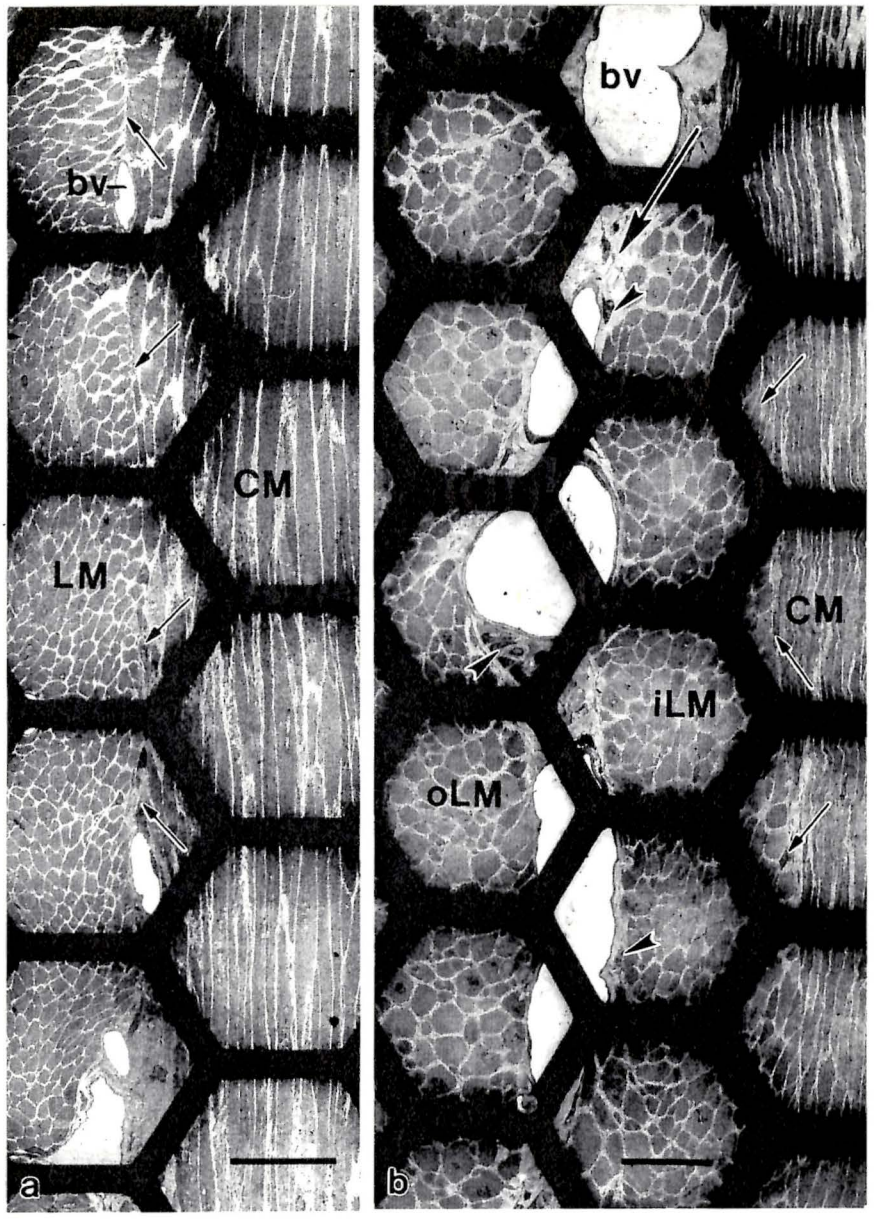

Figure 5.8

Figure 5.9: *Narrow regions between circular and longitudinal muscles at higher magnifications*

a. A medium magnification micrograph of a narrowed region of the myenteric plexus. The longitudinal (LM) and circular muscle (CM) layers are separated by an interstitial cell (IC), its processes (arrows), the small nerve of the tertiary plexus (N), elastin (e) and collagen fibres. Small capillaries and macrophage-like cells are usually also present in this region. Note close apposition contact (arrowhead) between the interstitial cell and the longitudinal muscle cell. Bar, 5 μm.

b. An electron micrograph of the narrowed myenteric plexus showing a close apposition contact (arrow) between the extended mushroom-like process of the circular muscle cell (CM) and the interstitial cell (IC). The interstitial cells are distinguished by their elongated or angular contour of their bodies and long ramified processes. Their plasma membrane possesses caveolae (c) and is surrounded by basal laminae (bl). LM - longitudinal muscle cell. Bar, 1 μm.

c. In the small portion of the narrowed myenteric plexus the longitudinal (LM) and circular muscle (CM) cells are seen directly in apposition one to another. No close apposition contacts are observed between two plasma membranes. Gaps of 55 nm (circle)—100 nm (arrow) between the two types of muscle cells are found. No morphological specialization occurs on apposing plasma membranes of either longitudinal or circular muscle cells. Electron dense material seen in the gap between the longitudinal and circular muscle cells correspond to their basal laminae (bl). In the remaining part of the narrowed region muscle layers are separated as usual by ICC processes, small nerves, collagen and elastin fibres. The arrowhead shows the gap ($\approx$100 nm) between two neighbouring circular muscle cells. Bar, 500 nm.

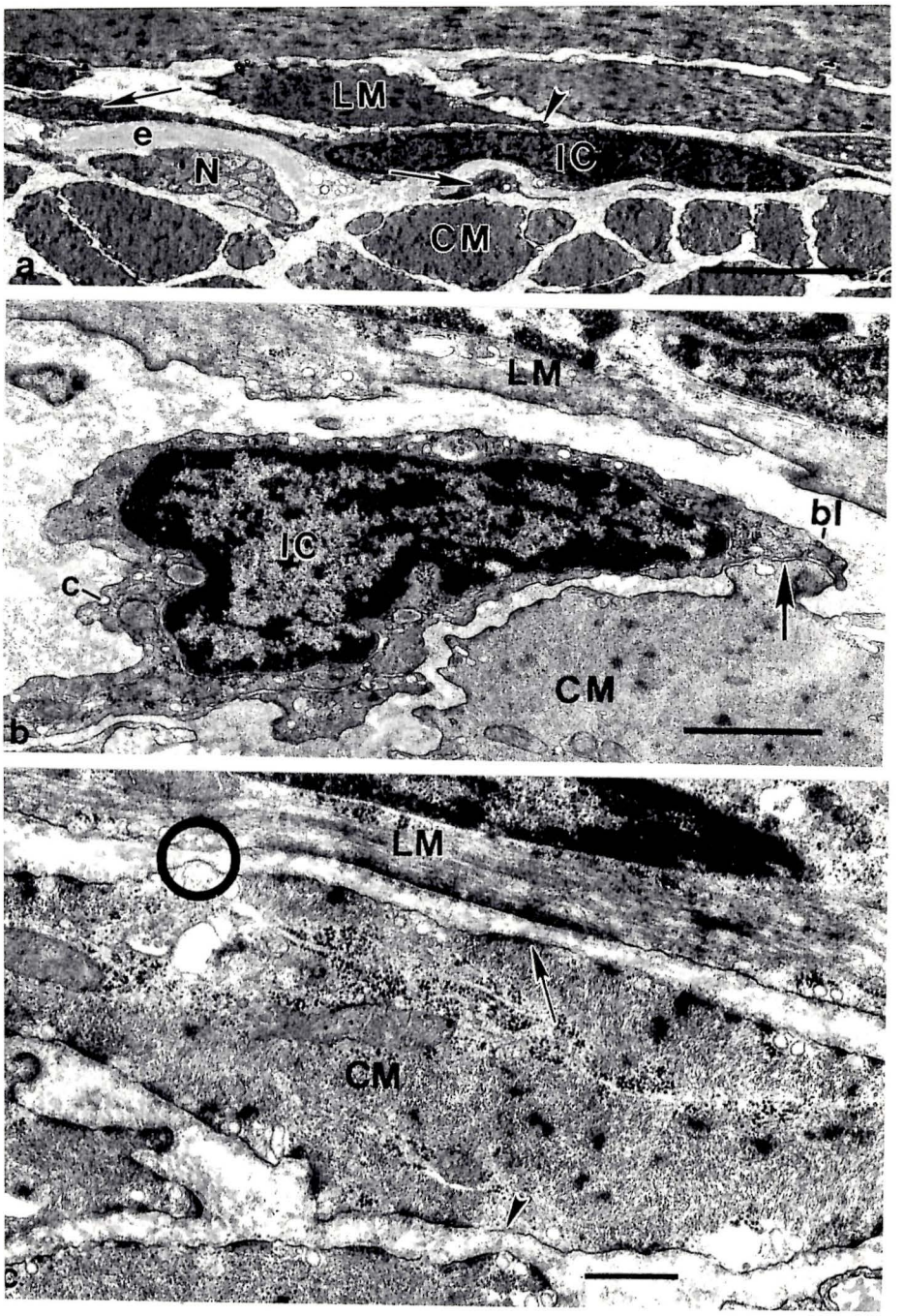

Figure 5.9

5.5 Discussion

5.5.1 Origin of membrane potential gradient

Using a full thickness (FT) colon wall preparation, cross-sectionally cut along the long axis of the circular muscle layer, it was revealed that there is a resting membrane potential gradient of approximately 23 mV in the circular muscle: the submucosal surface is at −71 mV, the myenteric plexus surface at −48 mV. The present study shows that if longitudinal muscle is removed from the circular muscle, the membrane potential at the myenteric plexus surface drops to −62 mV. The RMP throughout the circular muscle is then constant at approximately −62 mV except at the submucosal surface where for the first 76 μm the membrane potential is constant at −72 mV after which a sharp gradient develops such that at 200 μm the membrane potential is −64 mV. However, when we remove the ICC network located at the submucosal surface, this 8 mV gradient in the submucosal border disappears and the RMP of the CM cells is about −62 mV throughout (Chapter 4; see also [69]). Thus, after removal of the ICC network and the longitudinal muscle layer, the resting membrane potential within the circular muscle layer is uniform. Hence, the resting membrane potential gradients in the circular muscle *in situ* are caused by the *pulling forces* originating from different cell types with different electrical activities in both the myenteric and the submucosal borders. Data of the present study indicate that there is no need for a hypothesis stating that the RMP gradient is caused by the heterogeneity in properties of circular muscle cells [17]. If such heterogeneity existed this would have been maintained after cutting away the longitudinal muscle.

The cells in the network of ICC and smooth muscle cells, located at the submucosal surface of the circular muscle layer, are intrinsically at a very hyperpolarized

level, around −80 mV. This was shown by recording from an "ICC-rich" preparation consisting of the ICC network and a few adjoining smooth muscle cell layers [69]. Within the full thickness tissue, circular muscle cells adjoining this network and having an intrinsic RMP of approximately −62 mV become hyperpolarized resulting from the pull by the more hyperpolarized ICC network cells, creating phase I of the membrane potential gradient in the submucosal border. Moving away from the submucosal surface, the intrinsic resting membrane potential of the circular muscle cells become more dominant leading to the more steady phase II. This gradual transformation of resting membrane potential from phase I to phase II is consistently observed in the ICC-CM preparations. Thus, phase I of the RMP gradient is dependent only on the local interactions between the submucosal ICC network and circular muscle cells.

The longitudinal muscle cells are markedly depolarized compared to circular muscle cells. The resting membrane potential at the myenteric plexus surface was −45 mV when recorded in isolated longitudinal muscle. Attached to circular muscle, in a full thickness preparation, the membrane potential was −48 mV at the myenteric plexus surface whereas it was still −44 mV in the middle of the longitudinal muscle layer. Coupling of longitudinal muscle to circular muscle apparently pulls up myenteric circular muscle cells by 14 mV but pulls down longitudinal muscle cells by only 3 mV. Pulling of circular muscle by longitudinal muscle leads to phase III of the membrane potential gradient in full thickness preparations, and consistently, phase III is not observed in ICC-CM preparations without the longitudinal muscle. The mechanism of electrical communication leading to dominant pulling of longitudinal muscle over circular muscle is not clear and will need further experimentation to be resolved.

The plateau potential of the ICC-CM preparations hyperpolarized only in the submucosal border and remained very similar in the rest of the circular muscle. The transient hyperpolarization of the plateau potential is likely caused by the intrinsic difference in K^+ conductance between the submucosal ICC-network cells and the circular muscle cells. We have shown that circular muscle preparations without the presence of the submucosal ICC network are spontaneously quiescent due to high K^+ conductance ([62] and Chapters 3–4). In the myenteric border of the full thickness preparations, the plateau potential gradually depolarizes. This may be associated with the accompanying resting membrane potential depolarization. Such an association is also seen after depolarization with increasing extracellular K^+ concentration [3], extracellular field stimulation [52]; carbachol [3] or TEA [2]. Changes in the plateau potential in the myenteric border of the FT preparations are unlikely due to intrinsic differences in K^+ conductance of circular muscle cells since no change in plateau potential or RMP was observed in the ICC-CM preparations.

5.5.2 Structural basis for pulling of membrane potential

In parallel with the heterogeneous electrical activity, the morphology, in particular the gap junction distribution, is not homogeneous in the musculature of canine colon. In the submucosal surface, circular muscle cells are coupled to one another and to ICC forming a three dimensional network by gap junctions [14]. A high density of gap junctions was only found in the submucosal border (up to 7 layers of circular muscle). The electron micrograph shown in figure 5.10 depicts a very high number of gap junctions (arrows) between circular muscle cells at this location. Hence, the electrical activities from different cell types in the submucosal border can be coupled through low resistance pathways resulting in *signal averaging effects* (−80 mV in the

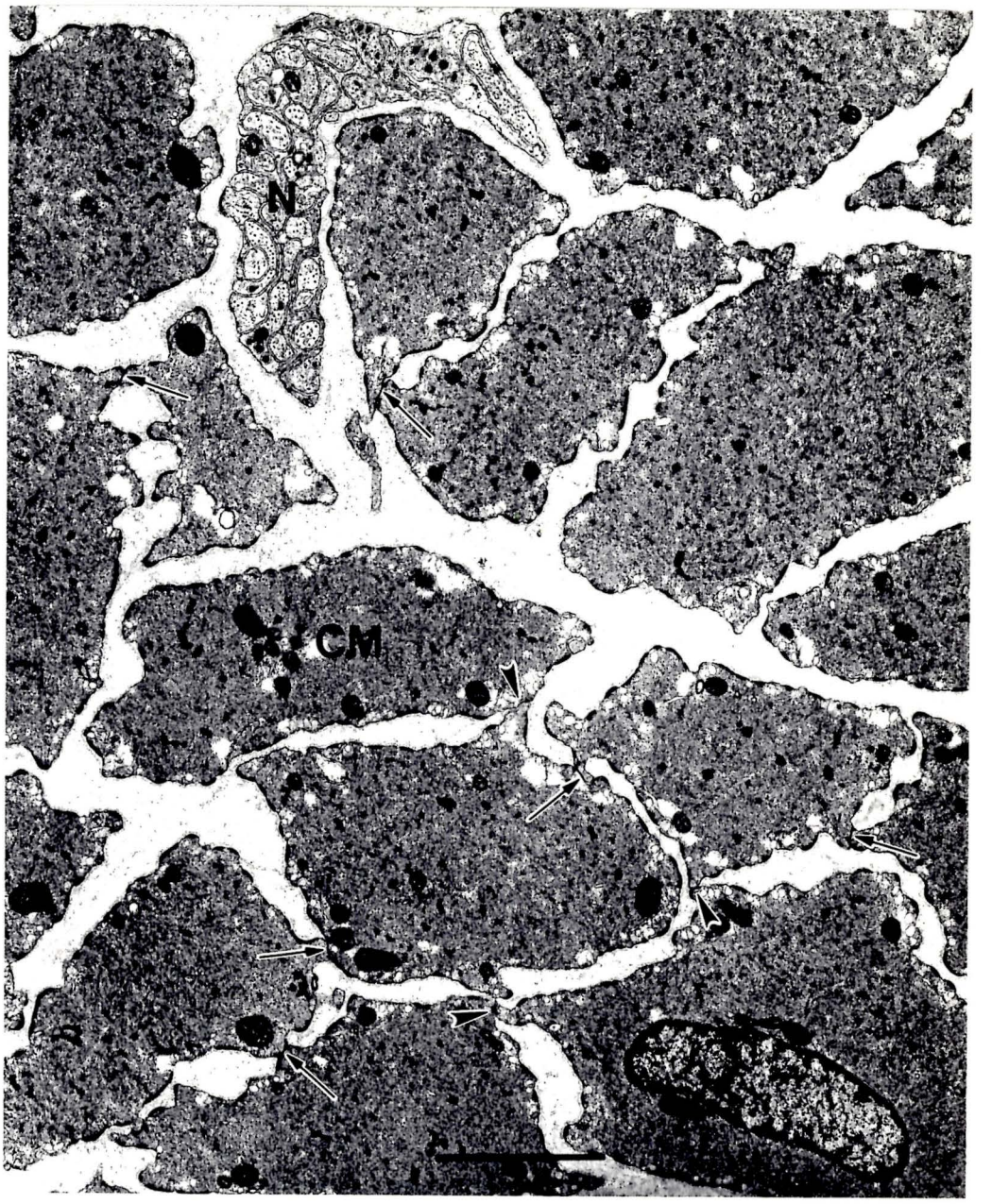

Figure 5.10: *High magnification micrographs of inner circular muscle.*
A cross section through the inner border of circular muscle (CM) layer near the submucosal border showing many gap junctions (arrows) between circular muscle cells. In the circular muscle layer, only the inner sub-division (up to 7 cellular layers) is well-coupled by gap junctions. N—nerve. Bar, 2 μm.

ICC network coupled to −62 mV in circular muscle averaging to −72 mV). Consistently, in the submucosal border, the area of constant resting membrane potential (0–76 μm) is similar to the area of high gap junction density (0–≈45-70 μm, including the submucosal ICC network). In the myenteric plexus area, small ICC processes coupled with either longitudinal or circular muscle cells were found in many narrow regions between circular and longitudinal muscle (see figure 5.9b and [15]). Thus, it is likely that ICC play a role in communication between the two muscle layers in the myenteric plexus area. Similarly, electrical communication between the two muscle types through interstitial cells has been suggested previously to occur in the small intestine of the cat [36, 79].

Circular muscle cells in the body of the circular muscle were found to form close appositions and intermediate contacts (≈60 nm); however, gap junctions can hardly be found. Despite lack of gap junctions, the electrical oscillations are synchronized since the slow wave frequency throughout the entire circular muscle is not different (the ultimate proof of perfect synchronization of electrical activity has to come from simultaneous recording of slow waves at different locations, showing constant phase relation in time). The structural data suggest that circular muscle cells may be coupled through a mechanism involving non-low-resistance pathways. Similarly, in the narrow regions of the myenteric plexus, the longitudinal and circular muscle cells are communicating apparently without the need of gap junctions. Although, under very rare occasions, tiny gap junctions can be found between the ICC processes and either muscle cell types, the relative effectiveness of tiny gap junctions and large areas of directly apposing membranes in permitting electrical coupling deserves further research. An alternative coupling mechanism, electric field coupling, has been shown to be theoretically feasible in cardiac and smooth muscle cells [73, 75].

5.5.3 Active propagation of slow waves in circular muscle

The present study provides additional evidence that slow waves originate in the network of interstitial cells of Cajal and smooth muscle cells located in the submucosal border. Slow waves generated in this pacemaker area propagate actively into the circular muscle layer. Evidence for active propagation is as follows: (1) the upstroke and plateau amplitudes of slow waves in the ICC-CM preparations remain unchanged after the first one third of the circular muscle layer (passive propagation would have caused an exponential decay). In addition, the upstroke and plateau amplitudes of the ICC-CM preparations were about 3 times larger than those of the FT preparations indicated the "apparent" exponential decay of upstroke and plateau amplitudes in the FT preparations could be a secondary effect of the decrease in resting membrane potential; (2) the slow wave duration stays very similar throughout the entire circular muscle (see also [2, 3]). Passive propagation would have increased the slow wave duration as propagating across the circular muscle; and (3) slow waves with a normal amplitude upstroke potential can be recorded at the myenteric plexus border [2, 3]. Further evidence for active contribution of circular muscle cells comes from studies showing that electrical oscillations can be induced in the canine colonic circular muscle disconnected from the submucosal ICC network ([62]; Chapters 3 and 4). Furthermore, an inward current activated at ≈ -60 mV has been reported in circular muscle myocytes of canine colon in a patch study [61].

A previous study using a cross sectioned preparation, cut cross sectionally through circular muscle cells, reported a membrane potential gradient of 40 mV and loss of slow waves at the myenteric border [70, 71]; the conclusion was reached that slow waves propagated passively. Passive propagation would mean that calcium channels in the circular muscle cells would not be activated which in turn would mean

that circular muscle cells would not participate in the generation of contractile activity. This is of course unlikely. We opted for a preparation similar to that used by Bauer *et al.* for the canine stomach [9, 10, 11, 12], that was cut along the long axis of circular muscle in an attempt to preserve as much electrical coupling as possible. Interestingly our results have much in common with results from Bauer *et al.* in the stomach (maintenance of slow waves throughout the muscle layer and evidence for active propagation of slow waves). It is likely that a 1 mm thick preparation, cross sectioned through the short axis of circular muscle cells, loses integrity of communication pathways.

5.5.4 Origin of the spikes in circular muscle

The amplitude of spikes in the circular muscle of canine colon in this study did not follow an exponential decay function starting from the myenteric plexus, unlike reported previously [71]. In the five FT preparations which exhibited spikes up to 65% (starting from 100%) of the circular muscle, the maximum spike amplitude was found to be at ≈72%. Although it is possible that the spike like action potentials generated in the longitudinal muscle can propagate into the circular muscle and modify the electrical activity (since the muscle layers are electrically coupled), the result of the present study indicates that the spikes do not need to be generated by specialized cells located in the boundary between the longitudinal and circular muscle layers and then propagate passively into the circular muscle [65, 70]. Consistently, spikes have been observed in circular muscle with the longitudinal muscle and myenteric plexus removed in the presence of carbachol [3], TEA [2] and depolarization [50, 52]. In addition, the spike like action potentials can be induced by $BaCl_2$ and Bay K 8644 in spontaneously quiescent circular muscle preparations disconnected from

the submucosal ICC network, longitudinal muscle and myenteric plexus (Chapter 4). Thus, circular muscle cells have intrinsic properties enabling them to generate spikes. Appearance of spikes in the circular muscle depends solely on its level of excitation and has no dependence on specialized pacemaker cells in the myenteric plexus region.

Chapter 6

Selective accumulation of methylene blue by Interstitial Cells of Cajal in the canine colon with preservation of slow waves

6.1 Abstract

Interstitial cells of Cajal (ICC) of canine colon selectively accumulated methylene blue under physiological experimental conditions, which enabled us to record intracellular electrical activity and do methylene blue staining simultaneously. The ICC network at the submucosal border of canine colon was stained by incubation with 50 μM methylene blue for 45 min. The stained network was composed of regularly scattered ICC cell bodies interconnected by long processes. The ICC appeared to be a unilayer at the submucosal surface since no overlapping of ICC cell bodies was observed.

The ICC network connected the circular muscle cells along the longitudinal axis of the colon since the circular muscle layer was divided into circumferentially oriented lamellae separated by connective tissue. 50 μM methylene blue slightly decreased the resting membrane potential and increased the duration of slow waves, leading to an increase in the force of phasic contractions, with no significant influence on other slow wave parameters. Methylene blue had neither electrophysiological nor mechanical effect on circular muscle preparations from which the submucosal ICC network was removed, indicating that the excitatory effects of methylene blue on circular muscle were mediated by ICC. In summary, the three dimensional aspects of the submucosal ICC network can be visualized using staining with methylene blue. This staining does not affect physiological characteristics of smooth muscle cells.

6.2 Introduction

Electrophysiological data have accumulated to show that slow waves are generated in specific areas of the gastrointestinal smooth muscle wall. In the canine stomach [11] and small intestine of the cat [47, 77], dog [47], rabbit [47] and mouse [80], slow waves are generated at the myenteric border of the circular muscle. In the colon of cats [19, 25] and dogs [4, 33, 34, 49, 71], slow waves are generated at the submucosal surface of the circular muscle. In the areas where electrophysiological evidence exists for generation of pacemaking activity, the presence of a network of interstitial cells of Cajal (ICC) has been demonstrated by electron microscopic (EM) studies [14]. Although EM studies can show the ultrastructure of the ICC, it is extremely time consuming to reconstruct the cellular organization by transmission electron microscopy of sections.

In the canine colon, it has been suggested that a group of well coupled ICC and smooth muscle cells located at the submucosal surface of the circular muscle layer is necessary for the generation of slow waves [4, 71]. A specific staining to visualize the ICC network at the light microscopic level would illustrate the 3 dimensional aspects of the ICC network such as (i) cell body density, (ii) distribution characteristics of the processes, (iii) whether or not the ICC network would penetrate into the circular muscle layer. Using vital staining with methylene blue (reviewed in [6]), the ICC network has been demonstrated in the Auerbach's plexus of the small intestine of various species, such as the rabbit, guinea pig and mouse (see review by Thuneberg [81]). In contrast, methylene blue staining of the ICC network has never been demonstrated in the colon of any species.

To assess whether or not uptake of methylene blue served as a vital stain, microelectrode recordings to monitor the change in electrical activity of the preparation were performed whilst the staining procedure was in progress. The specificity of the action of methylene blue, that it selectively stains ICC with little or no effect on tissue function, has recently been put into question [67]. It was suggested that methylene blue may not be a specific probe for colonic ICC because it also stained smooth muscle cells and it abolished colonic slow waves at the submucosal surface. This conclusion was challenged by Thuneberg [82]. If ICC were to selectively accumulate methylene blue, ICC may be selectively killed using the photodynamic properties of methylene blue.

The main objective of the present study was to investigate the possibility that methylene blue could serve as a specific vital stain for the submucosal ICC network in the canine colon to study its three dimensional aspects. A second objective was to study the physiological effects of methylene blue on colonic circular muscle while it

was taken up by ICC.

6.3 Method

6.3.1 Tissue preparation

An area of 3 x 3 mm (with the ICC network at the submucosal border facing up) of the ICC-CM preparation was pinned flat on the Sylgard bottom of a holder, with a tail (3 mm wide x 10 mm long) suspended from one edge of the pinned area as described in Chapter 4. The holder was transferred to a muscle bath with circulating prewarmed oxygenated Krebs solution. The free end of the tail was tied to a force transducer for measurement of the mechanical activity of the strip. To address the specificity of the action of methylene blue on ICC, the effects of methylene blue on CM preparations were studied.

6.3.2 Microelectrode recordings

After a stable impalement was obtained by a micoelectrode, Krebs solution was substituted by Krebs containing 50 μM methylene blue. During exposure of the tissue to methylene blue, illumination was kept low (dim light). It was attempted to maintain the same impalement during the entire staining procedure (approximately 45 min). However, because of the contraction induced by methylene blue (see Results section), stable impalement sometimes was difficult to achieve. When the microelectrode popped out of a cell, a small tickle was applied to the microelectrode in order to regain impalement of the same cell. If stable recording was not resumed, the electrode would impale a cell located one layer deeper. Recordings were always made in the first few (not more than 5) layers of cells.

6.3.3 Mechanical contraction measurements

The method used for quantifying the force of contraction has previously been described by [54]. The effects of methylene blue (with and without the presence of TTX (0.5 μM) and atropine (0.5 μM)) on the ICC-CM and CM preparations were studied. The effectiveness of TTX and atropine was verified by nerve stimulation using electrical field [53] before incubation of methylene blue for 45 min. In addition, the CM preparations used was proven to be viable and excitable by exposing the 0.5 mM $BaCl_2$.

6.3.4 Light and electron microscopy

After the staining procedure, the Sylgard was removed from the holder with the tissue still in place. The preparation was then fixed in a modified Karnovsky fixative of the following composition: formaldehyde (2 %), gultaraldehyde (2 %), picric acid (0.2 %) and phosphate buffer 0.1 M. The pH of the fixative was adjusted to 7.5. The stained tissue was examined and photographed under a Leitz Dialux microscope. For electron microscopy, the aldehyde-fixed tissue was cut in 0.5 × 1 mm pieces, washed with phosphate buffer, fixed with 2 % osmic acid in 0.1 M phosphate buffer for 1 h, dehydrated in a graded series of ethanol, block- stained for 1 h in 1 % uranyl acetate in absolute alcohol, and taken through propylene oxide to epon (Merck). Ultrathin sections were post-stained with alcoholic uranyl acetate and lead citrate, and examined in a Philips 300 electron microscope.

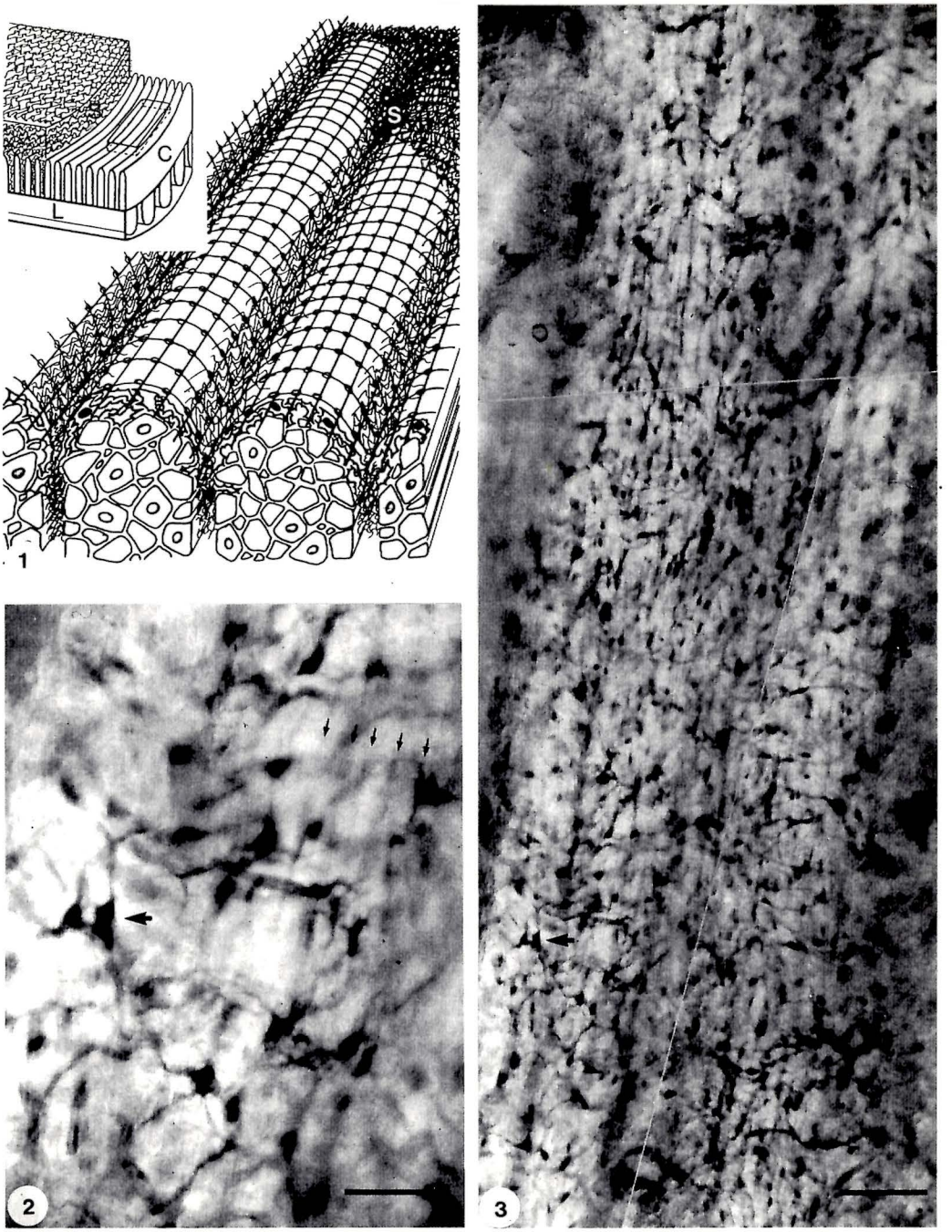

Figures 6.1—6.3

6.3.5 Data Presentation and statistical analysis

Data are presented as MEAN±SEM. The results in the mechanical contraction study were presented as the area under the curve for the period of 1 min. Hence, the analysis took into account both the tone and amplitude of phasic contraction of the strips. The statistical significance of the datum sets under different conditions were compared by student t-test.

6.4 Results

6.4.1 Selective accumulation of methylene blue by ICC

50 μM methylene blue stained the ICC network at the submucosal border of the canine colon circular muscle. Figures 6.2 and 6.3 illustrate the methylene blue stained ICC network in the submucosal plexus using light microscopy. Electron micrographs are shown in figure 6.5 demonstrating that the methylene blue stained branching cells are indeed ICC. In all preparations examined, 30–45 min exposure to 15 to 50 μM methylene blue resulted in a visible staining of ICC. During processing for electron microscopy, the dye is only partially preserved in the cells. However, irregular electron-dense deposits in the stained cells, as compared with controls, are probably derived from light microscopically visible intracellular precipitations of methylene blue picrate (figure 6.5). Methylene blue did not stain the circular muscle cells except for a few scattered cells in the innermost layer in direct contact with ICC. Damaged areas, such as the cut edges and locations where pins were pierced through the tissue, were coloured pale blue, 5 to 10 min after the start of the methylene blue perfusion, well before any observable accumulation of methylene blue in the ICC could be detected.

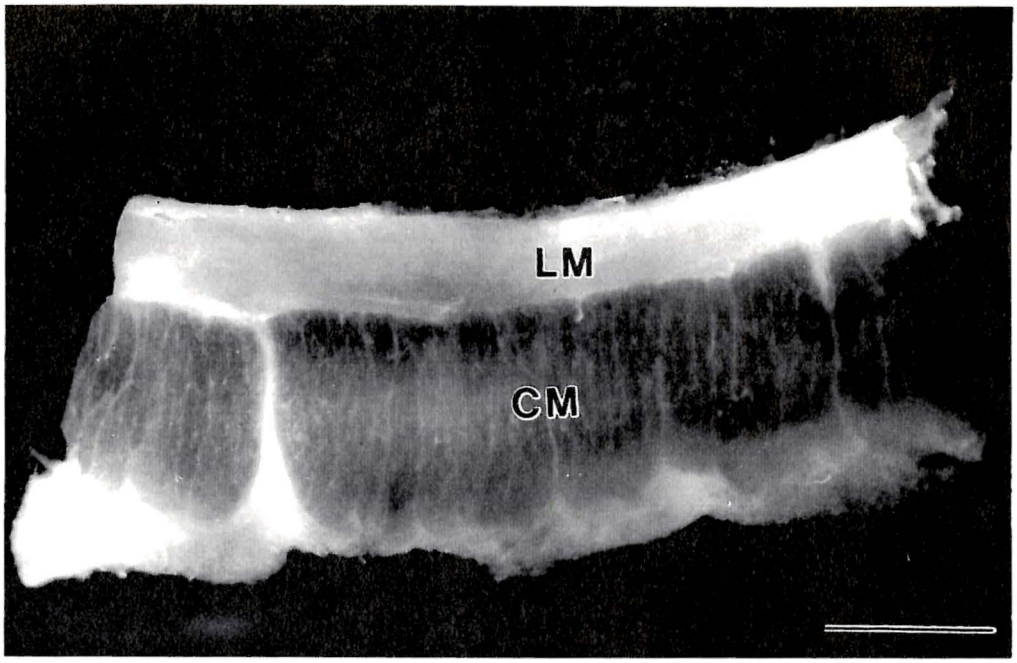

Figure 6.4: *Low magnification myographs of the canine colonic musculature.*
A hand-cut glutaraldehyde fixed preparation, cut along the transverse axis of the cirular muscle cells, illustrates the division of the circular muscle (CM) layer. LM — longitudinal muscle (× 22, bar 1mm).

In the actively stained areas, hardly any overlapping of ICC cell bodies was observed which suggests that the ICC network in the submucosal surface of canine colon is composed of a single layer of ICC which, connected through their processes, creates a three dimensional ICC network with adjacent smooth muscle cells covering the entire submucosal surface.

In all the methylene blue stained preparations, the submucosal ICC network was observed to be at different focal planes under the light microscope no matter how flat the preparation was laid out. The submucosal surface presented a smooth ridge-

Figure 6.5: *Electron micrographs of canine colon incubated with methylene blue.* (a) Tissues were incubated for 45 min at 37°C before fixation, similar to figures 6.2–6.3, except that the aldehyde fixative included picrate. Figure 6.5 shows the submucosal circular muscle border, with ICC (single asterisks), in contact with varicose axons of a small nerve (N) of the submuscular plexus. One ICC profile shows a reflexive gap junction and a gap junction (both encircled) with an irregularly branching smooth muscle cell (double asterisk), which contacts the cells of the circular muscle proper. Note that ICC as well as circular-muscle cells appear intact (×9,100; bar = 1 μm). (b) Higher magnification of ICC in figure 6.5a. Characteristic ultrastructural features of the ICC are recognized: a prominent basal lamina, numerous caveolae, numerous mitochondria in typical condensed configuration, tightly packed filaments, and few cisternae of rough endoplasmic reticulum. The only consistent change of ultrastructure, after methylene blue, was a dilatation of components, part of which could be recognized as smooth endoplasmic reticulum. These smaller vesicular structures most often appeared empty, whereas larger vesicles (arrows; secondary lysosomes) often contained conglomerates of deposits. Similar structures were seldom observed in control tissue. No consistent changes after methylene blue were seen in the smooth muscle cells (×21,000; bar = 1 μm).

and-grove appearance (see figure 6.2). Low magnification micrographs of thick hand-cut sections cut along the transverse axis of circular muscle illustrate the subdivision of circular muscle in thin circularly oriented lamellae (figure 6.4) separated by connective tissue septa forming ring-like structures around the circumference of the colon. A schematic diagram of the orientation and subdivision of the muscle layers is shown in figure 6.1.

To study the invagination of ICC into the circular muscle layer, four blocks from each of 38 samples were examined from 12 dogs. For each block, 5–10 ultrathin sections were examined to a depth of 30–50 cells. All sections included small or large connective tissue septa. ICC extended into septa to a depth of a few cells layers. Not a single ICC was observed deeper than 5 cells.

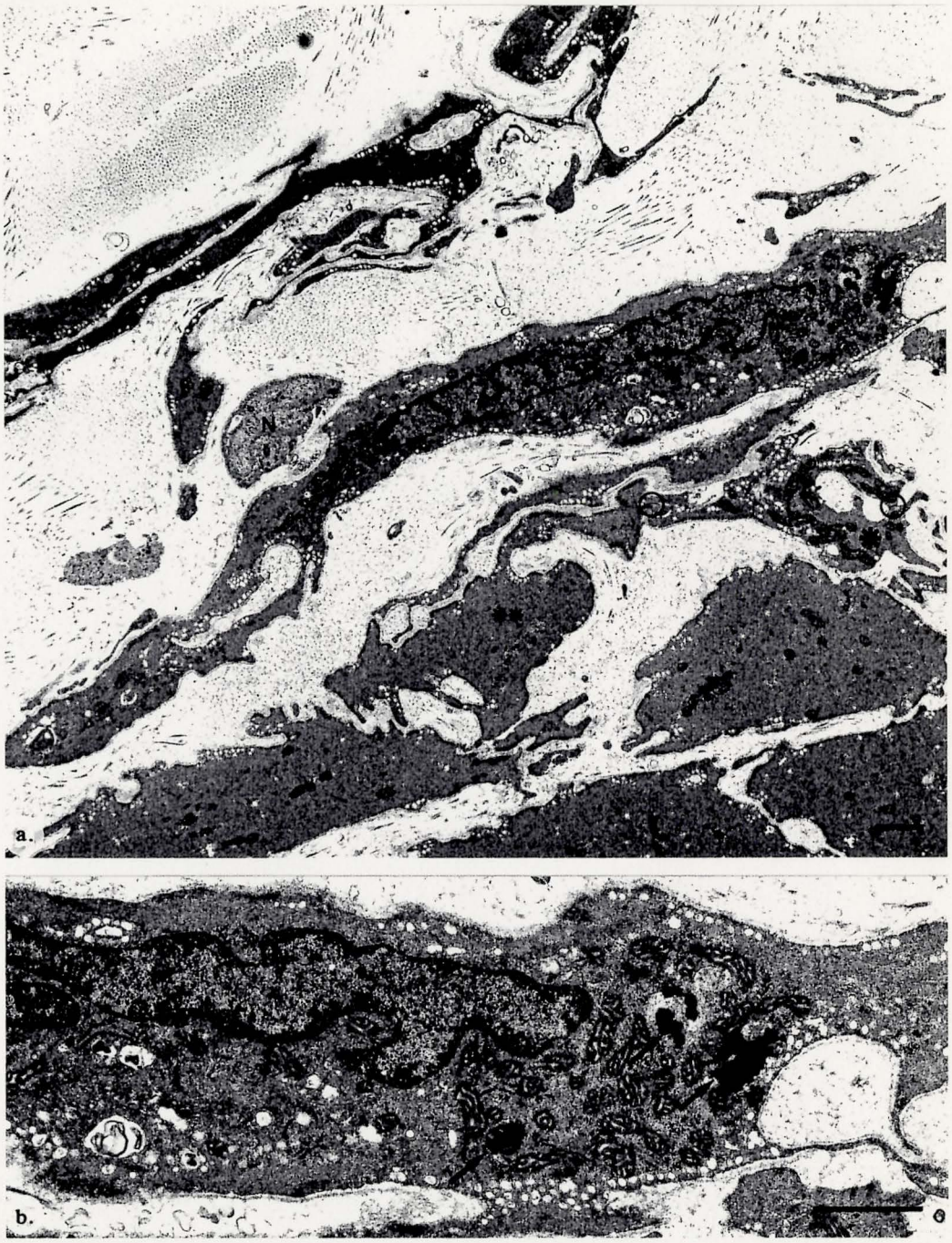

Figure 6.5

Table 6.1: *Pharmacological effects of 50 μM methylene blue on the slow wave parameters of canine colon.*

	KREBS	METHYLENE BLUE
RMP (mV)	−72.2±0.7	−70.0±0.8**
Frequency (cpm)	5.1±0.2	4.9±0.2
Duration (s)	3.4±0.3	5.0±0.6*
Upstroke Amplitude (mV)	37.6±1.2	36.0±1.2
Plateau Amplitude (mV)	31.8±1.4	30.3±1.3
Plateau Potential (mV)	−40.4±1.0	−39.7±0.8
Rate of Rise (mV/s)	174.7±19.1	134.9±11.3

(n=12)

* significantly different from the duration in Krebs solution ($P < 0.05$)

** significantly different from the resting membrane potential (RMP) in Krebs solution ($P < 0.01$)

Contacts made between ICC and smooth muscle cells were difficult to quantify. Those smooth muscle cells in direct contact with ICC had smaller profiles and a more branched appearance than circular muscle cells in the body of circular muscle. The study of thin sections by electron microscopy suggested that an ICC makes contact with up to 10 processes from neighboring ICC and smooth muscle cells.

6.4.2 Effect of methylene blue on slow wave activity

Methylene blue slightly decreased the resting membrane potential and increased the slow wave duration in ICC-CM preparations (table 6.1; figures 6.6 and 6.7). The resting membrane potential changed from −72.2±1.1 mV to −70.0±0.8 mV (n=12, $P < 0.01$) within the first 30 min. Thereafter, the resting membrane potential

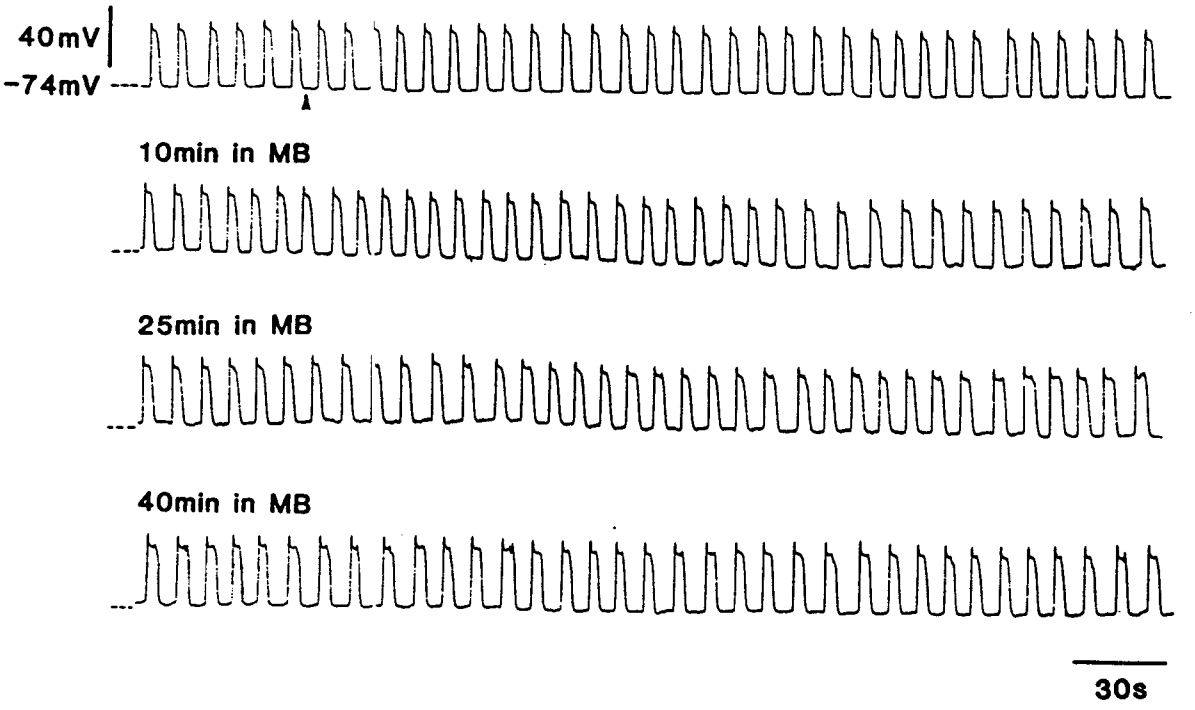

Figure 6.6: *Effects of 50 μM methylene blue on the colonic slow wave activity*
Intracellular recording of a cell at the submucosal surface of an ICC-CM preparation. The recording shows sections of a continuous recording from the same cell. Superfusion with 50 μM methylene blue (MB) was started at the arrow. The beginning of the second, third and fourth traces show slow waves after incubation in MB for 10 min, 25 min and 40 min, respectively. 50 μM MB slightly reduced the resting membrane potential (from −74 mV to −73 mV) and increased the slow wave duration. Note that a steady resting membrane potential was achieved after 15 min perfusion with 50 μM MB. In addition, MB also sporadically induced spikes on top of the longer duration slow waves after incubation for 30 min. The calibration bars apply to all traces. The dotted lines indicate the −74 mV resting membrane potential in all the traces.

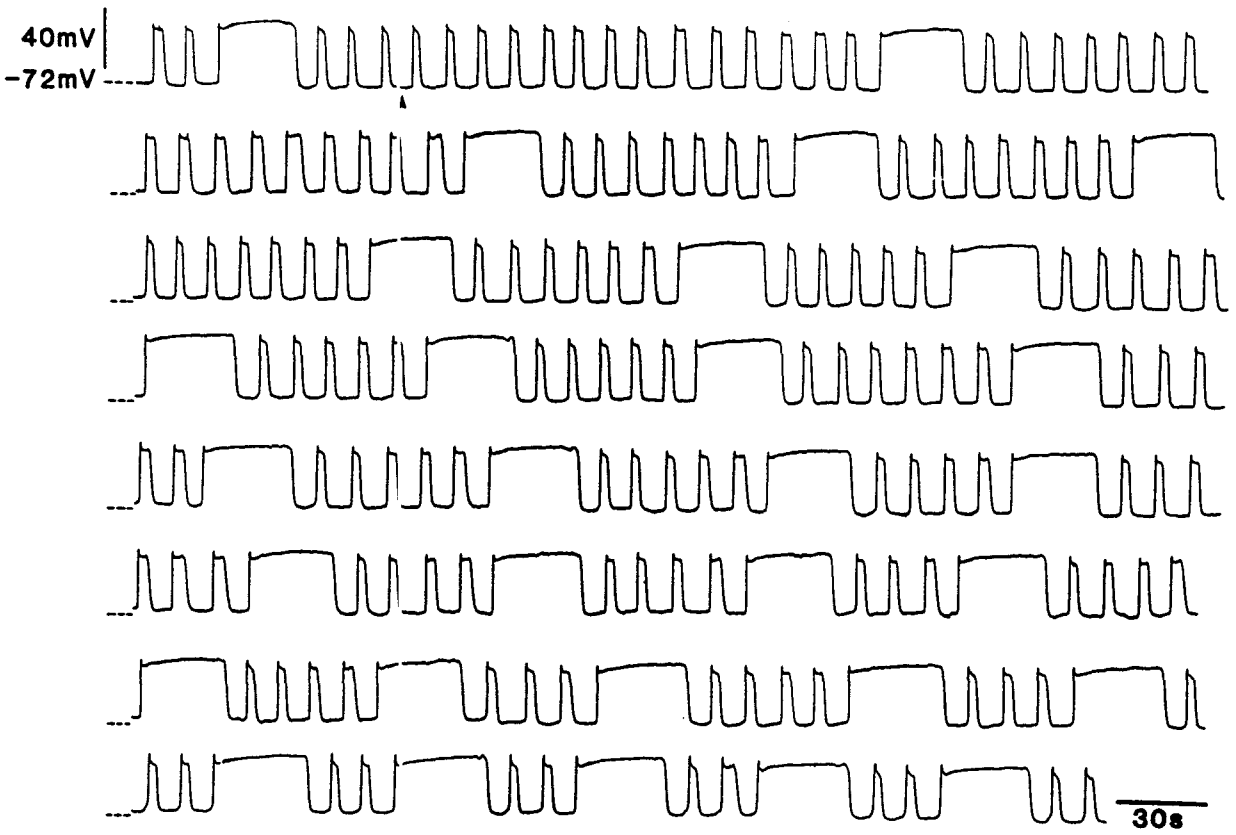

Figure 6.7: *Effects of 50 μM methylene blue on colonic slow wave activity exhibiting intermittent prolonged slow waves.*

Intracellular recording of a cell at the submucosal surface of an ICC-CM preparation. The experiment shows a continuous recording from the same cell during a 45 min incubation period with methylene blue (MB). Similar to figure 6.6, the resting membrane potential of slow waves decreased slightly (from −72 mV to −70 mV) and became steady after about 15 min. Note that in addition to prolongation of slow waves, the appearance of the long duration slow waves became more frequent as the MB incubation period increased. The calibration bars apply to all traces. The dotted line indicate the −72 mV resting membrane potential in all the traces.

Table 6.2: *Mechanical excitation of ICC-CM and CM strips by methylene blue and* $BaCl_2$

Preparations	Krebs	Atropine+TTX	Methylene blue	$BaCl_2$
ICC-CM (n=24)	0.3±0.1	0.2±0.1	0.5±0.1*	3.4±0.6[1,***]
ICC-CM (n=18)	0.4±0.1	—	0.6±0.1**	3.5±0.8[2,**]
CM (n=25)	—	—	—	3.3±0.5

[1] n = 21; [2] n = 12

* significantly different from that in atropine + TTX ($P < 0.05$)

** significantly different from that in Krebs solution ($P < 0.01$)

*** significantly different from that in methylene and atropine + TTX ($P < 0.01$)

All data are in the unit of $mN \cdot min/mm^2$

remained unchanged for the rest of the staining procedure. Superfusion with 50 μM methylene blue also increased the slow wave duration (from 3.4 ± 0.3 s to 5.0 ± 0.6 s, n=12, $P < 0.05$). The effect of 50 μM methylene blue on other slow wave parameters, such as upstroke amplitude, plateau amplitude, frequency and rate of rise, were insignificant. In parallel with membrane depolarization and increase in slow wave duration, the amplitude and duration of phasic contractions were enhanced by 50 μM methylene blue (table 6.2).

In the CM preparations, the circular muscle cells were quiescent with a resting membrane potential equal to -63.3 ± 0.7 mV (n=3) which was consistent with results reported previously (see Chapter 4; [69]). The electrical activity remained identical

to control for the entire 45 min perfusions with 50 μM methylene blue.

6.4.3 Mechanical excitation by methylene blue

In contrast to CM preparations (n=25), in which 50 μM methylene blue neither changed the tone nor induced any phasic contraction during 45 min incubation, the force of phasic contractions of ICC-CM preparations (n=18) was increased from 0.4 ± 0.1 mN·min/mm^2 to 0.6 ± 0.1 mN·min/mm^2 (representing a 1.5 times increase). In the presence of TTX and atropine (n=24) methylene blue excited the ICC-CM strips from 0.2 ± 0.1 mN·min/mm^2 to 0.5 ± 0.1 mN·min/mm^2 (representing a 2.3 times increase), indicating that methylene blue excited the colonic circular muscle probably not through an action on active intrinsic nerves. The mechanical contraction data from ICC-CM and CM strips under different conditions are summarized in table 6.2.

To demonstrate that the CM preparations were viable, despite the fact that they could not be excited by methylene blue, all ICC-CM and CM strips were subjected to $BaCl_2$. In the presence of 0.5 mM $BaCl_2$, consistent with our previous observations (Chapters 3 and 4, [62]), all 25 CM strips contracted phasically with the normalized force equal to 3.3 ± 0.5 mN·min/mm^2 which was not significantly different from the force of contraction generated by $BaCl_2$ in the ICC-CM preparations with and without the presence of TTX and atropine (table 6.2).

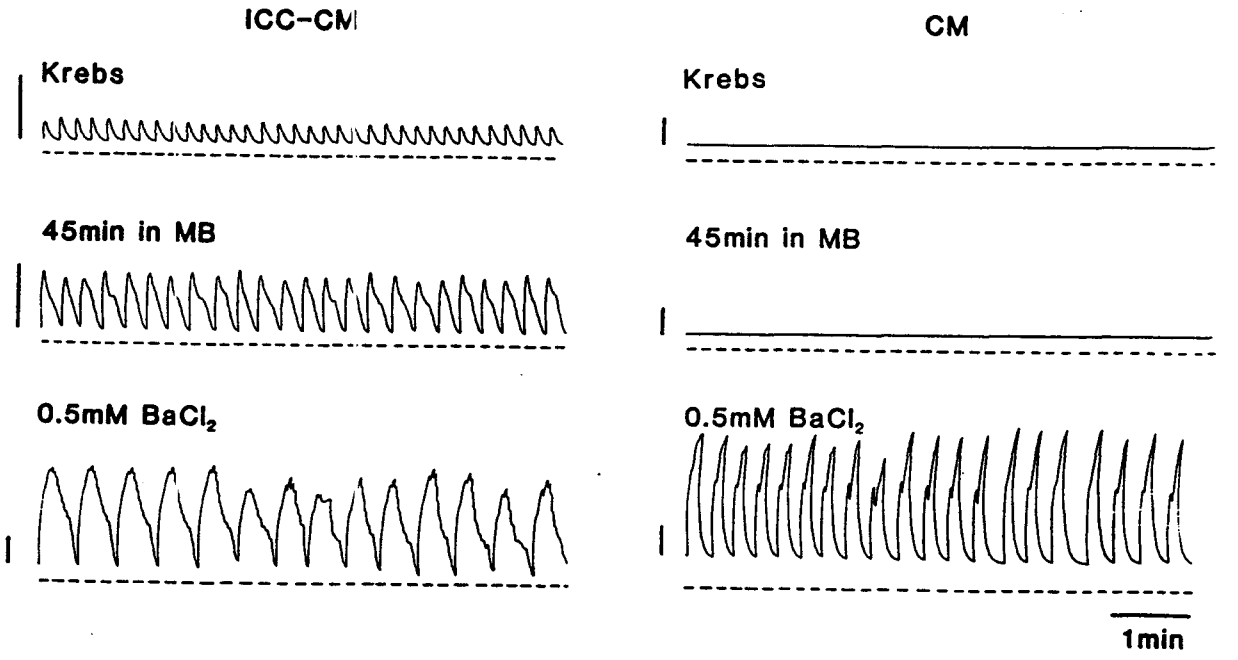

Figure 6.8: *Effects of 50 μM methylene blue on phasic contractions of ICC-CM and CM preparations.*

After 45 min incubation with methylene blue (MB), the amplitude of phasic contractions in the ICC-CM preparations increased dramatically without change in tone which was consistent with the fact that the resting membrane potential only decreased slightly in the presence of 50 μM MB. MB had no effect on the CM preparation. 0.5 mM $BaCl_2$ evoked phasic contraction in the CM preparation and further increased the amplitude of phasic contraction in the ICC-CM preparations. The tone in both preparations was increased in the presence of $BaCl_2$. The dotted line indicates the tone of preparations in Krebs and MB. All the calibration bars represent 3 mN/mm^2 *except* in the CM preparations under Krebs and MB solutions in which the calibration bars represent 0.3 mN/mm^2.

6.5 Discussion

6.5.1 Methylene blue is a specific probe for staining of canine colon submucosal ICC

Using methylene blue staining, the 3 dimensional aspects of the ICC network at the submucosal border of the canine colon were visualized. Consistent with the electronmicroscopic study performed by Berezin *et al.* [14], the submucosal ICC network forms a syncytium. In the present study, we observed hardly any overlapping of ICC cell bodies indicating that the ICC network in the submucsoal surface (submuscular plexus) of canine colon is composed of a single layer of ICC which, connected through their processes, creates a three dimensional ICC network with adjacent smooth muscle cells in the submucosal border.

The circular muscle layer of the canine colon was seen to be divided into discrete, circularly oriented lamellae, separated by connective tissue septa. This organization is much more elaborate than previously described [84] and bring into the question how the activity of the circular muscle is synchronized along the long axis (axial direction) of the colon. *In vivo* recordings from the dog colon revealed a cyclic occurrence of bursts of contractions propagating in the anal direction at a speed of 3–20 cm/min [68]. Similarly, Fioramonti *et al.* [39] recorded propagation of spike bursts at 14 cm/min. An *in vitro* study in the cat colon showed that slow waves were phase locked in the axial direction and were propagating at a velocity around 18 cm/min [26]. Furthermore, this study clearly indicated that the downstream propagation occurred through neither the circular nor the longitudinal muscle layer but through the submucosal network of interstitial cells of Cajal. The present study provides a structural basis for this observation. The methylene blue staining makes it clear at a

light microscopic level that the ICC network runs continuously, crossing the septa, at the submucosal surface. There are infoldings of the network but ICC extended into septa to a depth of only a few cell layers.

Methylene blue accumulates in ICC of canine colon, while it does not accumulate in smooth muscle cells except for (in some preparations only) a small number of smooth muscle cells, presumably those in gap junctional contact with ICC [14]. It is feasible that methylene blue, following accumulation in the ICC cytoplasm, spreads through gap junctions into smooth muscle cells.

As reported by Thuneberg *et al.* [82, 83], methylene blue is an effective indicator of tissue viability. Accumulation as well as rejection is dependent on the viability of the cells. If cells are damaged, the mechanism to accumulate or to reject methylene blue will be lost, and the cells will become coloured pale blue. We confirmed this for the canine colon since cut edges and cells damaged by pinning turned pale blue, while the entire circular muscle layer (with the noted exception in the submucosal border) remained unstained after 45 min in 50 μM methylene blue. Our data suggest therefore that pale blue colouring of tissue by methylene blue [67] may indicate extensive tissue damage.

6.5.2 The excitatory effects of methylene blue

Methylene blue caused slight but consistent excitation of circular smooth muscle preparations that included the submucosal ICC. The excitation (depolarization with prolongation of slow waves) was markedly less than that caused by an IC_{50} of the excitatory drugs carbachol (cholinergic agonist acting through blockade of K conductance) [3], TEA (a K channel blocker) [2] and substance P (excitatory neuropeptide) [54]. Prolongation of the slow waves is a feature common to all excitatory actions,

including current induced depolarization [52], hence should not be seen as an activity specifically mediated by intrinsic nerves as proposed previously [66]. Indeed, the excitatory effects of methylene blue were not mediated by active intrinsic nerves as the methylene blue induced contraction in the ICC-CM preparations was not abolished by TTX and atropine. It is most likely caused by a direct effect on interstitial cells of Cajal since 50 μM methylene blue did not electrophysiologically nor mechanically affect circular muscle preparations without the intact submucosal ICC network.

One might hypothesize that the excitatory effects of methylene blue in the canine colon could be caused by inhibition of nitric oxide (NO) synthesis since (i) methylene blue has been shown to inhibit NO synthesis in vascular smooth muscle [60, 85] and (ii) it has recently been demonstrated that the non-adrenergic non-cholinergic (NANC) inhibitory neural action in the canine colon is mediated by nitric oxide or a similar L-arginine derived compound since the NANC inhibitory response is blocked by Nω-monomethyl-arginine and reversed by a high concentration of L-arginine but not D-arginine (Huizinga and Tomlinson, unpublished). However, preincubation of the ICC-CM preparations with Nω-monomethyl-arginine (at concentrations previously shown to be sufficient to completely block the NO synthesis has no effects on the methylene blue induced contraction. Therefore, it is very unlikely that methylene blue excites the colonic circular muscle through the inhibition of NO synthesis unless there is an NO synthesis pathway that cannot be inhibited by Nω-monomethyl-arginine, located in the submucosal ICC network.

6.5.3 The photosensitivity of methylene blue

The photodynamic action of methylene blue is well-known [6, 42], if not understood chemically, and is in recent years investigated as a possible means to inactivate or

kill, in a selective way, bladder tumour cells [42]. It is therefore necessary, in a study of methylene blue, that experimental conditions are chosen that allow the distinction between effects of methylene blue per se and methylene blue plus light.

The small amount of depolarization and increase in slow waves duration by methylene blue reported in the present study were caused by the actual excitatory effects of methylene blue and were not an artifact of the dim light environment since performance of some experiments in complete darkness or slight increases in light intensity altered neither the electrical nor the mechanical effects of methylene blue.

A previous report noted that methylene blue caused abolishment of slow waves in the canine colon owing to depolarization of the circular muscle [67], at a concentration 5 times lower than the one used in our study. The most likely explanation is that the dramatic depolarization was caused by illumination of the methylene blue-exposed tissue, similar to that observed in the mouse small intestine [82, 83]. In preliminary experiments, we have observed such dramatic changes in slow wave activity following illumination of our methylene blue-stained colonic preparations. In addition to the effects on slow wave activity, specific ultrastructural changes in ICC were observed after exposure to light.

In summary, the present study a) shows the first application of the use of methylene blue as a specific stain for colonic ICC. It characterizes the 3 dimensional aspects of the canine colon submucosal ICC network, b) proves that methylene blue works as a vital stain since the capacity to generate action potentials by the tissue remains present; and, c) suggests the possibility of producing selective damage to ICC (making use of the photodynamic action of methylene blue) after selective accumulation of methylene blue by ICC.

Chapter 7

Concluding remarks

7.1 Physiological roles of ICC

Since the hypothesis proposed by Thuneberg in 1982 that ICC are the intestinal pacemaker cells [80], research has been devoted to investigate the role of ICC in control of gastrointestinal motility. Although direct proof of ICC as the pacemaker cells in the gastrointestinal tract is not available, the physiological importance of ICC is beyond doubt. Results presented in this thesis provide insights into the physiological roles of ICC in canine colon physiology.

7.1.1 As pacemaker cells

Slow waves have been recorded in a submucosal interstitial cell of Cajal by validating that the impalement of the microelectrode was in an ICC using electron microscopy [4]. However, this did not prove that slow waves recorded were indeed generated by the ICC since these cells in the submucosal border are extensively electrically coupled by gap junctions to smooth muscle cells [14]. Thus, the activity could have been

generated in the neighbouring cells and propagated to the site of recording. Using the circular muscle preparation without the intact submucosal ICC network (Chapter 3 and 4), we showed that, in this tissue, the ability of generating spontaneous slow waves was abolished. Although electrical oscillations can be induced, the ionic conductances and metabolic dependence of the induced electrical oscillations are very different from the spontaneous and sustained slow waves recorded at the submucosal surface of ICC-CM preparations. Therefore, these results demonstrate that slow waves, or more precisely *pacemaker potentials*, are not generated in the circular muscle.

Studies using the CM preparation have not yet proven that ICC per se are the pacemaker cells in colon. Because of the mechanical dissection, a few layers of smooth muscle were removed with the submucosal ICC when preparing the CM preparations. Therefore, we cannot exclude the possibility that the submucosal network, including the submuscular plexus and the immediately adjacent smooth muscle cells, is responsible for the generation of pacemaking potentials. In fact, a group of well coupled ICC and circular muscle cells has been hypothesized to be essential for producing slow wave activity in the canine colon [4, 71]. In the methylene blue study (Chapter 6), we revealed the presence of a one-cell-thick irregular branching smooth muscle cells, orientated obliquely (sometimes even orthogonally) to the neighbouring circular muscle cells, located in between the submuscular plexus and the ordinary circular muscle cells. Structurally speaking, there is no reason to deny the hypothesis that the network of ICC including the immediately adjoining irregularly branching smooth muscle cells in the submucosal surface is, as a unit, the pacemaker generating slow waves in the canine colon.

7.1.2 As an intercellular communication pathway

While studies devoted to the pacemaker role of ICC in generating slow waves are harbouring the literature, evidence for the role of ICC in facilitating intercellular communication is negligible. Morphologically, it is logical to conceive that ICC increase the efficiency in electrical communication between cells because ICC possess a lot of long processes which terminate at smooth muscle cells and other ICC. Apart from the results discussed in Chapter 5, which suggest that longitudinal and circular muscle cells may communicate through directly apposing membranes in the narrow areas of the myenteric plexus, ICC may serve as an intercommunication pathway between the muscle layers, in particular in the thicker myenteric regions where immediately apposing membranes between the two types of muscle cannot be estabished. Close contacts between ICC processes and the two muscle types have been identified, although very infrequent, in thick myenteric plexus regions [15].

Preliminary experiments indicated that it was very difficult to record a electrotonic pulse by a microelectrode in the myenteric surface of the longitudinal muscle with the circular muscle removed using the Abe-Tomita set-up discussed in Chapter 2. However, leaving the circular muscle on and orienting the strip in the way that the long axis of the circular muscle was located in the stimulating chamber, an electrotonic pulse injected into the circular muscle was seen to propagate into the longitudinal muscle next to the myenteric plexus. Figure 7.1 illustrates the effects of hyperpolarization on the pattern of electrical oscillations in the circular and longitudinal muscle of a FT preparation. Within the context of intercellular communication, this figure shows that the muscle layers at the myenteric interface are electrically coupled which may well be via myenteric ICC. Gap junctions, which may facilitate electrotonic coupling, are the highest in density at the interface between the muscle

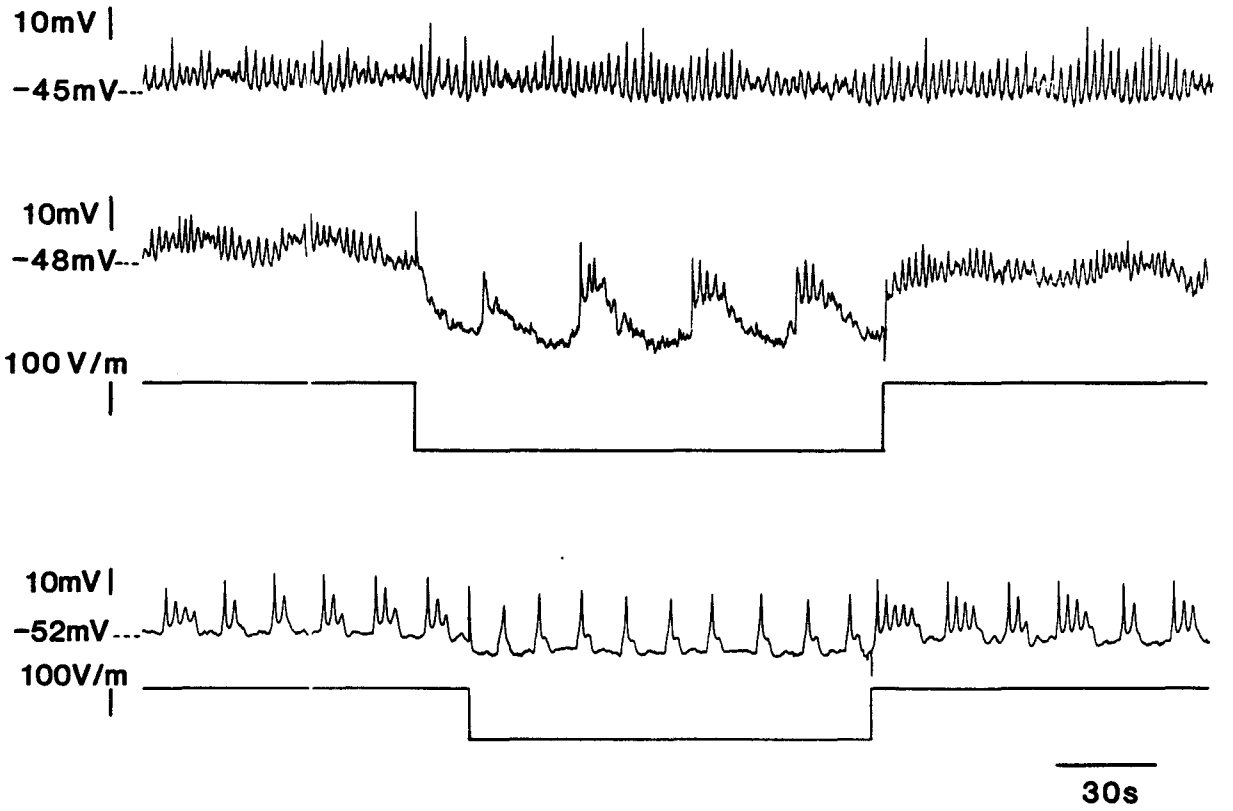

Figure 7.1: *Effects of hyperpolarization induced by extracellular electrodes in the FT preparations.*

A FT preparation is mounted in the Abe-Tomita bath set-up with the long axis of the circular muscle stretched in the stimulating chamber. The first panel displays the electrical activity in the middle of longitudinal muscle layer. The second panel shows the electrical activity in a longitudinal cell very close to the myenteric plexus. When hyperpolarizing the impaled cell to approximately −60 mV, slow-wave-like underlying oscillations, having a frequency of about 2 cpm, with spikes superimposed on the plateau were observed. The last panel demonstrates the electrical activity at about 80% of the circular muscle and its voltage dependence. Note the difference in frequency of the underlying oscillations.

layers than in the myenteric border of either muscle types.

7.1.3 As a modulator of the frequency of bursts

The ability of the canine colon longitudinal muscle to exhibit bursting oscillatory activity and its dependent on extrinsic stimuli have long been intriguing and interpreted as a potential animal model for human colon [59] which exhibits a wide range of oscillation frequencies including bursting activity [20, 58, 59]. However, the mechanism of how the bursting frequency is regulated is unknown. The bursting activity is observed in the longitudinal muscle of canine and human colon without a recordable underlying potential. Figure 7.1 indicates that in the FT preparation, it is possible to observe the underlying oscillations in the longitudinal muscle by hyperpolarization. Therefore, it allows us to speculate that perhaps the underlying oscillatory potential during the bursting activity is masked by the normally depolarized longitudinal muscle cells. If the myenteric ICC are responsible for a certain kind of pacemaking activity, they may be responsible for the generation of underlying oscillatory potentials that regulate the frequency of bursts but *not* for the generation of spike-like-action-potentials (see Chapters 4 and 5).

7.1.4 As a metabolite supplier

There is no doubt that the excitability of circular muscle cells disconnected from the submucosal ICC network is dramatically depressed. Our results suggest that this is caused by a high K^+ conductance. A possible explanation for this is that, in intact tissue, the submucosal ICC are producing certain metabolite(s) (ICC are metabolically active as indicated by the numerous and large mitochondria) which diffuse to the neighbouring circular muscle cells leading to the maintenance of the

circular muscle excitability. One of the candidates is ATP. Deficiency in ATP not only reduces cellular metabolic activity but may also decrease the cell excitability resulting from activating the ATP sensitive K^+ conductance [32].Consistently, abundant gap junctions are found in this region to provide a cytoplasmic continuity for metabolic coupling (see next section).

7.2 Physiological roles of gap junctions

7.2.1 Metabolic coupling

As indicated in the last section, the most obvious role of gap junctions is to allow sharing of intracellular metabolic substances between cells, termed as "metabolic coupling". There may be a type of cells (perhaps ICC in the canine colon) that continuously produce certain substances that is supplied to neighbouring cells (circular muscle cells). Such substances would be considered as trophic factors (as discussed in Chapter 4) for the target cells. In the canine colon, the slow wave frequency has been proposed to be regulated by a metabolic clock dependent on cyclic AMP [56]. The enormous number of large gap junctions found in the submucosal border of circular muscle can well be used for providing metabolic synchronization among pacemaker cells to generate a *local* pacemaker potential. In other words, metabolic equilibrium is necessary to be achieved in a minimum number of cells that need to fire synchronously in order to generate sufficient current to depolarize the membrane to reach the threshold for activating voltage-operated ionic channels to produce a subsequent membrane potential oscillation (see the following section). Thereafter, pacemaker potentials from different pacemaker loci (or *pacemaker units*) at the submucosal surface can be synchronized by electrical coupling.

7.2.2 Electrical coupling

It is obvious that gap junctions lead to membrane continuity between cells. The action potential in one cell can propagate to the next cell with a similar mechanism, explained by local circuit theory, as in the axon. This coupling mechanism allows electrical events to be coupled through a low resistance pathway. Based on the result discussed in Chapter 5, low resistance coupling has been shown electrically and morphologically to be the mechanism for electrical communication in the submucosal border of the circular muscle of canine colon.

Another passive membrane parameter, that is directly associated with resistance, is capacitance. Using the concept of relaxation oscillators, a computer model has been successfully developed for simulating the frequency gradient in the canine small intestine [30]. It was observed that the coupled frequency in intact tissue was higher than the intrinsic frequency in any location of the tissue. Incorporating a capacitive component in the coupling parameter of two bi-directionally coupled relaxation oscillators, it has been shown that the entrained frequency can be higher than the intrinsic frequency of either oscillator if the backward coupling coefficient exceeds a threshold level [7]. Such coupling properties may be operating for the canine small intestine in which the entrained frequency is higher than the highest intrinsic frequency in isolated segments of the canine small intestine. In addition to the resistive component, the capacitive component plays an important physiological role in electrical coupling between small segments of tissue with oscillations of different intrinsic characteristics, hence is referred to as resistive-capacitive (RC) coupling. However, the capacitive component of gap junctions has not yet been identified. Until then, one has to be cautious to refer gap junction coupling to RC coupling.

Low resistance coupling may also play a role in electrical communication

between the two muscle layers at the myenteric plexus through tiny gap junctions between ICC processes and smooth muscle cells. A similar speculation can be made for the circular muscle; however, the presence of tiny gap junctions in the circular muscle layer is unclear. Are these cells coupled by gap junctions that cannot be recognized by electron microscopy? If there are such connections, is that the major pathway for electrical coupling? If such connection does not exist, how are these cells electrically coupled? The same questions are important in other tissues, such as longitudinal muscle of intestine and mouse myometrium before parturition [63], in which electrical oscillations are perfectly synchronized and yet no gap junctions can be identified so far.

In intestinal smooth muscle, the mechanism through which electrical oscillations are synchronized is unclear. In heart tissue, such as the sino-atrial node [16] and ventricular tissue of lower mammals [73, 75], similar questions have been asked owing to the low frequency of appearance and small size of gap junctions. Based on the electric field theory, a theoretical model has been developed to show that electrical oscillations can successfully propagate down a chain of cells between which no low resistance pathways exist [75]. Although it is promising that oscillations can propagate without gap junctions, the electric field coupling cannot be immediately accepted as the electrical coupling mechanism for the intestinal smooth muscle without observable gap junctions since these cells are of different dimensions and possess different passive membrane parameters than vascular muscle cells.

7.2.3 Disadvantage of gap junction coupling

Many morphologists and physiologists believe that gap junctions are the only means for electrical coupling, yet a *severe* drawback of low resistance coupling in active

areas, in particular the pacemaker region, is often overlooked; it is the problem of *current shunk*. For a pacemaker cell to generate an action potential, it requires to produce an active current that is sufficient enough to depolarize the cell membrane to activate corresponding ionic channels so as to complete the entire action potential. If pacemaker cells are connected by low resistance pathways, the active current will leak to neighbouring cells before it can depolarize the membrane *unless* the neighbouring cells are producing active current of similar magnitude simultaneously. It has been suggested that because of the problem of current shunk, the gap junction density is the lowest in the core of the sino-atrial node than in any other parts of the heart tissue [73]. However, it cannot be easily envisioned in the canine colon whose pacemaker region is filled with gap junctions.

7.2.4 Gap junctions create a current sink in the canine colon pacemaker area

The primary difference between the motor function of a heart and a colon is that the period of rhythmic contractions that appears in the entire heart is in the order of seconds and cells contract sequentially with a time delay of milliseconds depending on the propagating velocity of action potentials; whereas, the period of phasic contractions during persistalic motion in the colon is in the order of minutes or even hours *in vivo*. While cells in one region are contracting, the downstream cells may be relaxing for minutes. Therefore, the heart requires only one pacemaker spot to control its motor function; whereas, to differentiate the motor function in different segments of the colon, it requires a pacemaker sheet covering the entire submucosal surface with pacemaking activity very similar in a (or a few) circumferential lamella(e) but, at the same time, very different in the downstream (axial) direction. The connective

tissue in septa (as discussed in Chapter 6), dividing the column of circular muscle into ring-like lamellae around the colon lumen, can conceivably serve as an insulator to minimize electrical interference from neighbouring lamellae which may possess a different oscillating pattern at the same time. In view of this situation, it may *not* be advisable to have the entire sheet of submucosal pacemaker region perfectly electrically coupled.

Unlike the circular muscle, the ICC, presumably the pacemaker cells, are continuous even around the connective tissue septa. ***Electrical uncoupling in the submucosal ICC network relies on the presence of gap junctions.*** The initiation mechanism of action potentials in the heart is by sequential activation and inactivation of voltage sensitive ionic channels; whereas, in the colon, they are initiated by metabolic activity regulated by cyclic AMP. Thus, synchronization of electrical events between pacemaker cells in the heart can be purely electrical in nature. However, in the colon, metabolite equilibrium between pacemaker cells is more important to successfully generate a pacemaker potential. When metabolite balance is achieved in a pacemaker unit by diffusion through gap junctions, cells within the unit will fire simultaneously and generate a slow wave but only at the core of the pacemaker unit. Active current generated in the boundary of the unit will shunk to cells outside this pacemaker unit through gap junctions unless metabolite equilibrium in the neighbouring units has also been achieved and fire simultaneously. Undoubtedly, it is impossible to accomplish metabolite equilibrium in the entire submucosal surface of canine colon. Thus, different regions of colon can have different patterns of pacemaking activity.

Having highly permeable gap junctions to uncouple different pacemaking loci also allows spatial modification of motor function in different segments of the colon by extrinsic stimuli, such as neural inputs, since ICC are in close vicinity of nerve

varicosities [14]. For those pacemaker units that received the extrinsic stimuli, they exhibit a modified pattern of electrical activity which is different from the neighbouring pacemaker units outside this stimulated domain. These different patterns of electrical activity cannot interfere with each other (except in the boundary interfaces where small noise may appear but will decay exponentially according to passive membrane parameters) because active current generated in the boundary of either regions will shunk immediately through gap junctions to the 3-dimensionally well-coupled low-resistance network. This theory may extend to the sino-atrial node where gap junction density increases towards the boundary [16] so as to electrically uncouple the nonpacemaker cells from pacemaker cells to minimize passive electrotonic interference to the pacemaker core. However, morphological and physiological studies leading to the understanding of the anisotropic properties of gap junction permeability (intrinsic or extrinsic) and/or distribution along the circumferential and axial directions to provide perfect circumferential synchronization in circular muscle lamellae for creating a propulsive ring-like contraction, and at the same time to allow electrical uncoupling in the axial direction to permit generation of different patterns of pacemaker activity need to be performed.

It is important to realize that the statement "gap junctions increase the efficiency of electrical coupling" is *not* always true. In some cases, as in the canine colon, if gap junctions were there to provide prefect electrical coupling for signal propagation in the submucosal surface, differentiation in motor functions in different regions would be prohibited. Gap junctions can definitely promote electrical coupling in a passive system. In an active system, the role of gap junctions in electrical coupling (perhaps uncoupling) has to be interpreted with caution.

Chapter 8

Extension of work

8.1 Physiological aspects

8.1.1 Phase relationship between electrical oscillations

Experiments performed in the FT preparations were implemented by an intracellular electrode that records slow waves at different locations of the circular muscle during different time domains. Although the similar slow wave frequency at different locations suggests that slow waves are probably synchronized in the circular muscle, double electrode experiments showing a perfect phase relationship are essential for coming to the conclusion that slow waves are indeed synchronized. Simultaneous recordings in the longitudinal and circular muscles will provide additional knowledge about electrical interaction between the muscle layers at the myenteric plexus, in particular the SLAPs at the interface.

8.1.2 Selective action of methylene blue

As discussed in Chapter 6, the photo-oxidation of methylene blue leads to selective damage of cells in which methylene blue is actively accumulated. Our preliminary results indicated that illumination of ICC-CM preparations after 45 min incubation with methylene blue abolished slow waves. An important question that has not been fully resolved is whether the smooth muscle cells are damaged by methylene blue plus light. A way to test the circular muscle viability is its reaction to $BaCl_2$ (see Chpaters 3 and 4). Therefore, it is important to find out whether Ba^{2+} induced oscillations in CM preparations can be abolished by incubation with methylene blue followed by illumination. A negative result suggests that abolishment of slow waves in the ICC-CM preparations after treatment with methylene blue plus light is caused by selective damage of ICC. In that case, we can say that the generation of slow waves require vital ICC. It will give an additional piece of evidence showing that it is exclusively the ICC that generate pacemaker activity in the canine colon.

8.2 Theoretical aspects

To theoretically test several hypotheses about coupling mechanisms, a computer model can be developed reflectively, in particular, focusing on the heterogeneous aspect of slow waves across the circular muscle resulting from interactions between different cell types with oscillations of different intrinsic characteristics. Successful development of a computer model which possesses physiological characteristics of slow waves will allow us to examine the system in ways that could not be studied *in vitro* and could provide understanding of situations occurring *in vivo*.

8.2.1 Oscillator modelling for slow wave origin

A mapped clock oscillator has been established by Bardakjian and co-workers [8]. The mapped clock oscillator is a general type of nonlinear oscillator and consists of two interrelated compartments, a "clock" and a "mapping unit". The clock is characterized by a pair of nonlinear differential equations which describe the trajectory of a point in a two dimensional state plane. The mapping unit is a manifest station which can be at the same location as the clock or at a different location. The model description has been presented by Bardakjian and Lau [8]:

$$\dot{u}_1 = \omega[u_2(1+S_\phi) + u_1(1+S_\alpha - u_1^2 - u_2^2] \tag{8.1}$$

$$\dot{u}_2 = \omega[-u_1(1+S_\phi) + u_2(1+S_\alpha - u_1^2 - u_2^2] \tag{8.2}$$

$$S_\alpha = C_\alpha \cdot R \cdot x \tag{8.3}$$

$$S_\phi = C_\phi \cdot R \cdot x \tag{8.4}$$

$$R = [1 + (\frac{2\pi r}{\arctan(\frac{u_1}{u_2})^{2N}}]^{-\frac{1}{2}} \tag{8.5}$$

$$\mu = \sqrt{u_1^2 + u_2^2} \tag{8.6}$$

$$y = a_o + \Sigma_{\kappa=1}^{k}[a_\kappa \mu T_\kappa(\frac{u_2}{\mu}) + b_\kappa u_1 U_{\kappa-1}(\frac{u_2}{\mu})] \tag{8.7}$$

where x is the input stimulus,

y is the output oscillation,

r is the refractory parameter,

u_1 and u_2 are the clock variables,

C_α and C_ϕ are the switches (either 1 or 0) for α and ϕ portals, respectively.

T_κ $(\cdots)$ is the κ^{th} Chebyshev polynomial of the first type,

U_κ $(\cdots)$ is the κ^{th} Chebyshev polynomial of the second type, and

$[\omega, r, a_\kappa, b_\kappa]$ are the intrinsic model parameters

It is conceivable that the mapped clock oscillator is a potential model for the generation mechanism of colonic slow waves. The clock component represents the intracellular metabolic clock. The mapping unit manifests at the cell membrane, producing a membrane potential oscillation.

8.2.2 Propagation mechanism of slow waves

There is a major question related to the propagation mechanism of slow waves across the circular muscle layer, that is what the minimum number of gap junction channels needed to effectively allow passive signal propagation in a network of mapped clock oscillators adapted to the colonic physiological conditions is. Results of such a study can provide information on the relative importance of low resistance coupling and field coupling in slow wave propagation across the layer.

The next challenge is to simulate the oscillatory waveforms across the circular muscle. It is important to realize that the system is likely to be synchronized; however, there is a clear gap junction density gradient across the layer. Thus, it is not difficult to imagine that while the relative importance of the low resistance coupling component in determining the coupling coefficient is diminishing away from the submucosal surface, the electric field coupling component is increasing. That is, the coupling coefficient is a spatially dependent variable. Harmony of the two components produces a high enough coupling coefficient for prefect synchronization of electrical activity. Successfully simulating the heterogeneous nature of electrical activity across the circular muscle using the notions discussed may solidify the hypothesis that electrical communication can occur between intestinal smooth muscle cells without the need for gap junctions.

8.2.3 Chaos in proximal colon

Regular 6 cpm slow waves have been shown in canine proximal colon *in vitro* using tissue of a few square milimeters. *In vivo*, antiperistaltic motion was observed long ago in 1902 [18]. Therefore, it is obvious that the normally recorded 6 cpm slow waves in the proximal colon appear to be more chaotic[1] *in vivo*. It is an example that non-periodic oscillations can be appeared after coupled to other oscillators even if they all possess periodic oscillations individually. Generation of a chaotic oscillating pattern in the canine stomach has been modelled and can be produced by two coupled mapped clock oscillators with the same regular intrinsic characteristics by either a radial stimulation (affecting the amplitude) or a tangential stimulation (affecting the frequency) or a cartesian stimulation along one or other clock variables [45]. The extrinsic stimulus can come from distal neural inputs originating from the ileum. It has also been theoretically shown that using either mixed (both positive and negative) feedbacks or multiple negative feedback loops with different delays, complex periodic and aperiodic, chaotic rhythms are possibly produced from a regular oscillating pattern [43]. It suggests that a chaotic oscillating pattern in a point of the proximal colon can also be originated, without the need of any extrinsic input, by self-feedbacks along the axial direction which arrive at the discussed point at different time delays. After adapting mapped clock oscillators to the canine colonic electrical oscillations, it is interesting to investigate the chaotic behaviours of the nonlinear mapped clock oscillators with known physiological parameters under normal and pathological conditions because regularity does most of the time not exist in physiological situations.

[1] *chaos* is defined as aperiodic dynamics in deterministic systems in which there is a sensitive dependence of the temporal evolution on the initial conditions [43].

Bibliography

[1] Abe, Y. and Tomita, T. Cable properties of smooth muscle. *J. Physiol.(Lond)*, 196:87–100, 1968.

[2] Barajas-López, C. and Huizinga, J.D. Heterogeneity in spontaneous and tetraethylammonium induced intracellular electrical activity in colonic circular muscle. *Pflugers Arch.*, 412:203–210, 1988.

[3] Barajas-López, C. and Huizinga, J.D. Different mechanisms of contraction generation in circular muscle of canine colon. *Am. J. Physiol.*, 256:G570–G580, 1989.

[4] Barajas-López, C., Berezin, I., Daniel, E.E. and Huizinga, J.D. Pacemaker activity recorded in interstitial cells of Cajal of the gastrointestinal tract. *Am. J. Physiol.*, 257:C830–C835, 1989.

[5] Barajas-López, C., Den Hertog, A. and Huizinga, J.D. Ionic basis of pacemaker generation in dog colonic smooth muscle. *J. Physiol.(Lond)*, 416:385–402, 1989.

[6] Barbosa, P. and Peters, T.M. The effects of vital dyes on living organisms with special reference to methylene blue and neutral red. *Histochem-J.*, 3:71–93, 1971.

[7] Bardakjian, B.L. and Diamant, N.E. Electronic models of oscillator to oscillator communications. In N. Sperelakis and W.C. Cole, editors, *Cell interaction and gap junctions*, chapter 14. CRC Press, 1989.

[8] Bardakjian, B.L. and Lau, M.M. The refractory properties of mapped clock oscillators representing smooth muscle electrical oscillations. *Frontier in Smooth Muscle Research (Emil Bozler Symp.)*, 327:627–634, 1990.

[9] Bauer, A.J. and Sanders, K.M. Gradient in excitation-contraction coupling in canine gastric antral circular muscle. *J. Physiol.(Lond)*, 369:283–294, 1985.

[10] Bauer, A.J. and Sanders, K.M. Passive and active membrane properties of canine gastric antral circular muscles. *Am. J. Physiol.*, 251:C268–C273, 1986.

[11] Bauer, A.J., Publicover, N.G. and Sanders, K.M. Origin and spread of slow waves in canine gastric antral circular muscle. *Am. J. Physiol.*, 249:G800–G806, 1985.

[12] Bauer, A.J., Reed, J.B. and Sanders, K.M. Slow wave heterogeneity within the circular muscle of the canine gastric antrum. *J. Physiol.(Lond)*, 366:221–232, 1985.

[13] Benham, C.D., Bolton, T.B., Lang, R.J. and Takewaki, T. The mechanism of action of Ba^{2+} and TEA on single Ca^{2+}-activated K^{+}-channels in arterial and intestinal smooth muscle cell membranes. *Pflugers Arch.*, 403:120–127, 1985.

[14] Berezin, I., Huizinga, J.D. and Daniel, E.E. Interstitial cells of Cajal in the canine colon: a special communication network at the inner border of the circular muscle. *J. Comp. Neurol.*, 273:42–51, 1988.

[15] Berezin, I., Huizinga, J.D. and Daniel, E.E. Structural characterization of interstitial cells of Cajal in myenteric plexus and muscle layers of canine colon. *Can. J. Physiol.Pharmacol.*, In press, 1991.

[16] Brown, H.F. Electrophysiologoly of the sinoatrial node. *Physiol. Rev.*, 62(6):505–530, 1982.

[17] Burke, E.P., Reed J.B. and Sanders, K.M. Role of sodium pump in membrane potential gradient of canine proximal colon. *Am. J. Physiol.*, 254:C475–C483, 1988.

[18] Cannon, W.B. The movements of the intestines: Studies by means of the Röntgen rays. *Am. J. Physiol.*, 6:251–277, 1902.

[19] Caprilli, R. and Onori, L. Origin, transmission and ionic dependence of colonic electrical slow waves. *Scand. J. Gastroenterol.*, 7:65–74, 1972.

[20] Chow, E. and Huizinga, J.D. Myogenic electrical control activity in longitudinal muscle of human and dog colon. *J.Physiol.(Lond)*, 392:21–34, 1987.

[21] Christensen, J. Motility of the colon. In Leonard R. Johnson, editor, *Physiology of the Gastrointestinal Tract, Volume 1*, pages 695–722. Raven Press, New York, 1987.

[22] Christensen, J. and Hauser, R.L. Circumferential coupling of electric slow waves in circular muscle of cat colon. *Am. J. Physiol.*, 221:1033–1037, 1971.

[23] Christensen, J. and Hauser, R.L. Longitudinal axial coupling of slow waves in proximal cat colon. *Am. J. Physiol.*, 221:246–250, 1971.

[24] Christensen, J. and Rasmus, S.C. Colon slow waves: size of oscillators and rates of spread. *Am. J. Physiol.*, 223:1330–1333, 1972.

[25] Christensen, J., Caprilli, R. and Lund, G.F. Electric slow waves in circular muscle of cat colon. *Am. J. Physiol.*, 217:771–776, 1969.

[26] Conklin, J.L. and Du, C. Pathways of slow-wave propagation in proximal colon of cats. *Am. J. Physiol.*, 258:G894–G903, 1990.

[27] Dahms, V., Prosser, C.L. and Suzuki, N. Two types of 'slow waves' in intestinal smooth muscle of cat. *J. Physiol.(Lond)*, 392:51–69, 1987.

[28] Daniel, E.E. and Chapman, K.M. Electrical activity of the gastrointestinal tract as an indication of mechanical activity. *Am. J. Digest. Disease.*, 8:54–102, 1963.

[29] Debski, L.K. and Bowes, L., Kingma Y.J. and Gill R. Longitudinal and circular muscle of the canine colon have different and characteristic electrical and mechanical activities. In Claude Roman Dr. Sc., editor, *Gastrointestinal Motility*, pages 397–403. MTP Press Ltd., Hingham, 1983.

[30] Diamant, N.E., Rose, P.K. and Davison, E.J. Computer simulation of intestinal slow-wave frequency gradient. *Am. J. Physiol.*, 219:1684–1690, 1970.

[31] Droogmans, G. and Callewaert, G. Ca^{2+}-channel current and its modification by the dihydropyridine agonist BAY K 8644 in isolated smooth muscle cells. *Pflugers Arch.*, 406:259–265, 1986.

[32] Dunne, M.J. and Petersen, O.H. GTP and GDP activation of K^+ channels that can can be inhibited by ATP. *Pflugers Arch.*, 407:564–565, 1986.

[33] Durdle, N.G., Kingma, Y.J., Bowes, K.L. and Chambers, M.M. Origin of slow waves in the canine colon. *Gastroenterology*, 84:375–382, 1983.

[34] El-Sharkawy, T.Y. Electrical activities of the muscle layers of the canine colon. *J. Physiol.(Lond)*, 342:67–83, 1983.

[35] El-Sharkawy, T.Y., MacDonald, W.M. and Diamant, N.E. Characteristics of the slow wave activity of the canine colon. In J. Christensen, editor, *Gastrointestinal Motility*, pages 415–423. Raven Press, New York, 1983.

[36] Elden, L. and Bortoff, A. Electrical coupling of longitudinal and circular intestinal muscle. *Am. J. Physiol.*, 246(9):G618–G626, 1984.

[37] Elliott, T.R. and Barclay-Smith, E. Antiperistalsis and other muscular activities of the colon. *J. Physiol. (Lond.)*, 31:272–304, 1904.

[38] Farraway, L. and Huizinga, J.D. Potassium channel activation by cromakalim affects the slow wave type action potential of colonic smooth muscle. *Am. J. Pharmacol. Exp Ther.*, 257(1):35–41, 1991.

[39] Fioramonti, J., Garcia Villar, R., Bueno, L and Ruckebusch Y. Colonic myoelectrical activity and propulsion in the dog. *Dig. Dis. Sci.*, 25:641–646, 1980.

[40] Gabella, G. Intercellular junctions between circular and longitudinal intestinal muscle layers. *Z. Zellforsch. Mikrosk. Anat.*, 125:191–199, 1972.

[41] Giles, W.R. and Shibata, E.F. Voltage clamp of bull-frog cardiac pace-maker cells: a quantitative analysis of potassium currents. *J. Physiol.*, 368:265–292, 1985.

[42] Gill, W.B., Taja, A., Chadbourne, D.M., Roma, M. and Vermeulen, C.W. Inactivation of bladder tumor cells and enzymes by methylene blue plus light. *J. Urol.*, 138:1318–1320, 1987.

[43] Glass, L., Beuter, A., and Larocque, D. Time delays, oscillations , and chaos in physiological control systems. *Math. Biosci.*, 90:111–125, 1988.

[44] Hagiwara, S. *Membrane Potential-Dependence Ion Channels in Cell Membrane: Phylogenetic and Developmental Approaches.* Raven Press, New York, 1983.

[45] Hanson, P.E., Bardakjian, B.L. and Diamant, N.E. Chaos in a computer model of two coupled gastric oscillators. *CMBEC-15-CCGB*, Toronto:115–116, 1989.

[46] Hara, Y. and Szurszewski, J.H. Effect of potassium and acetylcholine on canine intestinal smooth muscle. *J. Physiol.(Lond)*, 372:521–537, 1986.

[47] Hara, Y., Kubota, M. and Szurszewski, J.H. Electrophysiology of smooth muscle of the small intestine of some mammals. *J. Physiol.(Lond)*, 372:501–520, 1986.

[48] Hille, B. *Ionic Channels of Excitable Membranes.* Sinauer Associates Inc., Sunderland, Massachusetts, 1984.

[49] Huizinga, J.D. Action potentials in gastrointestinal smooth muscle. *Can.J.Physiol.Pharmacol.*, in press, 1991.

[50] Huizinga, J.D. and Barajas-López, C. Ionic and cellular basis for slow-wave-type and spike-like action potentials. *Prog. Clin. Biol. Res.*, 327:605–615, 1990.

[51] Huizinga, J.D. and Chow, E. Electrotonic current spread in colonic smooth muscle. *Am. J. Physiol.*, 254:G702–G710, 1988.

[52] Huizinga, J.D., Barajas-López, C. and Chow, E. Generation of spiking activity in circular muscle cells of the canine colon. *Can. J. Physiol. Pharmacol.*, 65:2147–2150, 1987.

[53] Huizinga, J.D., Berezin, I., Daniel, E.E. and Chow, E. Inhibitory innervation of colonic smooth muscle cells and interstitial cells of Cajal. *Can. J. Physiol. Pharmacol.*, 68:447–454, 1990.

[54] Huizinga, J.D., Chang, G., Diamant, N.E. and El-Sharkawy, T.Y. Electrophysiological basis of excitation of canine colonic circular muscle by cholinergic agents and substance p. *J. Pharmacol. Exp. Ther.*, 231:692–699, 1984.

[55] Huizinga, J.D., Chow, E., Diamant, N.E. and El Sharkaway, T.Y. Coordination of electrical activities in muscle layers of the pig colon. *Am. J. Physiol.*, 252:G136–G142, 1987.

[56] Huizinga, J.D., Farraway, L. and Den Hertog, A. Effect of voltage and cyclic AMP on frequency of slow wave type action potentials in canine colonic smooth muscle. *J. Physiol.*, 442:31–45, 1991.

[57] Huizinga, J.D., Farraway, L. and Den Hertog, A. Initiation of the slow wave type action potentials in colonic smooth muscle involves a non-L-type calcium conductance. *J. Physiol.*, 422:15–29, 1991.

[58] Huizinga, J.D., Stern, H.S., Chow, E., Diamant, N.E., and El-Sharkawy T.Y. Electrophysiologic control of motility in the human colon. *Gastroenterology*, 88:500–511, 1985.

[59] Huizinga, J.D., Stern, H.S., Chow, E., Diamant, N.E., and El-Sharkawy T.Y. Electrical basis of excitation and inhibition of human colonic smooth muscle. *Gastroenterology*, 90:1197–1204, 1986.

[60] Ignarro, L.J. Biological actions and properties of endothelium-derived nitric oxide formed and released from artery and vein. *Circ. Res.*, 65:1–21, 1989.

[61] Langton, P.D., Burke, E.P. and Sanders, K.M. Participation of ca currents in colonic electrical activity. *Am. J. Physiol.*, 257:C451–C460, 1989.

[62] Liu, L.W.C. and Daniel, E.E. and Huizinga, J.D. Colonic circular muscle without the network of interstitial cells of Cajal can generate slow waves through different mechanisms. *J. Gastrointest. Motility.*, In press, 1991.

[63] Miller, S.M., Garfield, B. and Daniel, E.E. Improved propagation in myometrium associated with gap junction during parturition. *Am. J. Physiol.*, 256:C130–C141, 1989.

[64] Sabourin, P.J., Kingma, Y.J. and Bowes, K.L. Simultaneous measurment of electrical activity from two colonic smooth muscle layers using a dual sucrose gap appartus. *I.E.E.E. Trans. Biomed. Eng.*, 37(5):509–514, 1990.

[65] Sanders, K.M. Colonic electrical activity: concerto for two pacemakers. *N. I. P. S.*, 4:176–180, 1989.

[66] Sanders, K.M. and Smith, T.K. Enteric neural regulation of slow waves in circular muscle of the canine proximal colon. *J. Physiol.(Lond)*, 377:297–313, 1986.

[67] Sanders, K.M., Burke, E.P. and Stevens, R.J. Effects of methylene blue on rhythmic activity and membrane potential in the canine proximal colon. *Am.J.Physiol.*, 256:G779–G784, 1989.

[68] Sarna, S.K., Cordon, R. and Cowles, V. Colonic migrating and nonmigrating motor complexes in dogs. *Am. J. Physiol.*, 246:G355–G360, 1984.

[69] Serio, R., Barajas-López, C., Daniel, E.E., Berezin, I., and Huizinga, J.D. Slow wave activity in colon: role of network of submucosal interstitial cells of Cajal. *Am. J. Physiol.*, 260:G636–G645, 1991.

[70] Smith, T.K., Reed, J.B. and Sanders, K.M. Interaction of two electrical pacemakers in muscularis of canine proximal colon. *Am. J. Physiol.*, 252:C290–C299, 1987.

[71] Smith, T.K., Reed, J.B. and Sanders, K.M. Origin and propagation of electrical slow waves in circular muscle of canine proximal colon. *Am. J. Physiol.*, 252:C215–C224, 1987.

[72] Smith, T.K., Reed, J.B. and Sanders, K.M. Effects of membrane potential on electrical slow waves of canine proximal colon. *Am. J. Physiol.*, 255:C828–C834, 1988.

[73] Sperelakis, N. Electric field model: an alternative mechanism for cell-to-cell propagation in cardiac muscle and smooth muscle. *Gastroint. Mot.*, 3(2):64–82, 1991.

[74] Sperelakis, N. and Lehmkuhl, D. Ionic interconversion of pacemaker and non-pacemaker cultured chick heart cells. *J. Gen. Physiol.*, 49:867–895, 1966.

[75] Sperelakis, N. and Marschall, R.A. Propagation down a chain of excitable cells by electric field interactions in the junctional clefts: effect of variation in extracellular resistance, including a "sucrose gap" simulation. *I.E.E.E. Biomed. Eng.*, 30(10):658–664, 1983.

[76] Sperelakis, N. and Schneider, M.F. and Harris, E.J. Decreased K^+ conductance produced by Ba^{++} in frog sartorius fibers. *J. Gen. Physiol.*, 50:1565–1583, 1967.

[77] Suzuki, N., Prosser, C.L. and Dahms, V. Boundary cells between longitudinal and circular layers: essential for electrical slow waves in cat intestine. *Am. J. Physiol.*, 250:G287–G294, 1986.

[78] Szurszewski, J.H. Electrophysiological basis of gastrointestinal motility. In L.R. Johnson, editor, *Physiology of the Gastrointestinal Tract, Volume 1*, pages 383–422. Raven Press, New York, 1987.

[79] Taylor, A.B., Kreulen, D. and Prosser, C.L. Electron microscopy of the connective tissue between longitudinal and circular muscle of small intestine of cat. *Am. J. Anat.*, 150:427–442, 1977.

[80] Thuneberg, L. Interstitial cells of Cajal: intestinal pacemaker cells? *Adv. Anat. Embryol. Cell Biol.*, 71:1–130, 1982.

[81] Thuneberg, L. Interstitial cells of Cajal. In G. S. Schultz, J. D. Wood, and B. B. Rauner, editors, *Handbook of Physiology, the gastrointestinal system*, pages 349–386. American Physiological Society, Bethesda, U.S.A., 1989.

[82] Thuneberg, L. Methylene blue as a pharmacological probe of intestinal pacemaker activity;letter; comment. *Am.J.Physiol.*, 258:G992–G994, 1990.

[83] Thuneberg, L., Johansen, V., Rumessen, J.J. and Andersen, B.G. Interstitial cells of Cajal: Selective uptake of methylene blue inhibits slow wave activity. In C. Roman, editor, *Gastrointestinal Motility*, pages 495–502. MTP Press Limited, Lancaster, 1983.

[84] Ward, S.M. and Sanders, K.M. Pacemaker activity in septal structures of canine colonic circular muscle. *Am. J. Physiol.*, 259:G264–G273, 1990.

[85] Wolin, M.S., Cherry, P.D., Rodenburg, J.M., Messina, E.J. and Kaley, G. Methylene blue inhibits vasodilation of skeletal muscle arterioles to acetylcholine and nitric oxide via the extracellular generation of superoxide anion. *J. Pharmacol. Exp. Ther.*, 254:872–876, 1990.

List of publications

1. Huizinga, J.D. and Liu, L.W.C.. Role of calcium channels in pharmacological modulation of gastrointestinal motilty, in *Calcium Antagonists: Pharmacology and Clinical Research*, edited by Christen, M.O.. Raven press: New York, 1991. (accepted)

2. Huizinga, J.D., Liu, L.W.C., Blennerbassett, M., Thuneberg, L., and Molleman, A.. Intercellular communication in smooth muscle. *Experientia.* (submitted)

3. Liu, L.W.C., Daniel, E.E. and Huizinga, J.D.. Excitability of canine colon circular muscle disconnected from the network of interstitial cells of Cajal. *Can. J. Physiol. Pharmacol.*. (accepted, based on Chapter 3).

4. Liu, L.W.C. and Huizinga, J.D.. Properties of the circular muscle of canine colon disconnected from pacemaker cells. *J. Physiol. (Lond).* (submitted, based on Chapter 4).

5. Liu, L.W.C. and Huizinga, J.D.. Electrophysiological and structural communication between circular and longitudinal muscle of canine colon. *J. Physiol. (Lond).* (submitted, based on Chapter 5).

6. Liu, L.W.C., Thuneberg, L., Daniel, E.E. and Huizinga, J.D.. Selective accumulation of methylene blue by interstitial cells of Cajal in the canine colon with preservation of slow waves. *Am. J. Physiol.*. (submitted, based on Chapter 6).